Analysis of intermediates of the methionine and polyamine metabolism by liquid chromatography-tandem mass spectrometry

Dissertation

zur Erlangung des Doktorgrades der Naturwissenschaften (Dr. rer. nat.)
an der Fakultät für Chemie und Pharmazie
der Universität Regensburg

vorgelegt von

Axel Peter Stevens

aus Friedrichsdorf

Mai 2011

Diese Doktorarbeit entstand in der Zeit von Oktober 2006 bis März 2011 am Institut für Funktionelle Genomik der Universität Regensburg.

Die Arbeit wurde angeleitet von Prof. Dr. Peter J. Oefner.

Promotionsgesuch eingereicht am 09.05.2011

Kolloquiumstermin: 29.06.2011

Prüfungsausschuss:	Vorsitzender:	Prof. Dr. Jörg Heilmann
	Erstgutachter:	Prof. Dr. Frank-Michael Matysik
	Zweitgutachter:	Prof. Dr. Peter J. Oefner
	Drittprüfer:	Prof. Dr. Wolfram Gronwald

Für meine Eltern & Heiner

Danksagung

Ein solches Werk entsteht nicht ohne die Hilfe anderer und diesen Personen möchte ich an dieser Stelle herzlich danken.

Beginnen möchte ich bei Prof. Peter Oefner, der mir die Möglichkeit gab, an seinem Institut zu promovieren, und mit seinen stets konstruktiven Fragen dazu beitrug, dass ich meine Ergebnisse kritisch hinterfragte. Sein konstantes Interesse an meiner Arbeit und seine Unterstützung, meine Ergebnisse auf nationalen und internationalen Tagungen zu präsentieren, zeigten mir die Wichtigkeit meiner Forschung.

Ein herzlicher Dank gebührt auch Prof. Frank-Michael Matysik, der sich nach dem Betreuen meiner Diplomarbeit in Leipzig auch bereiterklärt hat, Gutachter und Erstprüfer meiner Doktorarbeit in Regensburg zu sein. Weiterhin danke ich Prof. Wolfram Gronwald und Prof. Jörg Heilmann für Ihre Bereitschaft, die Funktion des dritten Prüfers und des Prüfungsvorsitzenden zu übernehmen.

Größter Dank gilt der direkten Betreuerin meiner Arbeit, der Leiterin der Metabolomics-Gruppe Frau Dr. Katja Dettmer-Wilde. Ihre Unterstützung bei meinen ersten Gehversuchen an der LC sowie die mir zugestandenen Freiräume während meiner Forschung und der Zusammenarbeit mit Kooperationspartnern habe ich immer sehr zu schätzen gewusst.

Ein weiterer Dank geht an alle Kollegen aus der Metabolomics-Gruppe – aktuelle wie ehemalige – Dr. Birgit Timischl, Dr. Hanne Kaspar, Dr. Wentao Zhu, Martin Almstetter, Stephan Fagerer, Steffi Stöckl, Magdalena Waldhier, Chris Wachsmut sowie Nadine Nürnberger für das nette Klima und den regen Ideenaustausch im Labor.

Den Kollegen von der Proteomic-Abteilung, Dres. Yvonne und Jörg Reinders, Sophie Schirmer, Anja Thomas, Nadine Assmann und Corinna Feuchtinger danke ich für ihre Hilfe bei diversen Quantifizierungsversuchen von MTAP. Leider ausgestorben, aber dennoch nicht vergessen, die Kolleginnen und der Kollege aus der Zellkultur Dr. Kathrin Renner-Sattler, Dr. Karin Eberhart und Jan Linnemann – vielen Dank für Eure Hilfe bei Fragen zur Zellkultur und das ein oder andere Frustbier nach Feierabend. Vielen Dank an Barbara Herte für den ein oder anderen lustigen Abend am Institut

und das stete Interesse am Quadle-Trip – auch wenn es mal nicht so läuft. Um den Flur zu komplettieren: Einen herzlichen Dank an die Kollegen vom KFB, Dr. Thomas Stempfl, Dr. Christoph Möhle, Jutta Schipka, Susanne Schwab und Corinna Unger für die Möglichkeit, diverse Proben bei Euch zu horsten, und die immer netten und aufmunternden Worte.

Ebenfalls nicht unerwähnt bleiben dürfen an dieser Stelle natürlich meine Kooperationspartner, denen ich für die fruchtbare Zusammenarbeit während dieses Projektes danken möchte: Dr. Katrin Singer, Dr. Eva Gottfried und Prof. Marina Kreutz von der Häma/Onko, Barbara Czech, Dr. Georgi Kirovski und PD Dr. Claus Hellerbrand von der Inneren Medizin I, Susanne Wallner und Prof. Anja Bosserhoff vom Institut für Pathologie sowie Dr. Oliver Grauer von der Neurologie. Ein ganz spezieller Dank geht an Dr. Martin Link von Institut für Analytische Chemie für seine Hilfe bei der Synthese von $^{13}C_5$-gelabeltem MTA sowie an Prof. Keijiro Samejima von der Musashino University in Tokio für das $^{15}N_3$-gelabelte Spermidin.

Ohne ihn wäre es nie dazu gekommen: Ein großes Dankeschön geht an meinen ersten Chemie-Lehrer Günther Winnen. Hätte er nicht mein Interesse an der Chemie geweckt und gefördert, vielleicht hätte ich was anderes studiert.

Das allergrößte Dankeschön geht an meine Eltern, dafür dass sie mich in den letzten Jahren immer unterstützt und fest an mich geglaubt haben.

Während meiner Promotion fand ich auch mein privates Glück. Liebe Ireen, dafür dass Du mich immer bedingungslos unterstützt, danke ich Dir von ganzem Herzen. Es tut gut, heimkommen zu können und jemanden zu haben, der einem zuhört und einen versteht.

I. Table of contents

II. Abbreviations and Acronyms

Ac	acetyl
AMD1	adenosylmethionine decarboxylase
°C	degree Celsius
CCl_4	carbon tetrachloride
CO_2	carbon dioxide
CE	collision energy
CE-MS	capillary electrophoresis-mass spectrometry
CE-QqQ-MS	capillary electrophoresis-triple quadrupole-mass spectrometry
Conc.	concentration
cps	counts per second
CXP	collision cell exit potential
dcSAM	decarboxylated *S*-adenosyl-methionine (*S*-Adenosyl-methionineamine)
DMEM	Dulbecco's Modified Eagle Medium
DNA	deoxyribonucleic acid
DTT	dithiothreitol
DP	declustering potential
EC	enzyme commission number
EDTA	ethylenediaminetetraacetic acid
eV	electron volt
FCS	fetal calf serum
FDA	federal drug administration
fmol	femtomol
g	gram
GC	gas chromatography
GC-MS	gas chromatography-mass spectrometry
GLP	good laboratory practice
h	hour
H_2O	water
HCC	hepatocellular carcinoma
HCl	hydrochloric acid
HFBA	heptafluorobutyric acid
HPLC	high performance liquid chromatography

HPLC-MS/MS	high performance liquid chromatography-tandem mass spectrometry
HPLC-UV	high performance liquid chromatography-ultra violet detection
i.d.	inner diameter
IDA	information dependent acquisition
IP-LC-MS	ion pair-liquid chromatography-mass spectrometry
IS	internal standard
k	rate constant
KH_2PO_4	potassium dihydrogen phosphate
K_2HPO_4	dipotassium phosphate
L	liter
LC	liquid chromatography
LC-ESI-MS/MS	liquid chromatography-electrospray ionization-tandem mass spectrometry
LC-FTICR-MS	liquid chromatography-Fourier transformation ion cyclotron resonance-mass spectrometry
LC-IT-MS	liquid chromatography-ion trap-mass spectrometry
LC-MS	liquid chromatography-mass spectrometry
LC-MS/MS	liquid chromatography-tandem mass spectrometry
LC-QqQ-MS	liquid chromatography-triple quadrupole-mass spectrometry
LC-UV	liquid chromatography-ultra violet detection
LLOQ	lower limit of quantification
ln	natural logarithm
LOD	limit of detection
M	molar
MALDI-TOF-MS	matrix assisted laser desorption/ionization-time of flight-mass spectrometry
MeOH	methanol
mg	milligram
min	minute
mio	million
mL	milliliter
mM	millimolar
mm	millimeter

MMP	matrix metalloproteins
MRM	multiple reaction monitoring
MS	mass spectrometry
MS^3	three dimensional mass spectrometry
MTA	5'-deoxy-5'-methylthioadenosine
MTAP	methylthioadenosine phosphorylase
MTR	5-methyltetrahydrofolate-homocysteine methyltransferase
MTR-!P	5'-deoxy-5'-methylthioribose-1-phosphate
m/z	mass to charge ratio
µg	microgram
µL	microliter
µM	micromolar
µmol	micromol
n	number of experiments
NaCl	sodium chloride
NAFLD	non alcoholic fatty liver disease
NASH	non alcoholic steatohepatitis
nM	nanomolar
nmol	nanomol
ODC	ornithine decarboxylase
p	value of probability
PCR	polymerase chain reaction
pH	potentia Hydrogenii
PI	product ion scan
pM	picomolar
pmol	picomol
ppm	parts per million
psi	pound per square inch
Put	putrescine
Q1 / q2 / Q3	first / second / third quadrupole
QC	quality control
qMS	quadrupole mass spectrometer
qTOFMS	quadrupole time of flight mass spectrometer
r^2	coefficient of determination

rMTAP	recombinant methylthioadenosine phosphorylase
rpm	revolutions per minute
RSD	relative standard deviation
RT	room temperature
s	second(s)
SAH	*S*-adenosyl-homocysteine
SAM	*S*-adenosyl-methionine
S.D.	standard deviation
SIM	single ion monitoring
S/N	signal to noise ratio
Spd	spermidine
Spm	spermine
STAT	signal transducer and activator of transcription
t	time
TCEP	Tris(2-carboxyethyl)phosphine hydrochloride
TOFMS	Time of flight mass spectrometer
tRNA	transfer ribonucleic acid
U/min	units per minute
ULOQ	upper limit of quantification
V	volt
vs.	versus
xg	times of gravitation force

1. Motivation

The methionine pathway covers the metabolism and catabolism of the essential amino acid methionine and overlaps with the polyamine synthesis. The *S*-adenosylated derivative of methionine, *S*-adenosyl-L-methionine (SAM) is an important methyl group donor in transmethylation reactions, whereupon *S*-adenosyl-L-homocysteine (SAH) is formed. SAM can also be decarboxylated and afterwards donates its *n*-propylamine group to the biosynthesis of the polyamines spermidine and spermine from putrescine. In this reaction 5'-deoxy-5'-methylthioadenosine (MTA) is formed. MTA can be recycled to methionine, the first step of this catabolism is an enzymatic reaction catalyzed by the enzyme methylthioadenosine phosphorylase (MTAP, EC 2.4.2.28).

It has been observed that many malignant tumors commonly lack or display reduced MTAP activity and therefore MTA should accumulate in tumors.

Aim #1: Development of a method to quantify MTA in biological samples.

A major obstacle in the study of MTA and its role in cancer development and progression has been the lack of a sensitive and specific analytical method for its direct quantification in cell lysates, cell culture media and tumor tissue specimens. Hence, a method for quantification of MTA was developed. Reversed phase liquid chromatography combined with electrospray ionization tandem mass spectrometry was chosen as analytical method, because of simple sample preparation. Only a protein precipitation is necessary to make the sample amenable to LC-MS/MS. To achieve high accuracy and reproducibility a stable isotope labeled standard ($^{13}C_5$-MTA) was synthesized. Low limits of detection and quantification were obtained using a triple quadrupole mass spectrometer (API 4000 QTrap) in the MRM mode. With this

method the postulated accumulation of MTA in MTAP lacking cells and tissues was proved.

Aim #2: Quantification of intermediates of the methionine and polyamine metabolism.

In an effort to further elucidate the molecular consequences of a lack of MTAP and a concomitant increase in intracellular MTA, the analytical method developed under #1 was expanded to all key intermediates of the methionine and polyamine metabolic pathways. The LC separation was optimized including the addition of an ion pair reagent and the modification of the gradient. This method was used to determine changes in metabolite concentration in these pathways in different cell lines and tumor biopsies.

Aim #3: Determination of the MTAP activity in cell culture samples and liver biopsies.

In the course of the application of the method to tissue specimens from the livers of mice with fatty liver disease as well as various tumors, it was observed that the protein levels of MTAP did not always correlate with the MTA concentration measured in the tissue specimens. In an effort to elucidate whether alterations in MTAP activity accounted for the lack of correlation, an LC-MS/MS based assay for the measurement of the enzymatic activity of MTAP was developed. Tissue specimens were lysed in K_2HPO_4/KH_2PO_4 buffer (pH=7.4) and labeled MTA was spiked in. To measure the decrease in labeled MTA over time aliquots were taken repeatedly over 10 minutes and subjected to LC-MS/MS. Relative rate constants were determined and compared between tissues.

2. Background

2.1 5'-Deoxy-5'-methylthioadenosine

5'-deoxy-5'-methylthioadenosine (MTA) is a modified analogue of adenosine with the 5'-hydroxy group of the sugar moiety being substituted by a methylthio-group (see Figure 1).

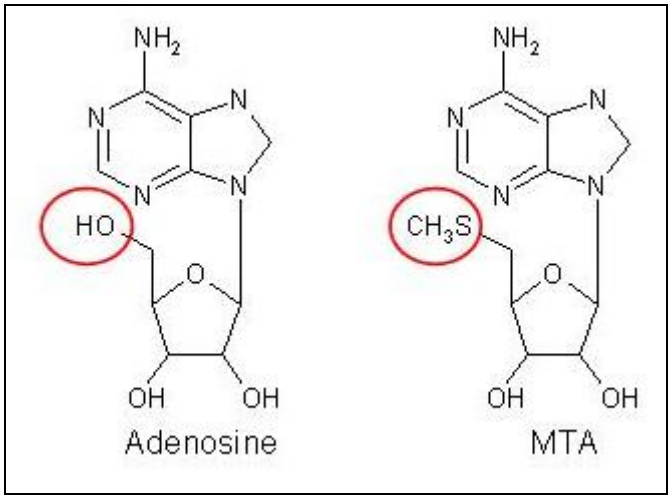

Figure 1: Structure of Adenosine and MTA.

MTA is synthesized from S-adenosyl-L-methionine (SAM), which is a condensation product of adenosine and L-methionine. SAM is decarboxylated and the *n*-propylamine group of the decarboxylated SAM (dcSAM) is used in the course of polyamine synthesis resulting in MTA as byproduct [1]. The first step of MTA catabolism is the cleavage of MTA to adenine and methylthioribose-1-phosphate, an enzymatic reaction catalyzed by MTA phosphorylase (MTAP, EC 2.4.2.28) [2]. The removal of accumulated MTA by MTAP is essential for the synthesis of polyamines and the salvage of methionine and adenosine [3]. Due to the involvement of MTA in polyamine synthesis, MTA is ubiquitously distributed, e.g. in rat tissues at concentrations of 2 to 7 nmol per gram fresh tissue weight as determined by HPLC-UV after sample preconcentration [4].

Studies reported, that cancer cells commonly lack MTAP expression [5-8]. Consequently, in MTAP-deficient cancer cells MTA is presumably not metabolized but accumulates intracellularly and/or is excreted [9]. This leads to an increased invasive potential of these cancer cells due to molecular mechanisms yet to be elucidated in detail [3,6,9-11]. Studies on malignant melanoma show that MTAP-deficiency correlates with tumor invasion and metastasis. *In vitro* data has shown that MTA leads to tumor progression by inducing matrix metalloproteins (MMP) in melanoma cells as well as in tumor associated fibroblasts [6,12]. It was furthermore observed that in melanoma patients tumor cells lacking MTAP show a worse response to interferon therapy [13].

Beside its role in tumor progression, MTA also affects cellular signaling pathways. Mowen et al. demonstrated that MTA influences the interferon signaling pathway caused by the reduction in methylated STAT (signal transducer and activator of transcription) which is required for activating the transcription of target genes [14]. Although this is critically discussed [6] Meyer et al. could show a positive correlation between MTAP expression and a response to an interferon-α treatment in patients with malignant melanoma [15]. Hence, MTA is of great interest in the filed of tumor research.

2.2 Quantitative analysis of 5'-deoxy-5'-methylthioadenosine

A major obstacle in the study of MTA and its role in cancer has been the lack of a sensitive and specific analytical method for its direct quantification in cell and tissue lysates as well as cell culture supernatants. Mass spectrometry has been applied to the analysis of urinary MTA. Liquid chromatography coupled to an ion trap MS yielded lower limits of detection (LODs) in the lower pmol range [16], while a LOD of

100 fmol was achieved using MALDI-TOF-MS [17]. However, data on absolute quantification, reproducibility and accuracy were reported for neither method. Further, there have been reports on the HPLC separation of MTA and its detection by means of UV absorbance [18-20]. Although LODs as low as 1 nmol were obtained using boronate affinity chromatography for pre-concentration of MTA, LC-UV has proven too insensitive and insufficiently selective for the direct analysis of MTA in tumor cells.

2.3 Methionine and polyamine metabolism

Since the analysis of MTA alone is insufficient to evaluate metabolic changes during the development and progression of a disease, the comprehensive analysis of intermediates of the methionine and polyamine metabolism is needed to understand the underlying mechanisms of these metabolic changes. Methionine is one of two sulfur-containing proteinogenic amino acids. Other than in protein synthesis, methionine plays an important role in the biosynthesis of cysteine, carnitine, taurine, and lecithine [21-23]. Its *S*-adenosylated derivative, *S*-adenosylmethionine (SAM), is an important methyl group donor in transmethylation reactions, whereupon *S*-adenosyl-L-homocysteine (SAH) is formed (Figure 2) [24]. SAH is hydrolyzed enzymatically to homocysteine and adenosine, and the former is recycled back to methionine through transfer of a methyl group from 5-methyltetrahydrofolate by the enzyme 5-methyltetrahydrofolate-homocysteine methyltransferase (MTR, EC 2.1.1.13) [25]. SAM can also be decarboxylated by adenosylmethionine decarboxylase (AMD1, EC 4.1.1.50) to *S*-adenosylmethionineamine (dcSAM), which subsequently donates its *n*-propylamine group in the biosynthesis of spermidine and spermine from putrescine, whereupon MTA is formed (Figure 2) [1]. MTA, in turn, can

be recycled back to methionine, the first step of which involves the phosphorolytic cleavage of MTA by methylthioadenosine phosphorylase (MTAP, EC 2.4.2.28) to produce adenine and 5'-deoxy-5'-(methylthio)ribose-1-phosphate [2,3].

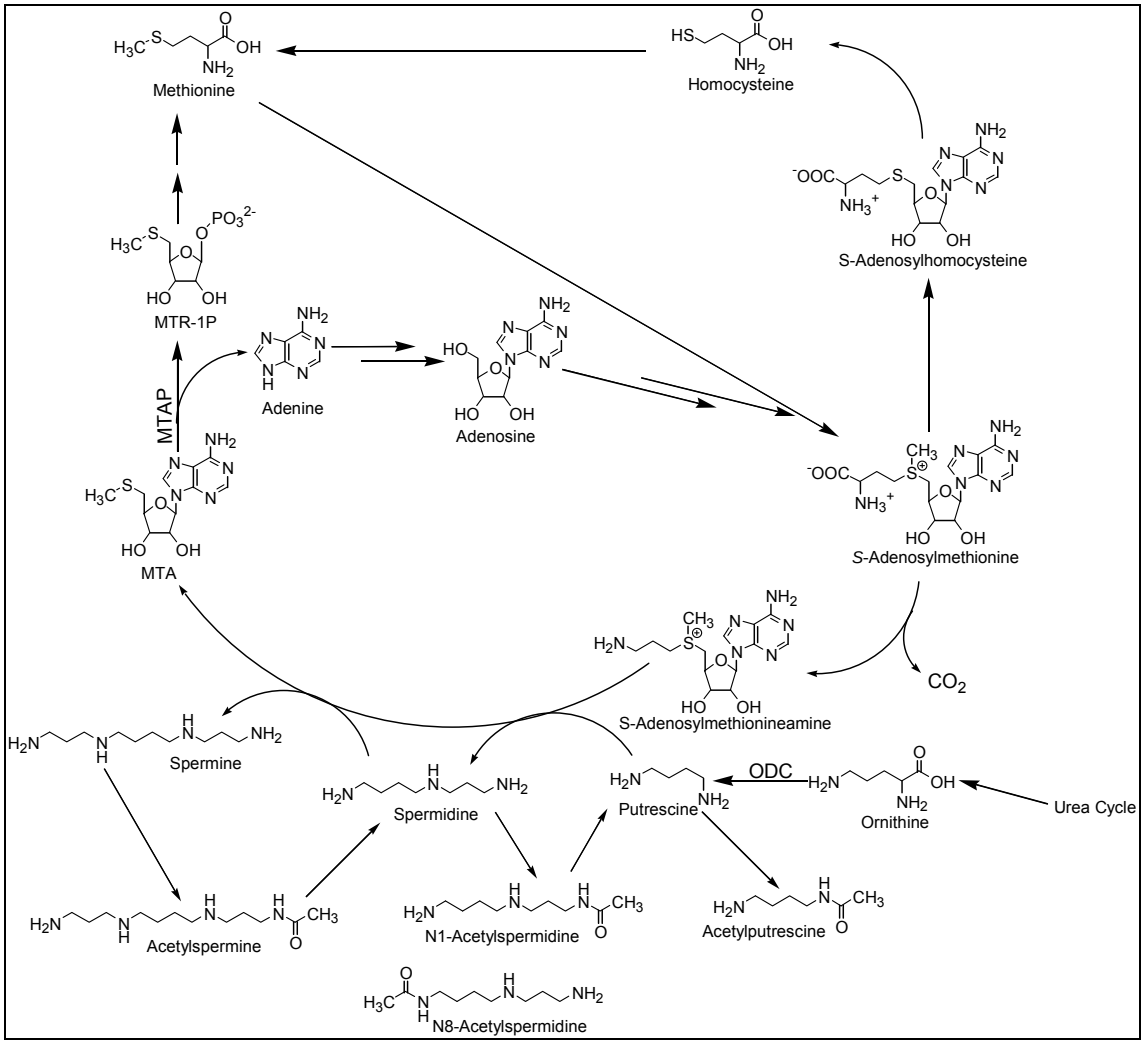

Figure 2: Scheme of the methionine and polyamine pathways.

Polyamines derive from the amino acid ornithine, which is decarboxylated in the initial rate-limiting reaction by the enzyme ornithine decarboxylase (ODC, EC 4.1.1.17) to yield putrescine [26]. Subsequently, putrescine gives rise to spermidine, which in turn provides the substrate for the formation of spermine. Polyamines play important roles in cellular growth, differentiation of eukaryotic cells, conformational stabilization of nuclear DNA, and methylation of tRNA. Acetylation of polyamines is required in the homeostatic maintenance of polyamine levels in mammalian cells within a relatively

constant range by rendering polyamines susceptible to either export out of the cell or enzymatic oxidation to lower polyamines [27].

Many malignant tumors lack or display reduced MTAP activity [3,6,10] resulting in an accumulation of MTA in MTAP lacking cells [12,28]. Polyamines are also known to concentrate in cancer cells and it has been reported that MTAP regulates ornithine decarboxylase (ODC) activity by downstream metabolites [29]. However, to date analytical methodology for the combined analysis of intermediates of both the methionine cycle and polyamine biosynthesis has lacked. In 2009 Cataldi et al. published a method using liquid chromatography coupled to hybrid linear quadrupole ion trap and Fourier transform ion cyclotron resonance mass spectrometer for the analysis of the methionine pathway including adenine, adenosine, homocysteine, homocystine, MTA, methionine, SAH and SAM [30]. In addition, methods have been developed for the determination of selected metabolites of either pathway.

Methods to quantify SAM and SAH by LC-MS/MS were developed by Gellekink et al. [25] and Krijt et al. [31]. Polyamines and their acetylated derivatives, on the other hand, have been determined by LC-MS/MS as carbamoyl [32] or as benzoyl derivatives by LC-UV [33]. Hakkinen et al. presented an LC-MS/MS method to quantify polyamines without derivatization [34]. Kammerer et al. determined MTA and adenosine after analyte enrichment by LC-IT-MS [16] and Porcelli et al. determined only MTA without prior enrichment by LC-UV [18]. For the analysis of amino acids numerous analytical methods are available, including GC-MS [35], LC-UV [36], CE-MS [37]. An IP-LC-MS method [38] includes additionally the quantification of homocysteine.

A comparison of these methods containing analytes and figures of merit is given in Table 1 on the next page.

Table 1: Method comparison for quantification of metabolites of the methionine and polyamine pathways.

Method	Analytes [a]	LOD	LOQ	Ref.
LC-FTICR-MS	Complete methionine pathway	0.01 – 1.8 µM	0.03 – 5.9 µM	[30]
LC-QqQ-MS	SAM SAH	n.d.	2 nM 1 nM	[25]
LC-QqQ-MS	SAM SAH	7.5 nM 15 nM	n.d	[31]
Carbamoyl derivatization and LC-IT-MS	Putrescine Ac-putrescine Spermidine Ac-spermidine	n.d.	1 ng/mL	[32]
Benzoyl derivatization and LC-UV	Putrescine Spermidine Spermine	57 pmol abs. 117 pmol abs. 124 pmol abs.	n.d	[33]
No derivatization and LC-QqQ-MS	Putrescine Spermidine N^1-Ac-spermidine N^8-Ac-spermidine Spermine ac-Spermine	n.d.	n.d.	[34]
LC-IT-MS	Adenosine MTA	0.1-9.6 pmol abs.	n.d.	[16]
MALDI-TOF-MS	Adenosine MTA	100 fmol abs.	n.d.	[17]
LC-UV	MTA	1 mM	n.d.	[18]
Propyl chloroformate derivatization and GC-MS	Methionine Ornithine	0.9 µM 0.3 µM	3.0 µM 0.9 µM	[35]
Ninhydrin derivatization and LC-UV	Methionine Ornithine	< 5 µM	n.d.	[36]
CE-QqQ-MS	Methionine Ornithine	0.7 µM 0.5 µM	n.d.	[37]
No derivatization and LC-QqQ-MS	Methionine Ornithine Homocysteine	n.d.	0.4 µM	[38]

[a] Only analytes of interest for this work are selected.

2.4 Kinetic studies of methylthioadenosine phosphorylase

The accumulation of MTA is not necessarily an indication of lower MTAP abundance, but can also point towards reduced MTAP activity. This can be assessed by measuring the enzymatic activity of MTAP. In the past only a few experiments were carried out to determine kinetic parameters of the MTAP enzyme. In 1984 Seidenfeld et al. described for the first time an assay to determine MTAP activity in rat prostate based on the use of ^{14}C-labeled MTA [4]. Six years later, based on this assay, Della Ragione et al. purified and characterized MTAP in human placenta and analyzed

MTAP activity [2]. Cacciapuoti measured MTAP activity in different types of archaeons (thermophilic bacteria) under high thermal conditions (70-80°C) [39-41]. All these assays are radio isotope assays and based on measuring the formation of [methyl-^{14}C]-5-methylthioribose-1-phosphate from [methyl-^{14}C]-MTA. The use of stable isotope labeled substrate and the analysis of substrate degradation by LC-MS/MS has not been described yet.

2.5 Mass spectrometry for metabolic profiling

Metabolomics aims at the comprehensive quantitative analysis of all low-molecular weight metabolites in a biological system [42]. Two complementary strategies are used in the field of metabolomics: metabolic fingerprinting and metabolic profiling.

Metabolic fingerprinting is the comparison of metabolic patterns (the fingerprint of a sample), that change during disease, toxin exposure, environmental or genetic alterations. This method does not intend to identify and quantify single metabolites, but to visualize metabolic differences between samples [42].

The second approach, metabolic profiling, is the qualitative and quantitative determination of selected analytes for example in a metabolic pathway or compound class. Analysis of amino acids is an example for metabolic profiling. A more direct approach of metabolic profiling is target analysis, where selected metabolites are measured, such as substrates, intermediates and products of enzymatic reactions [43]. In most cases, as in this work, metabolic profiling is hypothesis-driven. Metabolites are selected and analytical methods for quantification are developed to test a given hypothesis. In the present work, the metabolic consequences of a lack of MTAP with regards to up- and downstream metabolites in the methionine and polyamine pathways are under investigation.

An often used strategy for metabolic profiling experiments is the separation of the metabolites by a chromatographic technique and the detection and quantification for example by mass spectrometry. The chromatographic separation tremendously expands the capability for the analysis of complex samples [44]. Different types of mass spectrometers have been developed over time and are well suited for metabolite detection in profiling analysis.

2.5.1 Single quadrupole mass spectrometer

A quadrupole mass analyzer (qMS) consists of four circular parallel rods. A direct current is placed on pairs of opposing rods and overlaid with a radiofrequency. Ions are separated based on the stability of their trajectories in the electric field applied to the rods. At a given voltage ratio only ions of a certain *m/z* can pass through the quadrupole, while all others move on unstable trajectories. By changing the voltage ratio ions are successively scanned.

A single quadrupole mass spectrometer contains only one quadrupole and can be operated in two different modes, the full scan and the selected ion monitoring (SIM) mode. In the full scan mode the instrument scans the complete selected mass range, in the SIM mode only single selected masses are analyzed. The use of the SIM mode results in the advantage of either a higher duty cycle or in a longer scan time per mass. The higher duty cycle delivers more points over chromatographic peak meanwhile a longer scan time per mass results in a higher signal and better limits of detection (LODs) and lower limits of quantification (LLOQs) of the analytes. Using a single-quadrupole mass spectrometer combined with a GC it is possible to achieve LODs and LLOQs in the nanomolar range [35].

2.5.2 Time-of-flight mass spectrometer

In a Time-of-flight mass spectrometer (TOFMS) ions are accelerated by an electric field of known strength. This results in an identical kinetic energy of the accelerated ions and the velocity of the ions depends on their mass-to-charge ratio. Ions are pushed during the acceleration in a filed-free drift tube, the time the ions need to travel a given distance until they reach the detector is measured and the *m/z* ratio is calculated. Ions are pushed periodically into the field free flight tube. The pusher frequency is determined by the time required until the slowest ion reaches the detector. The first TOFMS-instruments were designed linear, i.e. the ions beam in the source has the same direction as the acceleration and the drift region. The detector is positioned at the end of the drift region [45]. To compensate for the energy spread of the ions during the acceleration in newer instruments a reflector is installed in the drift tube. This reflector doubles the length of the field-free drift and focuses identical ions with an energy spread [46]. To minimize the effects of energy spread an orthogonal acceleration was developed. The ion beam leaving the source is accelerated orthogonally into the field-free drift region. This minimizes the energy spread of the ions as a result of ionization and transfer to the accelerator [47].

TOFMS has only one operation mode, the mass range scan. The selected scan range has no influence on peak intensity, since the instrument does not change the acceleration frequency of the ions. Smaller scan ranges reduce only the size of the acquired data file of the analysis. Coupled to liquid chromatography LODs and LLOQs in the lower nanomolar range can be achieved [48-50], while in combination with capillary electrophoresis LODs and LLOQs are in the lower micromolar range [51]. A big advantage of TOFMS over qMS is the high mass accuracy with an error in the range of 2-5 ppm, which allows the generation of a possible molecular formula of

the detected ion. This feature can be used in metabolic fingerprinting to identify unknown compounds [52].

2.5.3 Triple quadrupole mass spectrometer

A triple quadrupole mass spectrometer, one type of a tandem mass spectrometer, consists of two quadrupoles, with a non mass resolving quadrupole in between. The first (Q1) and the third quadrupole (Q3) function as a mass filter, whereas the second quadrupole (q2) is used as a collision cell to provide collision-induced fragmentation of precursor ions selected in Q1. The fragments pass Q3, where they are scanned or filtered. Consequently, the instrument can be described as a “double single quad”. The combination of two mass filters and fragmentation enables different operation modes, such as product ion scan (PI), precursor ion scan, neutral loss scan and multiple reaction monitoring (MRM).

The PI scan is used to get structural information about an analyte. One quasi-molecular ion is selected in Q1, fragmented in q2 and the fragments are scanned in Q3. A precursor ion scan has the same principle as a PI scan, but the Q1 is scanned and Q3 filters one fixed mass out of the formed fragments. Thus defined precursor ions, e.g. glycosylated peptides, can be determined in a complex mixture due to formation of specific fragments [53]. During a neutral loss scan ions are scanned in Q1, fragmented in q2, and fragment ions with a given offset are scanned in Q3. Consequently, Q1 and Q3 are working in a dependent scan mode, i.e. the masses of Q1 and Q3 are synchronized and the mass of Q3 is reduced by the mass of the neutral loss to be analyzed (e.g. -44 for CO_2 in organic acids).

The triple quadrupole mass spectrometer is highly suitable for selective and sensitive quantification [54] by selecting the quasi molecular ion in Q1 and filtering the most

abundant fragment in Q3 out instead of scanning all fragments. This mode of double mass filtering is called MRM and yields the best LODs and LLOQs in the lower nanomolar range [55], since interfering noise is filtered out twice.

2.5.4 Quadrupole time-of-flight mass spectrometer

A quadrupole-time-of-flight mass spectrometer (qTOFMS) is a hybrid tandem mass spectrometer. It is constructed like a triple quadrupole but the third quadrupole is exchanged by a time-of-flight mass analyzer. This instrument can either be used as a TOFMS, to determine molecular masses with high accuracy, or as a triple quadrupole mass spectrometer. All fragments of the precursor ion selected in Q1 will be acquired and their masses will be determined with high accuracy. As mentioned above in the TOFMS section, the detector is pulsed and it is not possible to increase peak intensity by lowering the scanned mass range. Hence, this instrument is not as sensitive as the triple quadrupole mass spectrometer However, it offers the advantages that structural information and exact masses of the quasi-molecular ion and the resulting fragment ions can be determined. This type of instrument is commonly used in the field of proteomics [56], but also in metabolic studies, e.g. the transformation of tetrazepam to diazepam in the human body [57]. Furthermore this type of mass spectrometer can be used like a TOFMS in the field of metabolic fingerprinting and identification of unknowns [58,59].

2.5.5 Triple quadrupole linear ion trap (QTrap)

A QTrap mass spectrometer is a triple quadrupole mass spectrometer, where the third quadrupole can be used as a linear ion trap. By placing on lens each before and after Q3 it is possible to trap and accumulate ions in Q3. The benefit is a higher

sensitivity in the scan mode compared to a pure triple quadrupole instrument. Also, MS^3 experiments can be performed by using the trap function and successive MS experiments, e.g. a product ion scan in the trap after a MRM event [60-62]. To work in accordance with the GLP-rules it is necessary to use two MRM transitions (quantifier and qualifier trace) for identification of a metabolite [63]. This doubles the duty cycle of the instrument. Using a QTrap instrument an information dependent acquisition (IDA) experiment can be performed, e.g. a product ion scan in the linear ion trap after the occurrence of a MRM signal [64]. To confirm the presence of the metabolite, which causes the MRM signal at the expected retention time, this fragmentation pattern can be used instead of the second MRM (qualifier) trace. Since such an IDA experiment is faster than two MRM scans, the duty cycle will decrease and additional information (product ions) will be obtained [65,66].

2.6 Stable isotope techniques

Correct quantification is a major issue in analytical chemistry requiring appropriate calibration of the used system. In case of concentration analysis this can be performed by an external or an internal calibration.

With an external calibration the concentration of the analyte is determined by a calibration curve, which is acquired using standards at different concentration levels. An advantage of this method is the high sample throughput, because no additional calibration work, e.g. adding internal standards, has to be performed on each sample. A correction for variability during sample preparation and analysis is not possible. The addition of a known amount of a standard compound which is not present in the sample (e.g. norleucine in amino acid analysis) is a first approach to account for this. It corrects to some extent for problems during sample preparation and analysis, but

not for all, because the used standard is only similar but not identical with the analytes of interest. In liquid chromatography-mass spectrometry ion suppression is an additional problem [67]. It occurs during ionization if the ionization energy is not high enough to ionize all analyte molecules. Since not all analytes have the same ionization efficiency, different percentages of each analyte will be ionized. This effect depends on coeluting matrix components and varies during the chromatographic run and therefore a correction for ion suppression is not possible with only one standard.

The best way to correct for ion suppression and other matrix effects is to add a known amount of a stable isotope labeled analog of the analyte of interest, e.g. ^{13}C, ^{15}N or ^{2}H labeled compounds. These stable isotope labeled standards have the advantage that they show identical chemical, nearly identical physical properties and they are not radioactive. In case of liquid chromatography coupled to mass spectrometry analyte and standard show the same behavior during sample preparation, injection into the system, chromatographic separation (using deuterated internal standards a partial separation from the unlabeled analyte is possible) and ionization in the mass spectrometer. A distinction between analyte and stable isotope labeled standard is done by the mass spectrometer, where analyte and standard show different masses. A corresponding stable isotope labeled standard corrects the best for problems during sample preparation and analysis and the quantification of the analyte is as exact as possible.

Quantification can be performed with the ratio analyte / stable isotope labeled standard only, so called isotope dilution analysis [68]. The amount of stable isotope labeled standard, which causes the signal, is known and the analyte concentration is calculated as the ratio of both signals. Alternatively, a calibration curve using a standard dilution spiked with a known amount of stable isotope labeled standard can be generated. The calibration curve with internal standard is a combination of isotope

dilution analysis and quantification with an external calibration. This method (used in the presented work) allows a precise determination of LOD and LLOQ as well as quantification of analytes in the samples. A correction for problems during sample preparation and analysis is possible.

3. Quantification of 5'-deoxy-5'-methylthioadenosine

3.1 Introduction

The aim of the study was to develop a method to quantify 5'-deoxy-5'-methylthioadenosine (MTA) in various biological samples. As its structural analogue adenosine MTA is accessible for a direct analysis by reversed phase liquid chromatography coupled to mass spectrometry without any steps of derivatization. Consequently, no complex sample preparation is necessary, but a simple protein precipitation with methanol is used, to avoid column blocking. To achieve a good linearity and low detection and quantification limits, a stable isotope labeled internal standard was used. A shortened version of this chapter was published in the Journal of Chromatography B [28]. Parts of the results are also shown in [12].

3.2 Experimental

3.2.1 Chemicals

All solvents for sample preparation and LC-MS were HPLC grade and purchased from Fisher-Scientific (Schwerte, Germany). MTA was obtained from Sigma Aldrich (Taufenkirchen, Germany) and labeled adenosine from Omicron Biochemicals (South Bend, IN, USA). The water used was purified by means of a PURELAB Plus system (ELGA LabWater, Celle, Germany). All chemicals for synthesizing labeled MTA (thionylchloride, pyrimidine, ammonia and sodium methanethiolate) were purchased from Fluka (Taufenkirchen, Germany).

3.2.2 Internal standard preparation

Stable isotope labeled [1',2',3',4',5'-$^{13}C_5$]-MTA was synthesized in house according to Robins et al. [69]. A scheme of the synthesis is shown in Figure 3.

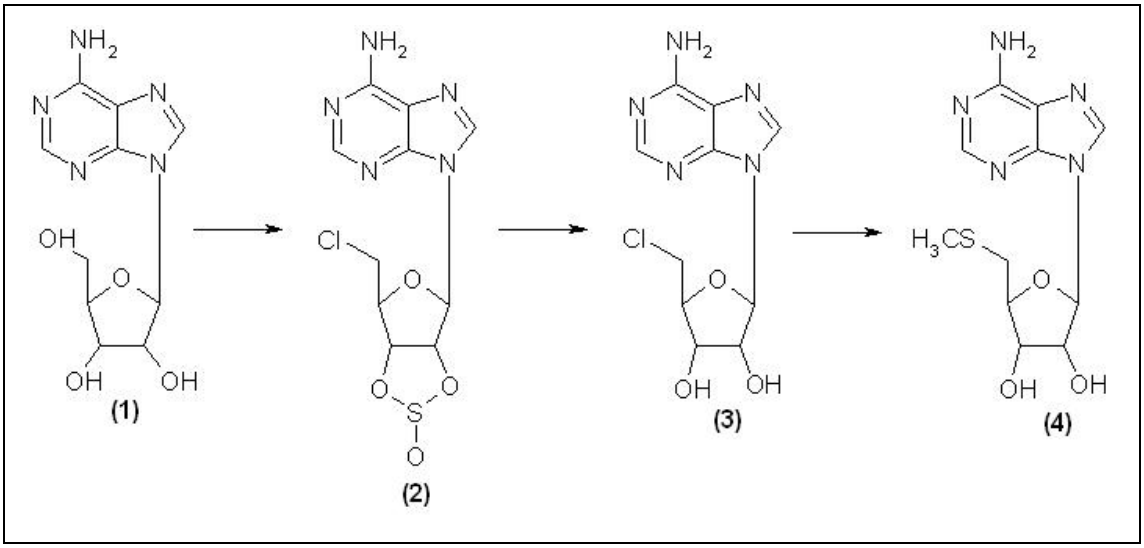

Figure 3: Scheme of the synthesis of methylthioadenosine as described by Robins et al. [69].

102 mg of $^{13}C_5$-labeled adenosine (1) were dissolved in a mixture of 0.1 mL pyridine and 1.5 mL acetonitrile. Cooled in an ice bath 0.15 mL thionylchloride were added drop wise and the reaction mixture was allowed to warm up over night. The solvents were removed by evaporation and the formation of white crystals (2) was observed (reaction step 1, method c). The crystals (2) were dissolved in a mixture of 2.5 mL methanol and 0.5 mL water. Afterwards 0.25 mL concentrated ammonia solution was added and the solution got a red color, presumably caused by rests of pyridine. The reaction mixture was stirred over 1 h at room temperature and the solvents were again evaporated. The reaction product (3) formed white crystals. The third step was made a little bit easier, due to the direct use of sodium methanethiolate instead of forming it in situ by the reaction of sodium hydrate and methanethiol. The product of step two (3) was dissolved in 3 mL dimethylformamide and 30 mg of sodium methanethiolate (dissolved in 2 mL dimethylformamide) were added dropwise to the stirred solution. During the reaction the reaction mixture was cooled at -30°C and

was allowed to warm up to ambient temperature after finishing the reaction. The mixture was stirred over night and the solvents were removed by evaporation. The residue was dissolved in 2.5 mL water, neutralized with HCl and cooled in the fridge. The crude product (4) was purified by recrystalization from MeOH/water (1:1, v/v, 10 mL). An overall yield of 29.7% (theoretical value 74.3%) was achieved and the stable isotope labeled MTA had an isotopic purity of 94%. A possible explanation of the lower yield could be the modification of the third step of the synthesis. This modification makes the synthesis easier, but could decrease the reaction efficiency. Furthermore the intermediate products were not purified during the synthesis and therefore side reactions are possible reason for the lower yield. The reason for the diminished isotopic purity was not found, the missing purification of the intermediate products in no reason therefore, because the unlabeled reagents alone can not form MTA.

A 2.24 mM stock solution of [1',2',3',4',5'-$^{13}C_5$]-MTA in water was prepared and further diluted with water to obtain a working solution of 224 nM, which was spiked into the samples and calibration standards. The final concentration of the internal standard in samples and standards was 22.4 nM.

A stock solution of unlabeled MTA was prepared in water and serially diluted over a concentration range of 1.0 mM to 12.5 pM. Spiking with internal standard was performed immediately before calibration. For calibration, 10 µL of internal standard were transferred into a 0.2-mL micro-insert (VWR, Darmstadt, Germany) in a 1.5-mL glass vial (Fisher-Scientific), dried by evaporation using an infrared vortex-vacuum evaporator (CombiDancer, Hettich AG, Bäch, Switzerland), and then reconstituted with 100 µL of the respective aqueous MTA standard.

3.2.3 Cell culture experiments and cell harvesting

The melanoma cell line Mel Im has been described in detail previously [70]. Further, two clones of Mel Im that either lack (Mock D) or express (Clone 5) *MTAP* were used [6]. Cells were grown at 37°C / 5% CO_2 in Dulbecco's modified Eagle medium (DMEM; PAN Biotech GmbH, Aidenbach, Germany) supplemented with penicillin (400 U/mL), streptomycin (50µg/mL), L-glutamine (300µg/mL) and 10% fetal calf serum (FCS; Sigma, Deisenhofen, Germany).

Melanoma cells, 200,000 each, were seeded in Falcon™ six-well-plates (Becton Dickinson GmbH, Heidelberg, Germany) and cultured in 2 mL DMEM as described above, for different periods of time. If not stated otherwise, cells were cultured for 24 h and were then harvested with trypsin (PAN Biotech GmbH). Cell culture medium samples were transferred in Eppendorf Cups and stored at -80°C until further preparation.

The adherently growing cells used in this study were harvested by incubation in 200 µL of either a solution containing 0.05% (w/v) trypsin and 0.02% (w/v) EDTA or 5 mM EDTA only. Trypsination was stopped after 5 min with 700 µL of cell culture medium. Following centrifugation at 100xg (5 min, room temperature), the supernatant was removed and the cell pellets were stored at -80°C until extraction. Alternatively, cells were scraped directly in pure methanol. To that end, 500 µL methanol spiked with 2.48 nmol/L stable isotope labeled MTA were added to the well after the cell culture medium had been removed and the cells were washed twice with 500 µL PBS buffer each. Cells were scraped, centrifuged (100xg, 5 min, room temperature) and the supernatant was collected. The cell pellet was washed twice with 200 µL methanol, centrifuged and all supernatants were combined. After drying and reconstitution in 100 µL of water the concentration of the internal standard should be 22.4 nM in case of 100% recovery.

The experimental work described in chapter 3.2.3 was performed by Susanne Wallner in the working group of Prof. Anja Bosserhoff at the Institute of Pathology, University of Regensburg.

3.2.4 Extraction of 5'-deoxy-5'methylthioadenosine from cell culture media

Methanol (600 µL) was added to 200 µL cell culture medium, followed by the addition of 10 µL internal standard (224 nM). The sample was vortexed and centrifuged at 9,000xg for 5 min at 4°C. The supernatant was transferred to a glass vial. The protein pellet was washed twice with 200 µL methanol and all supernatants were combined. The solvent was evaporated and the residues were reconstituted in 100 µL water.

A matrix spike and a standard addition experiment were carried out in cell culture media to check the efficiency of the extraction procedure and to evaluate ion suppression. To generate a representative matrix sample, 500-µL aliquots from 13 different cell culture media samples were combined. For the matrix spike experiment, aliquots of 200 µL of the matrix sample were spiked with MTA at three molar levels (resulting in final concentrations of 50 nM, 75 nM and 100 nM of MTA after reconstitution) and extracted as described above. For the standard addition, 200-µL aliquots of the matrix sample were extracted as described above. The obtained extract was then spiked with MTA at three levels (resulting in final concentrations of 50 nM, 75 nM and 100 nM after reconstitution). All samples were fortified with stable isotope labeled internal standard prior to extraction.

3.2.5 Extraction of 5'-deoxy-5'-methylthioadenosine from cell pellets

For the extraction of MTA from cell pellets, different solvent combinations (MeOH, MeOH/H_2O 50:50 v/v, acetonitrile, and acetonitrile/H_2O 50:50 v/v) were tested. Briefly, 600 µL of the different solvents were added to the frozen pellets and internal standard was spiked as described above. Then, the sample was slowly thawed on ice. To complete the cell lysis the cells were again shock-frozen in liquid nitrogen and thawed on ice. The freeze/thaw cycle was performed three times and the sample was vortexed in between each cycle. The sample was centrifuged at 9,000xg for 5 min at 4°C and the supernatant was transferred to a 1.5-mL glass vial. The pellet was washed twice with 200 µL of methanol and all supernatants were combined. The extract was further treated as described above.

For cell pellets, a standard addition experiment was carried out to evaluate ion suppression. The cell pellets were prepared as described above and a representative set of cell extracts was pooled. The experiment was carried out with cells removed by trypsin and EDTA, respectively. Ten µL of MTA standard solution with concentrations of 2.5, 5.0 and 7.5 µM were dried and then reconstituted with 100 µL of the pooled cell extracts. All concentrations were prepared in triplicate.

3.2.6 Lysis of malignant melanoma tissue samples

In a first approach we were interested, if the hypothesized accumulation of MTA can be observed in melanoma tumors. For that purpose biopsies (approx. 10-20 mg, tumor n=5 and healthy skin n=3) were weighted and then lysed in 50 µL of water by freezing in liquid nitrogen and thawing on ice. This freeze-thaw-cycle was performed three times and the lysates were treated afterwards as described above for the cell media pretreatment.

The experimental work described in chapter 3.2.6 was performed by Susanne Wallner in the working group of Prof. Anja Bosserhoff at the Institute of Pathology, University of Regensburg.

3.2.7 Analysis of 5'-deoxy-5'-methylthioadenosine in cell culture supernatants of different tumor cell lines and primary cells

Measurements of MTA were performed in the supernatants of different primary cell and tumor cell line cultures. Cell lines studied and their respective origins are listed in Table 2. Either 1.0 or 2.5 million cells were cultivated in six well plates (Corning, Amsterdam, The Netherlands) over 24 h at 37°C / 5% CO_2. The volume of the cell culture medium was adjusted to the cell count, i.e. 1.0 million cells were cultivated in 1.6 mL and 2.5 million cells in 4.0 mL. After 24 h cell culture medium was taken and stored at -80°C until further preparation.

Table 2: Cell type and name of the different cell lines and primary cells used for measurement of MTA in cell culture media.

Cell type	Cell line
Bladder carcinoma	J82, RT4
Brain tumor initiating cells	RAV 21, RAV 26
Colon adenocarcinoma	SW480, SW620
Breast carcinoma	MDA-MB-231, SKB R3, T47D
Glioblastoma	U87
Leukemia	Jurkat, THP-1
Melanoma	B16.SIY.E12 (mouse), Mel Im, Na8
Primary cells	CD8, Monocytes
Renal cell carcinoma	RCL1503, RH-556, RJ494

The experimental work described in chapter 3.2.7 was performed by Gabriele Hartmannsgruber in the working group of Dr. Eva Gottfried / Prof. Marina Kreutz at the Institute of Hematology and Oncology, University of Regensburg.

3.2.8 Instrumentation

Liquid chromatography-electrospray ionization tandem mass spectrometry (LC-ESI-MS/MS) was performed using an Agilent 1200 SL HPLC system (Böblingen, Germany) and a PE Sciex API 4000 QTrap mass spectrometer (Applied Biosystems, Darmstadt, Germany), which was equipped with a turbo ion spray source (completely controlled by Analyst version 1.4.2). The column oven was kept at 25°C. An Atlantis T3 3µm (1.0 i.d. x 150 mm) reversed phase column (Waters, Eschborn, Germany) was used. LC separation was carried out using a mobile phase consisting of 0.1% acetic acid in water (Solvent A) and 0.1% acetic acid in acetonitrile (Solvent B). The gradient employed was as follows: 0-10 min linear increase from 0% to 100% solvent B, hold at 100% solvent B for 5 min. The flow-rate was set to 125 µL/min. Sample volumes of 10 µL were injected.

The API 4000 QTrap mass spectrometer was operated in positive mode using turbo ion spray with the following parameters: gas 1 as 50, gas 2 as 30 and the curtain gas as 10 (all arbitrary units). The turbo ion spray source was heated to 250°C. The declustering potential was set to 60.0 V and the entrance potential to 10.0 V.

Quantitative determination was performed in the multiple reaction monitoring (MRM) mode using the following ion transitions: *m/z* 298.2 $(M+H)^+$ to *m/z* 136.1 (product ion) for MTA and *m/z* 303.2 $(M+H)^+$ to *m/z* 136.1 (product ion) for the internal standard ($^{13}C_5$-labeled MTA). Collision-induced dissociation was performed with nitrogen as collision gas. The collision energy and the collision exit potential were set at 23 eV and 9 V, respectively. The electron multiplier was set to 2100 V. All MS parameters were optimized by direct infusion and the source parameters by flow injection. Data analysis was performed using Analyst version 1.4.2.

3.2.9 Data analysis

Standard calibration curves were plotted as the chromatographic peak area ratio (MTA / IS) versus the corresponding nominal concentration ratio (MTA / IS). A $1/x^2$ weighted regression analysis was used to determine the slope, intercept and coefficient of determination (r^2). A two-tailed, unpaired, homoscedastic t-test was used to determine whether the means of the intra- and extracellular amounts of MTA measured in Mel Im clones either lacking or expressing MTAP were significantly different ($p < 0.05$). The same test was used to check whether the change of MTA concentration in FCS supplemented cell culture medium was significantly different.

3.3 Results and Discussion

3.3.1 Method validation

Figure 4 shows a product ion spectrum of MTA after ionization in positive mode. At *m/z* 298.2, the quasi molecular ion of MTA occurs and the main product ion is the protonated adenine at *m/z* 136.0, which was used to set up the MRM transition for quantitative analysis. The fragment at *m/z* 163.0 is the complementary fragment of the main product ion, the sugar group which is lost by forming the protonated adenine.

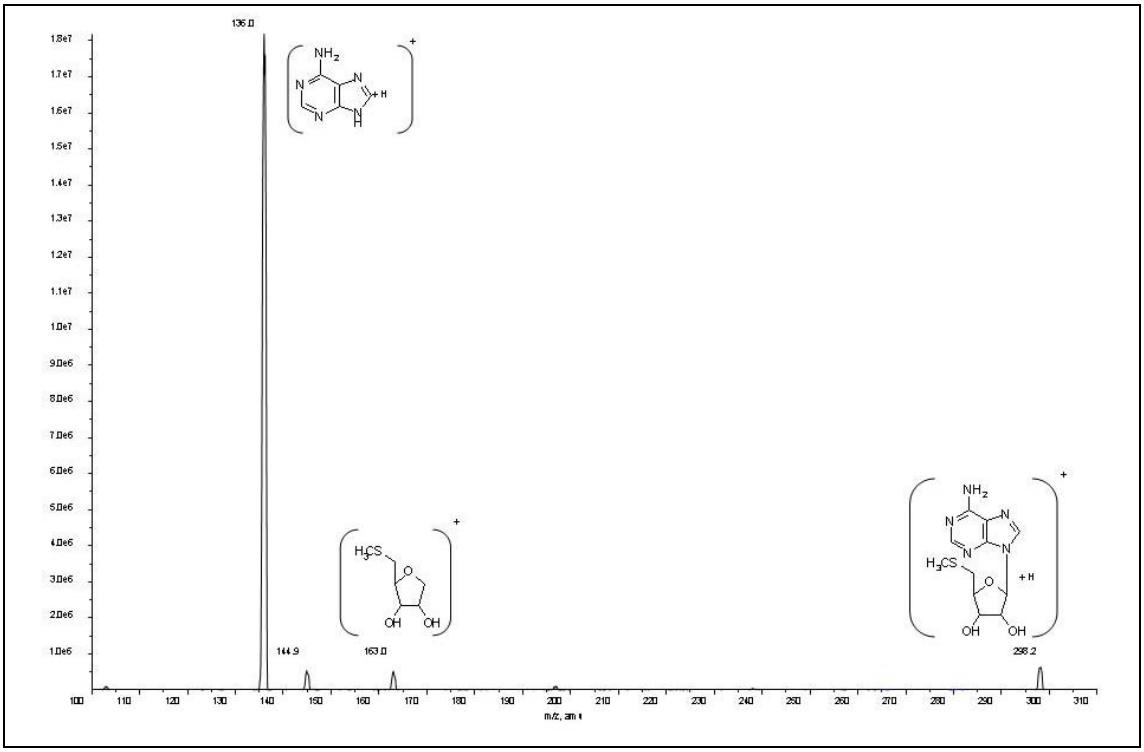

Figure 4: Product ion spectrum of MTA.

Representative MRM-chromatograms of an MTA standard, a cell culture medium sample and a cell pellet sample are shown in Figure 5. As can be seen, MTA elutes as a symmetric peak without any interferences even in the sample extracts.

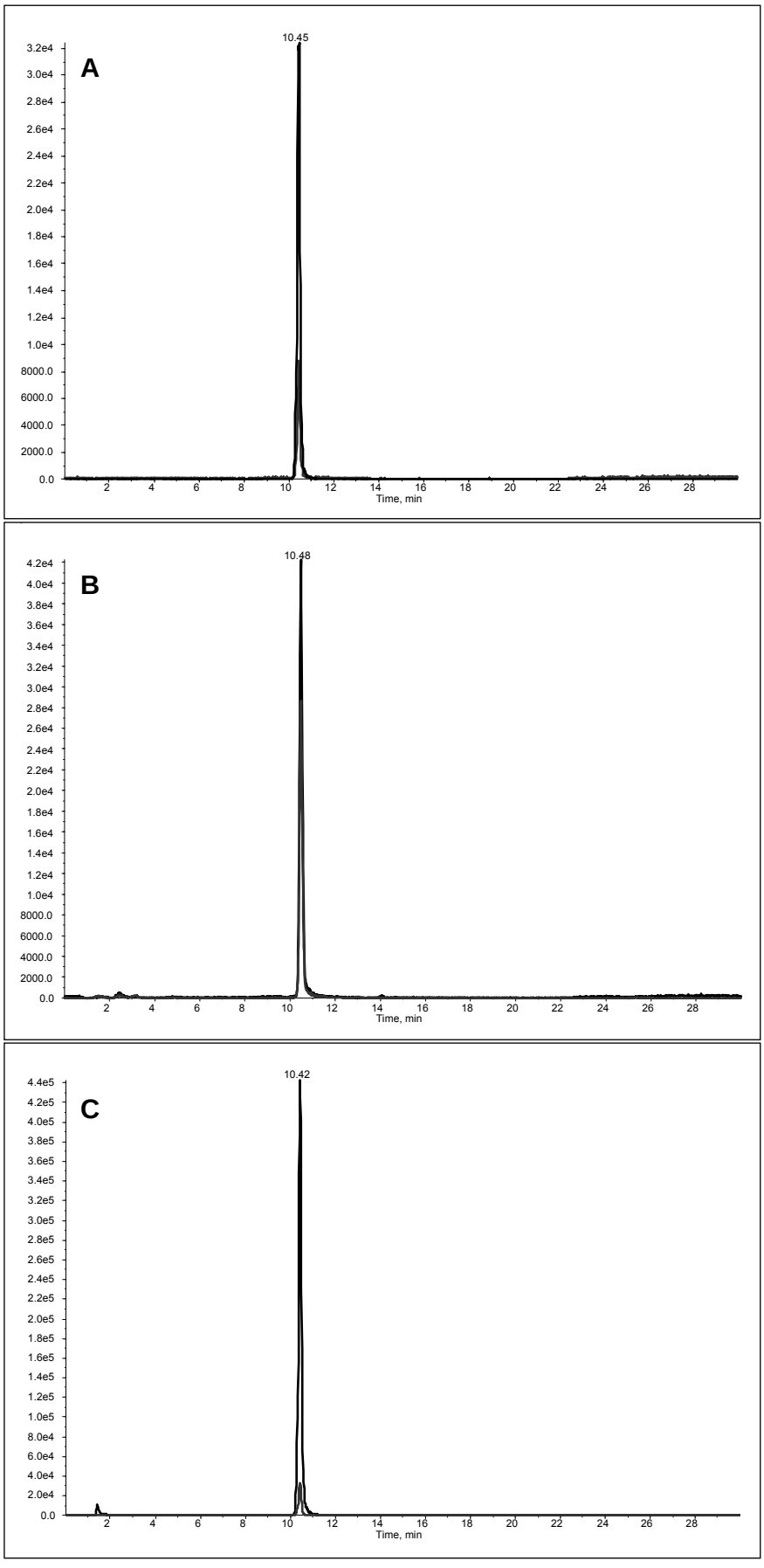

Figure 5: MRM-chromatograms of co-eluting unlabeled and stable-isotope labeled MTA (minor peak). (A) MTA standards, and methanol extracts of (B) cell culture medium and (C) Mel Im cell pellet.

A calibration was carried out using standards in the range of 12.5 pM to 1 mM. During analysis, it was observed that the internal standard contained small amounts of unlabeled MTA. Therefore, a calibration without internal standard was performed to determine the instrumental detection limit. This resulted in a limit of detection (LOD) of 62.5 pM at a signal to noise ratio (*S/N*) of 3. The lower limit of quantification (LLOQ) was defined as five times the background MTA level. Due to the contamination of the internal standard with unlabeled MTA the LLOQ was 2 nM and could be determined with an accuracy of 100.15% and an imprecision of 2.96%. This concords well with the FDA guidelines for bioanalytical method validation that require an analyte response at the LLOQ of at least 5 times the response compared to a blank and an accuracy and imprecision of 80-120% and <20%, respectively [71]. The calibration curve was linear from the LLOQ to 1 µM (intercept: 0.0212; slope: 0.949; r^2: 0.999). The relative standard deviation (RSD) of triplicate injections was 1.77%.

A matrix spike and a standard addition experiment of MTA in cell culture medium samples were carried out using three spike levels. Each experiment was performed in triplicate. Figure 6 shows the results in comparison to the calibration curve over this concentration range.

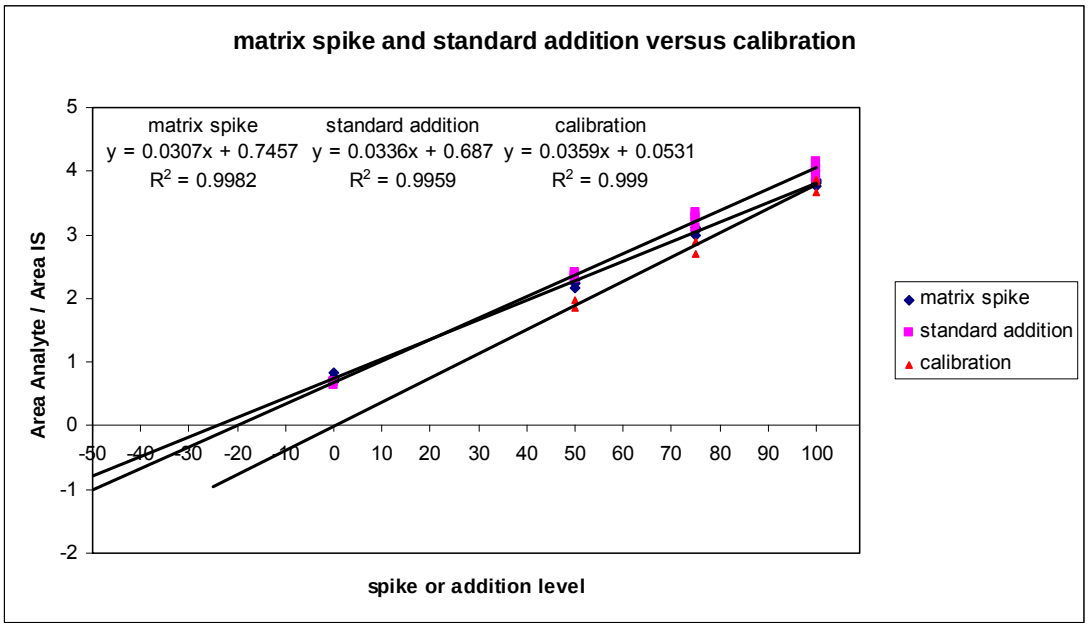

Figure 6: Matrix spike and standard addition experiment for cell media versus calibration curve with internal standard correction.

RSD values for triplicate samples in the matrix spike and standard addition ranged from 1.3 – 7.0% and 1.6 – 5.9%, respectively. It can be seen that the internal standard corrects very well for potential ion suppression or incomplete extraction because the slope of the three curves is similar. To further evaluate the extraction efficiency, the absolute areas of the MTA without internal standard correction were plotted versus the concentration (Figure 7).

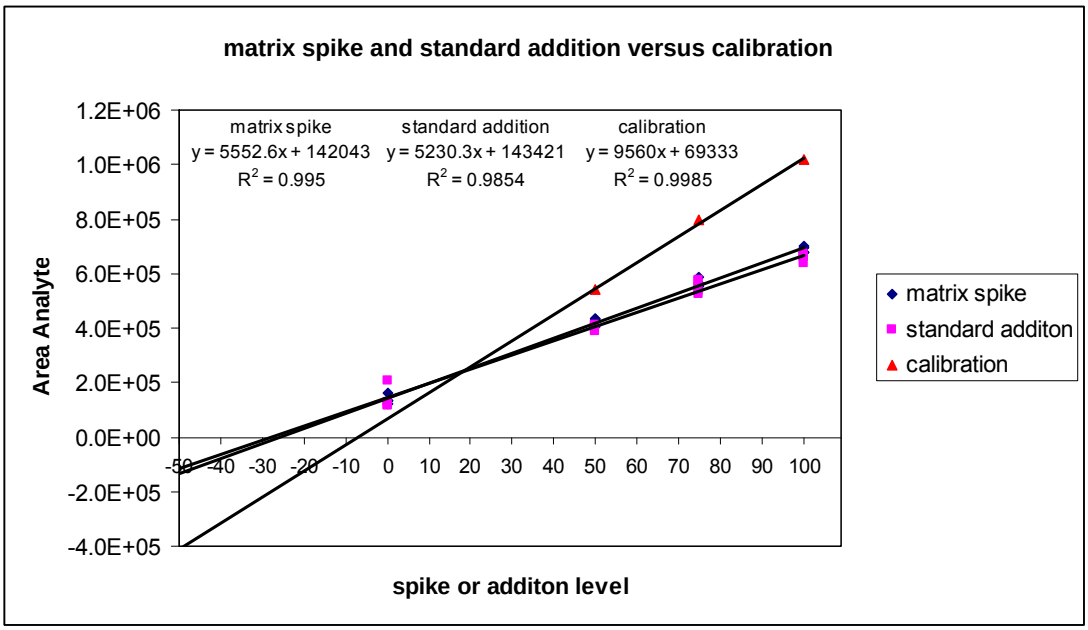

Figure 7: Matrix spike and standard addition experiment for cell media versus calibration curve without internal standard correction.

Interestingly, the RSD values were still in the range of 0.9 – 3.9% and 1.9 – 5.2% for the matrix spike and standard addition, respectively. Figure 7 shows a nearly identical slope for the matrix spike and the standard addition experiment. This demonstrates complete extraction of MTA from the sample. Using the values of the standard addition experiment as reference, recovery rates were calculated for the matrix spike samples, which ranged from 94.6 –112.4%. However, the slope of matrix spike and standard addition experiments is only 60% of the slope of the calibration curve, indicating substantial ion suppression. This observation is identical to the recovery of the internal standard from cell culture media, namely about 60%. However, as demonstrated above, the internal standard corrects for the ion suppression.

In addition to MTA excretion into the cell culture media, the intracellular levels were determined. For cell pellet extraction (pellets of 1,000,000 cells), different solvent combinations (MeOH, MeOH/H_2O 50:50 v/v, acetonitrile and acetonitrile/H_2O 50:50 v/v) were tested. Each experiment was performed in triplicate. The highest amount of

extracted MTA and the best recovery of the internal standard were achieved with pure methanol (see Figure 8 A and B).

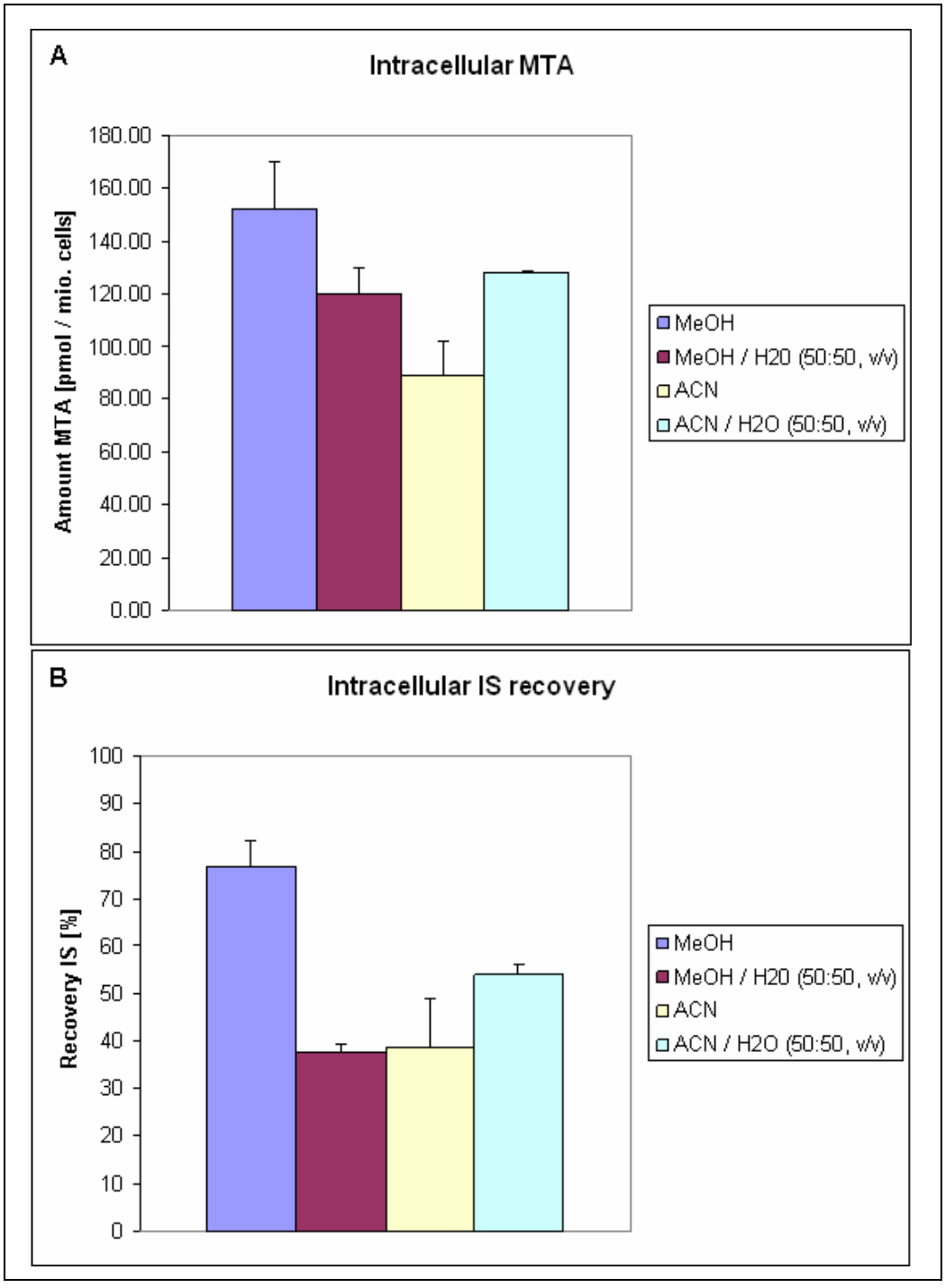

Figure 8: Detected absolute amount of MTA (A) and recovery of internal standard (B) in pellets of 1,000,000 cells each using different extraction protocols.

Metabolite leakage from adherently growing cells during harvesting can present a serious problem, if intracellular metabolite concentrations need to be determined. The conventional method to release cells is trypsination. In addition, we tested a

reportedly less aggressive method, namely a 5-mM EDTA solution. We also tested cell harvesting by scraping the cells directly in methanol spiked with IS. This procedure combines cell harvesting with cell extraction and should minimize metabolite losses caused by leakage. Each experiment was performed in triplicate. We observed very similar amounts of extracted MTA using EDTA or trypsination (Figure 9).

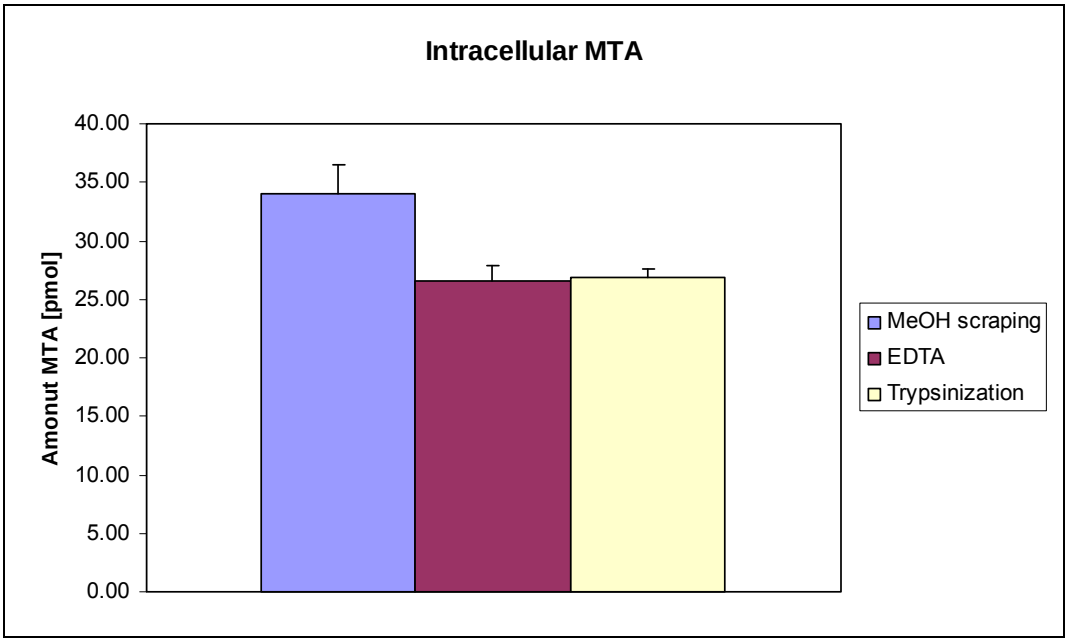

Figure 9: Arithmetic means and standard deviations of intracellular amount of MTA for three different cell harvesting procedures after incubation of 200,000 seeded Mel Im cells for 24 h.

With the methanol scraping protocol, the amount of extracted MTA was about 40% higher than for the other two methods (Figure 9). Hence, cell leakage must be similar for EDTA and trypsination. However, direct scraping does not allow the determination of cell count, a parameter often used for normalization in cell culture experiments. Overall, trypsination allowed the extraction of MTA and recovery of internal standard with the lowest imprecision, namely 2.82% and 2.33%, respectively. The respective values for EDTA were 5.32% and 4.52%, while those for scraping in pure methanol were 7.41% and 15.28%.

For cell pellets a standard addition experiment was carried out using three spike levels (n=3). Figure 10 shows the results of the standard addition experiment (A) and the corresponding recovery of the internal standard (B).

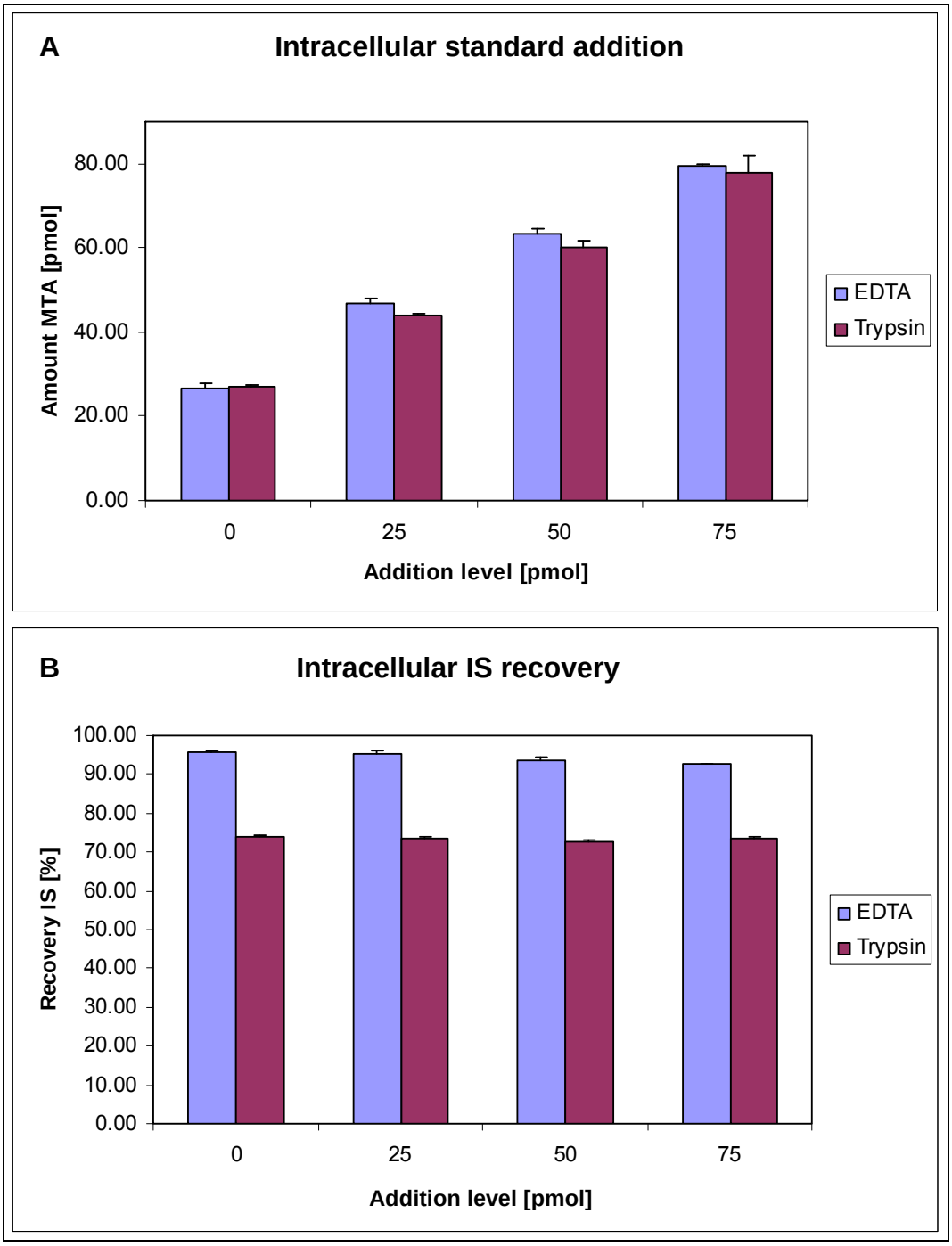

Figure 10: Arithmetic means and standard deviations of intracellular amount of MTA (A) and internal standard recovery (B) in standard addition experiments employing pellets of 200,000 Mel Im cells each.

Spike recoveries ranged from 70.44 to 81.87% and from 66.13% to 68.65% for EDTA and trypsination, respectively. Interestingly, the recovery of the internal standard was

between 95 – 97% for cells removed with EDTA, but only 75% for trypsinated cells. No significant difference in extracted MTA amount could be observed. The RSDs of the absolute MTA peak areas ranged from 0.6 – 3.7% and 0.2 – 0.9% for cells treated with EDTA and trypsin/EDTA, respectively.

Based on these results, trypsination was used in all subsequent experiments for cell detachment and the extraction of MTA from cell pellets was performed using pure methanol.

During sample analysis, quality controls (QC's) were measured after every 10 – 15 biological samples. The QC was 25 nM of MTA spiked with stable isotope labeled MTA. The calibration check samples yielded accuracy values of approximately 96%, and the recovery of the internal standard was about 97% in all QC's. The measured blanks (pure water) did not show MTA or internal standard.

3.3.2 Methylthioadenosine phosphorylase activity in fetal calf serum and stability of 5'-deoxy-5'-methylthioadenosine

In 1984, Riscoe et al. [72] observed MTAP activity in both native and heat-inactivated human and fetal calf serum (FCS). To investigate potential degradation of MTA during cell culture experiments, cell culture media with and without FCS were spiked with an MTA standard (with a final concentration of 300 nM) and incubated for 24 h at 37°C, to check for MTAP activity in FCS. To determine a potentially time-dependent decrease in the MTA concentration, samples were taken in triplicate at 0, 8 and 24 h. Figure 11 shows the concentration of MTA in both experiments.

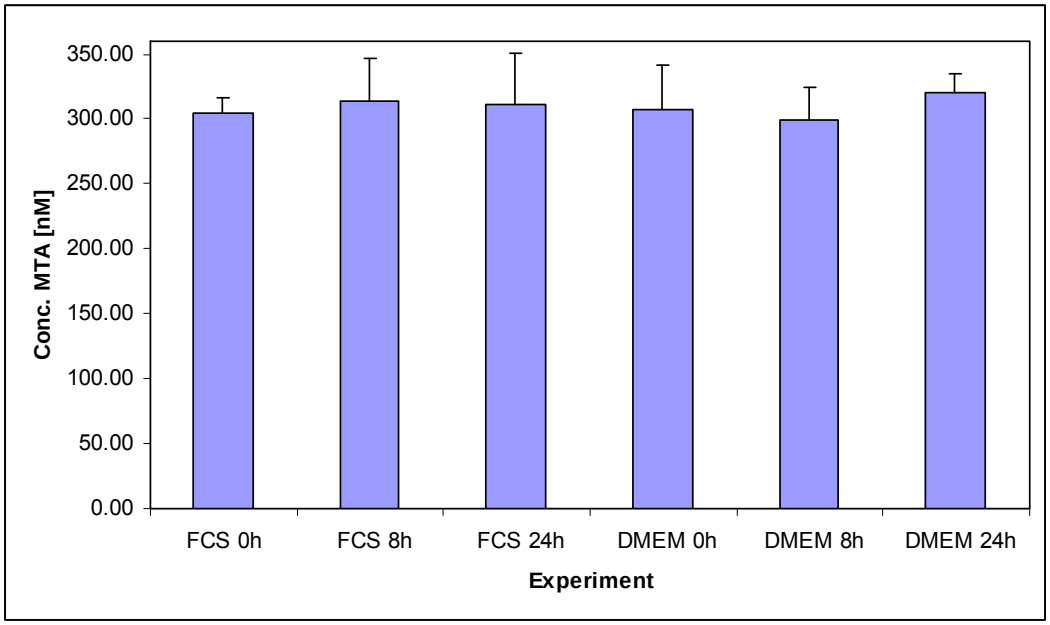

Figure 11: Stability of MTA in cell culture medium (DMEM) with and without FCS over 24 h at 37°C. Arithmetic means and standard deviations of MTA are shown at 0h, 8h and 24h (DMEM – DMEM without FCS; FCS – DMEM with FCS).

No significant change ($p=0.96$) in the MTA concentration was observed in the presence or absence of FCS, thus demonstrating that there is no significant MTAP activity in FCS, and that MTA is stable over 24 h at 37°C.

3.3.3 5’-Deoxy-5’-methylthioadenosine and melanoma cell lines

To measure the extracellular accumulation of MTA, 200,000 cells each of the parental Mel Im cell line were seeded in triplicate and cultured in 2 mL DMEM for 0, 2, 4, 6, 8, 16, 24, 30, 48, 72 and 96 h, before MTA was extracted from the cell medium and analyzed by LC-MS/MS. Extracellular concentrations of MTA reached a steady-state concentration of approx. 20 nM in the first 24 h of incubation (Figure 12).

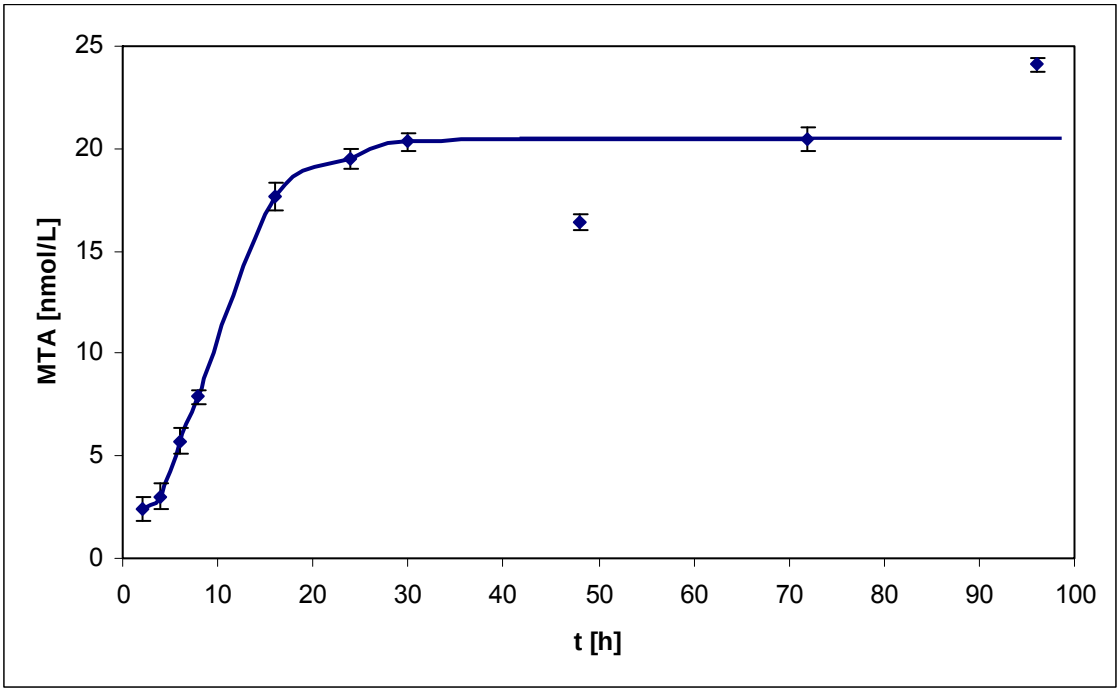

Figure 12: Accumulation of extracellular MTA in cell culture medium over time by culturing 200,000 cells in 2 mL DMEM for different time spans.

As a first test of the hypothesis that cells lacking MTAP do not metabolize MTA, two Mel Im cell clones that either lack (Mock D) or show expression of MTAP (Clone 5) [6] were analyzed. The clones showed a slight, albeit significant (p=0.0086), difference in extracellular MTA concentrations measured in quadruplicate after 24 h of incubation. The respective values for Mock D and Clone 5 were 11.6±0.2 nM and 12.7±0.4 nM. Intracellular amounts of MTA, in comparison, differed significantly (p=0.0012) by a factor of 4 (Figure 13). These values correlated inversely with MTAP expression.

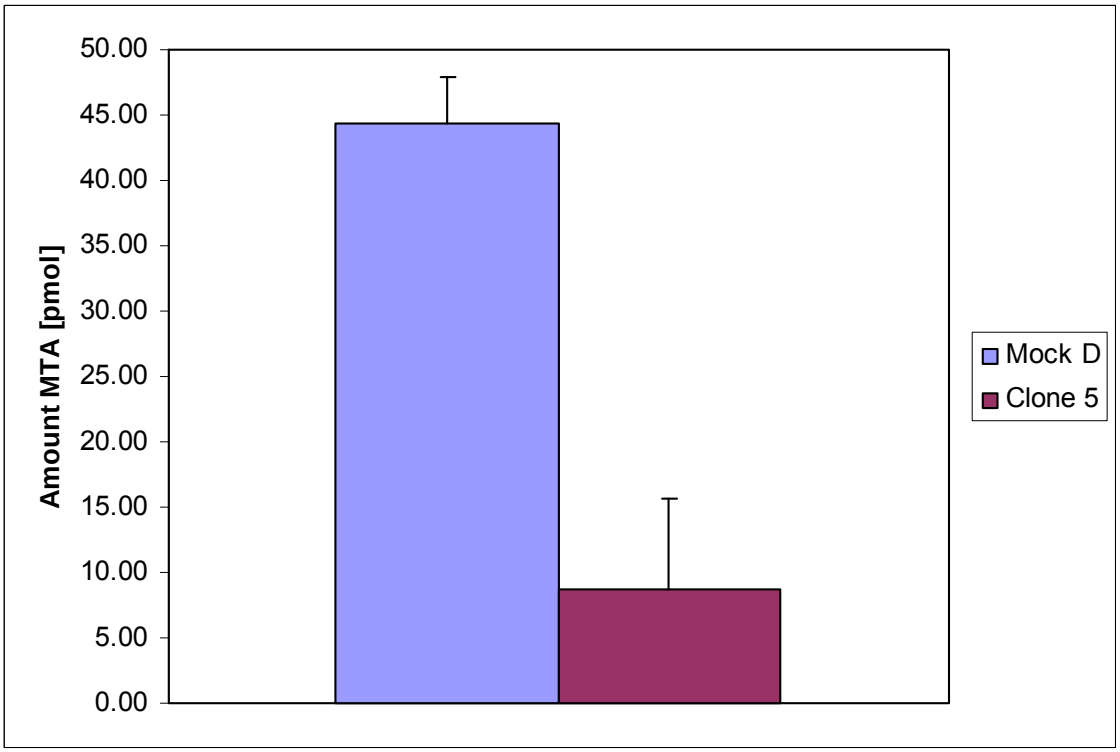

Figure 13: Absolute amount of intracellular MTA in 200,000 cells of two different Mel Im clones, which either lack (Mock D) or show expression of MTAP (Clone 5).

3.3.4 5'-Deoxy-5'-methylthioadenosine in malignant melanoma tumors

MTA was also analyzed in biopsies of malignant melanoma (n=5) and normal skin (n=3). Compared to the normal skin, MTA accumulated significantly (p=0.0016) in the malignant melanoma by a factor of 100 (Figure 14) due to the assumed lack of MTAP.

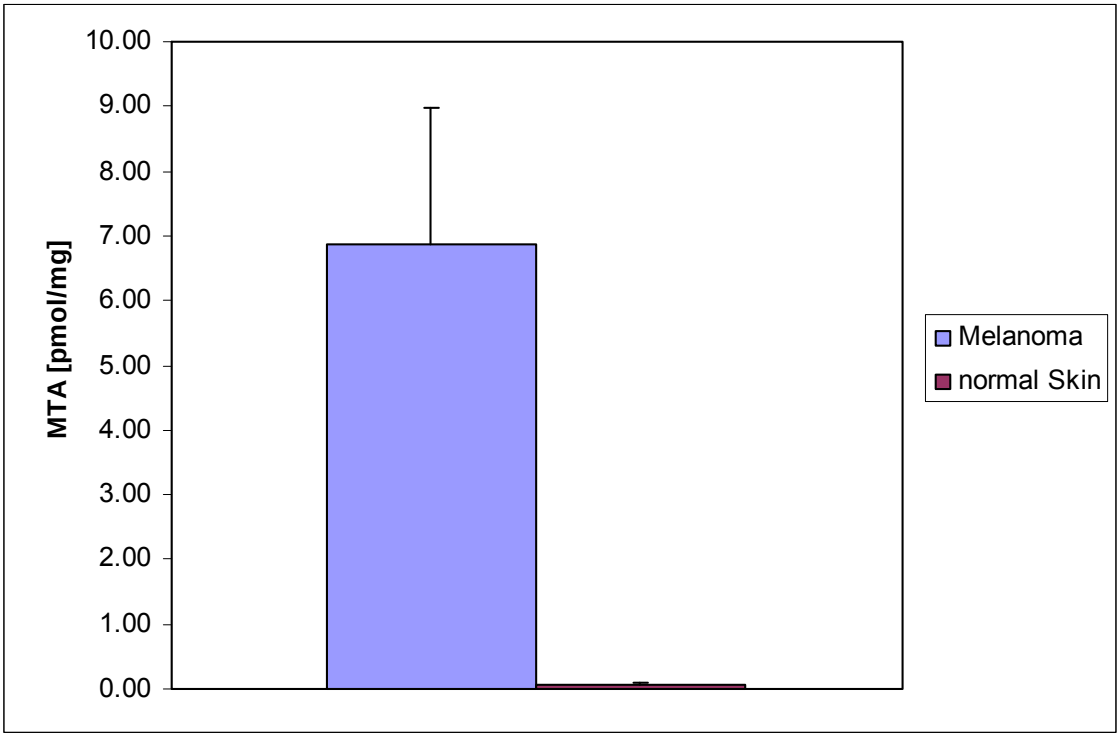

Figure 14: MTA concentration in biopsies of malignant melanoma (n=5) and normal skin (n=3) corrected for weight of the biopsy samples.

The mean concentration (±S.D.) of MTA in malignant melanoma was 6.869±2.095 pmol/mg tissue whereas that in normal skin was 0.064±0.018 pmol/mg. Biological variation explains the observed relative standard deviation of approximately 30%.

3.3.5 5'-Deoxy-5'-methylthioadenosine in the supernatant of different primary cells and tumor cell lines

Next, the concentration of MTA in cell culture media specimens of different tumor cell lines was determined. Figure 15 shows the concentrations of MTA in the cell culture media investigated after incubation for 24 h.

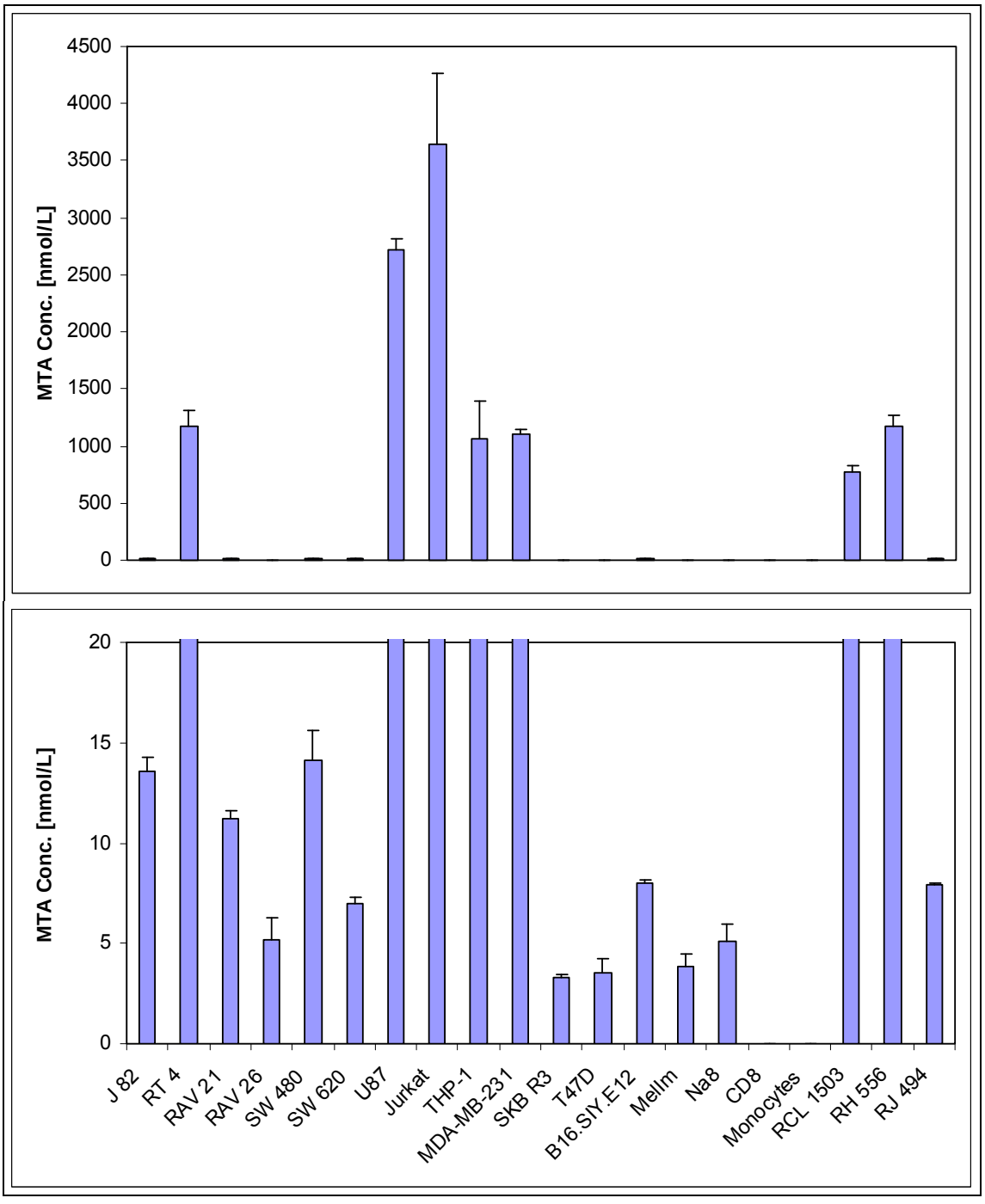

Figure 15: Concentration of MTA in cell culture media of different primary cells and tumor cell lines after incubation over 24 h (Lower graphic is a zoom-in of the upper graphic).

For most of the cell lines the MTA concentration in the medium after 24 h ranged between 3 and 15 nM. Interestingly, some cell lines excreted large amounts of MTA into the cell culture medium, including the glioblastoma cell line U87, the human T-cell leukemia cell line Jurkat, the human acute monocytic leukemia cell line THP-1, one bladder (RT4) and two out of the three investigated renal carcinoma cell lines. This results showed, that secretion of MTA into the cell culture medium was cell line specific and not cell type specific and it supports the hypothesis, that the excretion of MTA is somehow a controlled process and not driven by a concentration gradient. This hypothesis is supported by Hoffman et al. who demonstrated an unidirectional transport mechanism of SAH, the thioether metabolite of SAM [73] and furthermore by the corresponding intracellular MTA concentrations (Figure 16).

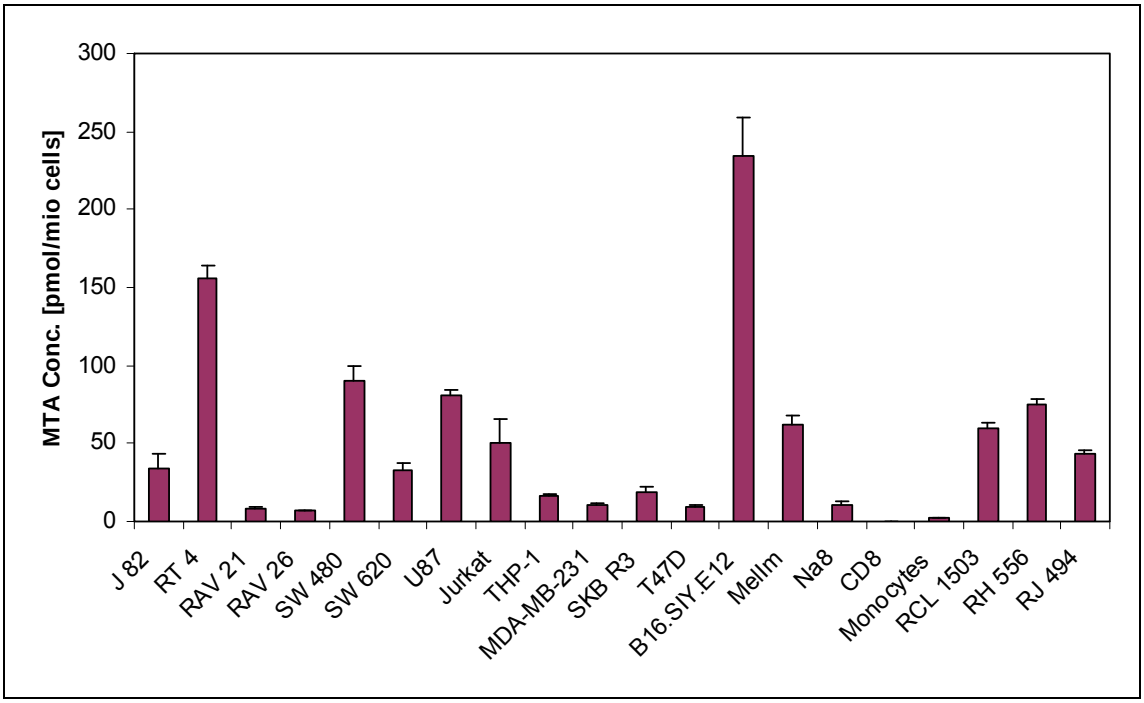

Figure 16: Intracellular concentration of MTA in cell pellets of different tumor cell lines after incubation over 24 h.

It is clearly visible, that the difference in the intracellular concentration is not as big as observed for the concentration in the cell culture medium. The three melanoma cell lines had a big difference in intracellular MTA concentration (234 vs. 61 vs. 10 pmol/mio cells) but showed all nearly the same MTA concentration in cell culture

medium of approximately 5 nM. The other way round was observed for the renal carcinoma cell lines, they showed nearly identical intracellular MTA concentrations of 60 nmol/mio cells but large difference in the MTA concentration in the cell culture medium (770 vs. 1170 vs. 8 nM). For the renal carcinoma cell lines Dr. Katrin Singer could show in her dissertation an inverse correlation of MTAP expression and MTA secretion to the cell culture media [74], i.e. the cell lines RCL 1503 and RH 556 have nearly no MTAP expression and therefore they excreted high amounts of MTA while the cell line RJ 494 show a slight MTAP expression and excreted nearly no MTA to the cell culture medium. These findings support the hypothesis that MTAP lacking cells accumulate and/or excrete MTA instead of metabolizing it [9].

Finally, CD8 T cells (not activated) and monocytes show no MTA secretion and only the monocytes had a very low intracellular MTA concentration. Both are primary cells and such cells are nearly not able to proliferate. In cell culture these cells can only be cultivated up to a few days [75]. Since polyamines and therefore also MTA were formed during cell proliferation, MTA is nearly not produced in this two primary cells and therefore consequently also not excreted to the cell culture medium.

3.4 Conclusions

An LC-ESI-MS/MS method was developed for the quantitative determination of MTA in cell culture media and cell pellets. The method was sensitive, precise and accurate in the concentration range of 2 nM – 1 µM. The LOD was determined at 62.5 pM. The method is reproducible with an RSD of triplicate injections of 1 – 7% in cell media and 0.2 – 3.7% in cell extracts, while biological reproducibility ranges from 2.1 – 32.6% in cell culture media and 3.5 – 31.4% in cell extracts. All quality controls showed an accuracy of 95 – 97% with an internal standard recovery of 97%.

An *in vivo* and *in vitro* accumulation of MTA in MTAP lacking samples could be demonstrated by cell culture experiments and analysis of real tumor samples.

The method developed will prove essential in the elucidation of utility of MTA as a diagnostic and/or prognostic tumor marker.

4. Quantitative analysis of the methionine and polyamine pathways

4.1 Introduction

To elucidate changes in the concentrations of intermediates of the methionine and polyamine pathways caused by a loss of MTAP activity, the method described in chapter 3 was expanded to all key metabolites of these pathways and liquid chromatography coupled to tandem mass spectrometry was chosen again as the analytical tool. Both extraction and separation had to be optimized. Stable isotope-labeled standards were used to correct for extraction, separation and ionization problems. A shortened version of this chapter was published in the Journal of Chromatography A [55] and parts of the results were also shown in [76].

4.2 Experimental

4.2.1 Chemicals

Solvents for sample preparation and LC-MS analysis were HPLC grade and purchased from Fisher-Scientific (Schwerte, Germany) and Merck (Darmstadt, Germany). Heptafluorobutyric acid (HFBA), adenine, homocysteine, methionine, putrescine, and spermidine were from Fluka (Taufenkirchen, Germany), while adenosine, 5'-deoxy-5'-(methylthio)adenosine, ornithine, *S*-adenosyl-L-homocysteine, *S*-adenosyl-methionine, spermine, acetylputrescine, N^8-acetylspermidine, acetylspermine, Tris(2-carboxyethyl) phosphine hydrochloride (TCEP), U-$^{13}C_4$-putrescine, and butane-d_8-spermine were from Sigma Aldrich (Taufenkirchen, Germany). N^1-acetylspermidine was from Wako Chemicals (Neuss, Germany), U-

$^{13}C_5$-adenine from Hartmann-Analytic (Braunschweig, Germany), [1',2',3',4',5'-$^{13}C_5$]-adenosine from Omicron Biochemicals (South Bend, IN, USA), d_7-ornithine from Cambridge Isotope Laboratories (Andover, MA, USA), and d_3-*S*-adenosylmethionine and 3,3,3',3′,4,4,4′4′-d_8-homocystine from CDN-Isotopes (Pointe-Claire, Quebec, Canada). [1',2',3',4',5'-$^{13}C_5$]-MTA was prepared in house according to Robins et al. [69] (see chapter 3.2.2), while U-$^{15}N_3$-spermidine was provided by Keijiro Samejima, Research Institute of Pharmaceutical Sciences, Musashino University, Tokyo, Japan, who had synthesized it according to Hara et al. [77]. The water used was purified by means of a PURELAB Plus system (ELGA LabWater, Celle, Germany).

4.2.2 Internal standard preparation and stock solutions

A stock solution of each stable-isotope labeled standard was prepared in aqueous 0.1 M acetic acid. The stable-isotope labeled standards were combined in a working solution containing 1 µM [1',2',3',4',5'-$^{13}C_5$]-MTA, 1µM [1',2',3',4',5'-$^{13}C_5$]-adenosine, 5 µM d_7-ornithine, 5 µM d_3-SAM, 5µM U-$^{13}C_5$-adenine, 10µM $^{15}N_3$-spermidine, 10 µM U-$^{13}C_4$-putrescine and 10 µM d_8-spermine, respectively. The final concentrations of the internal standards spiked into samples and calibration standards were 100 nM, 500 nM, and 1 µM, respectively. The addition of acetic acid had been reported to diminish the decomposition of SAM [78].

A standard solution of stable-isotope labeled homocysteine was obtained by reducing 32.1 mg of d_8-homocystine in 10 mL of a solution of 121 mg/mL TCEP in water. The resulting d_4-homocysteine concentration was 23.26 mM and the solution was diluted with 0.1 M acetic acid to a working concentration of 10 µM. The final concentration of d_4-homocysteine spiked into samples and standards was 1 µM.

Stock solutions of unlabeled standards were prepared in aqueous 0.1 M acetic acid and serially diluted over a concentration range of 500 µM to 0.5 nM. Spiking with internal standard was performed immediately before calibration. For calibration, 10 µL of each internal standard solution were transferred into a 0.2-mL micro-insert (VWR, Darmstadt, Germany) in a 1.5-mL glass vial (Fisher-Scientific), dried by evaporation using an infrared vortex-vacuum evaporator (CombiDancer, Hettich AG, Bäch, Switzerland), and then reconstituted with 100 µL of the respective aqueous standard. To avoid detector saturation, injection volumes of solutions containing between 7.5 µM and less than 75 µM of each standard were reduced from 10 to 2 µL, and halved again for standard solutions of ≥ 75 µM.

4.2.3 Cell culture and cell harvesting

The human hepatocellular carcinoma (HCC) cell line PLC (CRL-8024) [5] and the melanoma cell lines Mel Im and HTZ-19 [12,70] were grown at 37°C and 5% (PLC) and 8% (Mel Im and HTZ) CO_2, respectively, in Dulbecco's modified Eagle medium (DMEM; PAN Biotech GmbH, Aidenbach, Germany), which had been supplemented with penicillin (400 U/mL), streptomycin (50 µg/mL), L-glutamine (300 µg/mL), and 10% fetal calf serum (FCS; Sigma, Deisenhofen, Germany).

The adherently growing melanoma cells were cultured in six-well plates (Corning, NY, USA) and detached with 200 µL of 0.05% (w/v) trypsin and 0.02% (w/v) EDTA in Hanks' balanced salt solution (Sigma-Aldrich). Trypsination was stopped after 5 min by the addition of 700 µL of cell culture medium. Following centrifugation at 100xg (5 min, room temperature), the supernatant was removed. The cell pellet was washed with PBS buffer, centrifuged again (100xg, 5 min, room temperature), and the cell pellets were then stored at -80°C until extraction.

The adherently growing HCC cells were cultured in Corning 25cm^2 culture flasks (Corning) and harvested by trypsination using 2 mL trypsin solution as described above. Following centrifugation of detached cells at 700xg (5 min, 4°C), the supernatant was removed. The cell pellet was washed with PBS buffer, centrifuged (700xg, 5 min, 4°C), and then shock-frozen in liquid nitrogen and stored at -80°C until extraction.

The experimental work described in chapter 4.2.3 was done by Georgi Kirovski (HCC-cell line) and Susanne Wallner (melanoma cell lines), respectively, in the working groups of PD Dr. Claus Hellerbrand (Department of Internal Medicine I, University Hospital Regensburg) and Prof. Anja Bosserhoff (Institute of Pathology, University of Regensburg).

4.2.4 Analyte extraction from the pellets and spiking experiment

Metabolites are commonly extracted from cells and tissues with methanol (MeOH)/ water at a ratio of 80:20. To verify that 80:20 MeOH/water was also best suited for extracting metabolites of the methionine and polyamine pathways, different solvent combinations (pure MeOH, MeOH/0.1 M acetic acid 80:20 v/v, and MeOH/0.1 M acetic acid 50:50 v/v) were tested. Briefly, 600 µL of the different solvents were added to the frozen pellets and internal standard was spiked as described above. Then the sample was slowly thawed on ice. To complete the cell lysis, the cells were again shock-frozen in liquid nitrogen and thawed on ice. The freeze/thaw cycle was performed three times and the sample was vortexed between each cycles. The sample was centrifuged at 9,000xg for 5 min at 4°C and the supernatant was transferred to a 1.5-mL glass vial. The pellet was washed twice with 200 µL of

solvent and all supernatants were combined. The solvent was evaporated and the residues were reconstituted in 100 µL of aqueous 0.1 M acetic acid.

For cell pellets a spiking experiment was carried out to evaluate extraction efficiency and matrix effects. Prior to extraction, the cell pellets were spiked in quadruplicate with three different concentration levels and extracted as described above. The spiking concentrations were individually selected for each analyte based on the intracellular analyte concentration x (spike levels x/2, x, 2x) and extracted as described above.

4.2.5 Preparation of hepatic tissue samples

Hepatocellular carcinoma tissue samples and normal liver specimens were ascertained from patients undergoing partial hepatectomy. Informed consent had been obtained from all patients following approval of the study by the local Ethics Committee. These samples were obtained by PD Dr. Claus Hellerbrand from the Department of Internal Medicine I, University of Regensburg.

Tissue samples were weighted and homogenized in 600 µL of MeOH/0.1 M acetic acid (80:20, v/v) using “Precelly-Keramik-Kit 1.4 mm” vials (Peqlab Biotechnologie GmbH, Erlangen, Germany). The samples were homogenized twice at 5,500 rpm for 15 s with an intermediate 30-s pause (Peqlab Biotechnologie GmbH). Samples were centrifuged at 9,000xg for 5 min at 4°C, and the supernatant transferred to a 1.5-mL glass vial. The pellet was washed twice with 200 µL of the solvent, homogenized again, and all supernatants were combined. After solvent evaporation, the residues were reconstituted in 100 µL of 0.1 M acetic acid.

4.2.6 Hepatic tissue samples of mice with non-alcoholic steatohepatitis and liver cirrhosis

Non-alcoholic fatty liver disease (NAFLD) is characterized by the accumulation of fat in the liver in the absence of excessive alcohol abuse. It is typically related to insulin resistance and the so-called metabolic syndrome, the clinical manifestations of which include obesity, hyperlipidemia, diabetes mellitus type II, and high blood pressure. Non alcoholic steatohepatitis (NASH) is the most extreme form of NAFLD and regarded a major cause of liver cirrhosis [79]. To initiate the development of NASH, mice were fed a so-called Paigen diet containing 15% lard / cocoa butter, 1.25 % cholesterol and 0.5% sodium cholate over 30 weeks. This protocol was modified from [80,81]. The mice were sacrificed; the liver was resected and immediately frozen in liquid nitrogen and stored at -80°C until further sample preparation as described above.

Liver cirrhosis was induced by repeated intraperitoneal injection of CCl_4 (1 µL/g body weight) and the animals were sacrificed after three days [82]. The removed liver was immediately frozen with liquid nitrogen and stored at -80°C until further sample preparation as described above.

The experimental work described in chapter 4.2.6 was performed by coworkers of PD Dr. Claus Hellerbrand at the Department of Internal Medicine I, University of Regensburg.

4.2.7 Mice glioma tissue

The used brain tumor model was described previously by Grauer et al. [83] and the experimental work described in chapter 4.2.7 was carried Dr. Oliver Grauer (Department of Neurology, University of Regensburg). Briefly, to induce tumors mice

glioma cells (GL261) were harvested washed and the cell count was adjusted. A total of 100,000 cells were injected below the dura mater into the right cerebral hemisphere. Animals were observed daily and sacrificed after the occurrence of characteristic symptoms, such as hunched posture, reduced mobility and significant weight loss (>20%). The animals were perfused with 0.9 % NaCl solution and the tumor as well as the surrounding brain parenchyma resected. As a control the normal brain parenchyma from the tumor free left brain region was taken. Tissue samples were shock-frozen in liquid nitrogen and stored at -80°C until extraction. The further preparation was carried out as described in 4.2.5.

4.2.8 Renal carcinoma tissues

Renal carcinoma tissue samples and non-cancerous tissue specimens were ascertained from patients undergoing nephrectomy. Informed consent had been obtained from all patients following approval of the study by the local Ethics Committee. Samples were stored at -80°C until further preparation as described for hepatic tissue samples.

These samples were provided by Prof. Anja Bosserhoff from the Institute of Pathology, University of Regensburg.

4.2.9 Instrumentation

Liquid chromatography-electrospray ionization-tandem mass spectrometry (LC-ESI-MS/MS) was performed using an Agilent 1200 SL HPLC system (Böblingen, Germany) and a PE Sciex API 4000 QTrap mass spectrometer (Applied Biosystems, Darmstadt, Germany) equipped with a turbo ion spray source (completely controlled by Analyst version 1.5). The column oven was kept at 25°C. An Atlantis T3 3µm (2.1

i.d. x 150 mm) reversed phase column (Waters, Eschborn, Germany) was used. LC separation was carried out using a mobile phase consisting of 0.1% acetic acid and 0.025% HFBA in water (Solvent A), respectively in acetonitrile (Solvent B). The gradient employed was as follows: 0-4 min linear increase from 0% to 30% B, 4-8 min from 30% to 40% B, 8-8.1 min 40% to 100% B and hold at 100% B for 5 min. The flow-rate was 400 µL/min. If not otherwise noted, sample volumes of 10 µL were injected.

The API 4000 QTrap mass spectrometer was operated in positive mode using turbo ion spray with gas 1, gas 2, and curtain gas set at 50, 30, and 10 psi, respectively. The source was heated to 500°C. Quantitative determination was performed with multiple-reaction monitoring (MRM) using the parameters listed in Table 3.

Table 3: List of chromatographic retention time (RT), selected MRM parameters, loss off, declustering potential (DP), collision energy (CE), and collision cell exit potential (CXP) for each metabolite measured.

Analyte	RT [min]	Q1 mass	Q3 mass	Loss off	DP	CE	CXP
Adenine	5.70	135.9	119.1	- NH_3	76	33	8
Adenine-$^{13}C_5$	5.70	140.9	124.1	- NH_3	76	33	8
Adenosine	5.89	268.2	136.1	- sugar moiety	36	24	9
Adenosine-$^{13}C_5$	5.89	273.2	136.1	- $^{13}C_5$-sugar moiety	36	24	9
Homocysteine	2.96	136.2	90.1	- formic acid	31	17	6
Homocysteine-d_4	2.96	140.2	94.1	- formic acid	31	17	6
MTA	6.98	298.2	136.1	- sugar moiety	60	19	9
MTA-$^{13}C_5$	6.98	303.2	136.1	- $^{13}C_5$-sugar moiety	60	19	9
Ornithine	2.31	133.3	116.1	- NH_3	44	13	9
Ornithine-d_7	2.31	140.3	123.1	- NH_3	44	13	9
Putrescine	5.92	89.1	72.1	- NH_3	36	17	4
Putrescine-$^{13}C_4$	5.92	93.1	76.1	- NH_3	36	17	4
Acetylputrescine	5.32	131.2	72.1	- NH_2COCH_3	6	23	2
SAH	6.34	385.2	136.1	- sugar moiety	56	27	10
SAM	6.51	399.1	136.1	- sugar moiety	66	37	8
SAM-d_3	6.51	402.1	136.1	- d_3-sugar moiety	66	37	8
Spermidine	7.19	146.2	72.1	- $NH_2(CH_2)_3NH_2$	51	21	4
Spermidine-$^{15}N_3$	7.19	149.2	73.1	- $^{15}NH_2(CH_2)_3{}^{15}NH_2$	51	21	4
N1-Acetylspermidine	6.70	188.3	100.1	- $NH_2(CH_2)_4NH_2$	51	27	6
N8-Acetylspermidine	6.76	188.3	114.1	- $NH_2(CH_2)_3NH_2$	51	27	6
Spermine	7.48	203.2	112.1	- [$NH_2(CH_2)_3NH_2$ + NH_3]	66	27	8
Spermine-d_8	7.48	211.2	120.1	- [$NH_2(CH_2)_3NH_2$ + NH_3]	66	27	8
Acetylspermine	7.30	245.3	100.1	- $NH_2(CH_2)_3NH(CH_2)_4NH_2$	61	31	6

The electron multiplier was set at 2100 V. All MS parameters were optimized by direct infusion, the source parameters by flow injection. Data analysis was performed by Analyst version 1.5.1.

4.2.10 Data analysis

Standard calibration curves were plotted as the chromatographic peak area ratio (analyte / IS) versus the corresponding nominal concentration ratio (analyte / IS). A 1/x weighted regression analysis was used to determine the slope, intercept and coefficient of determination (r^2). An unpaired two tailed t-test was used to determine whether the means of analyte concentrations were significantly different ($p < 0.05$).

4.3 Results and Discussion

4.3.1 Chromatographic Optimization and Calibration

As mentioned in the introduction, this method is an expansion of the method described in chapter 3. Chromatographic separation was tried at first with the solvents and the gradient of the previous method. Figure 17 clearly indicates that the solvents and gradient of this method are insufficient to separate all analytes.

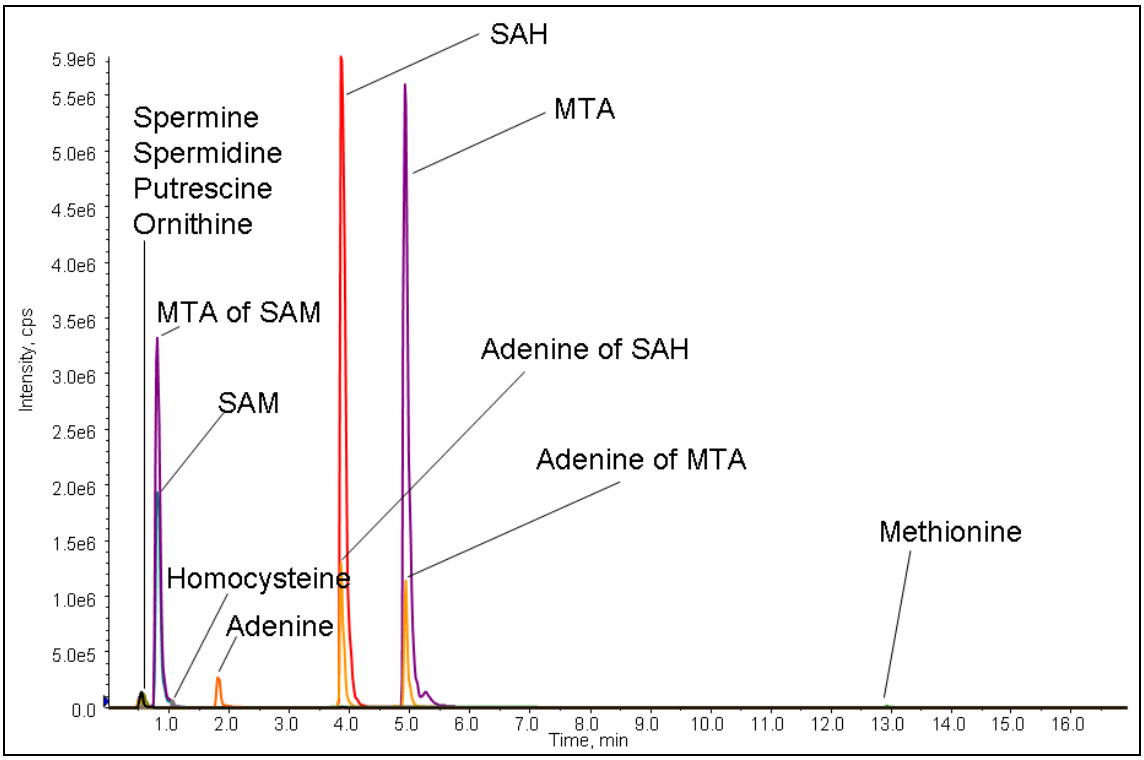

Figure 17: Chromatographic separation of a subset of the metabolites of the methionine and polyamine pathways. Chromatographic conditions from the method described in chapter 3 were used.

To achieve a higher retention of the polar analytes 0.025% HFBA were added to both solvents and the linear gradient was replaced by a stepwise gradient. Figure 18 shows a representative chromatogram of intermediates of the methionine and polyamine metabolism detected in an extract of a liver biopsy specimen. The method development started with a smaller set of analytes and was expanded over time. Therefore, more analytes are shown in Figure 18 than in Figure 17.

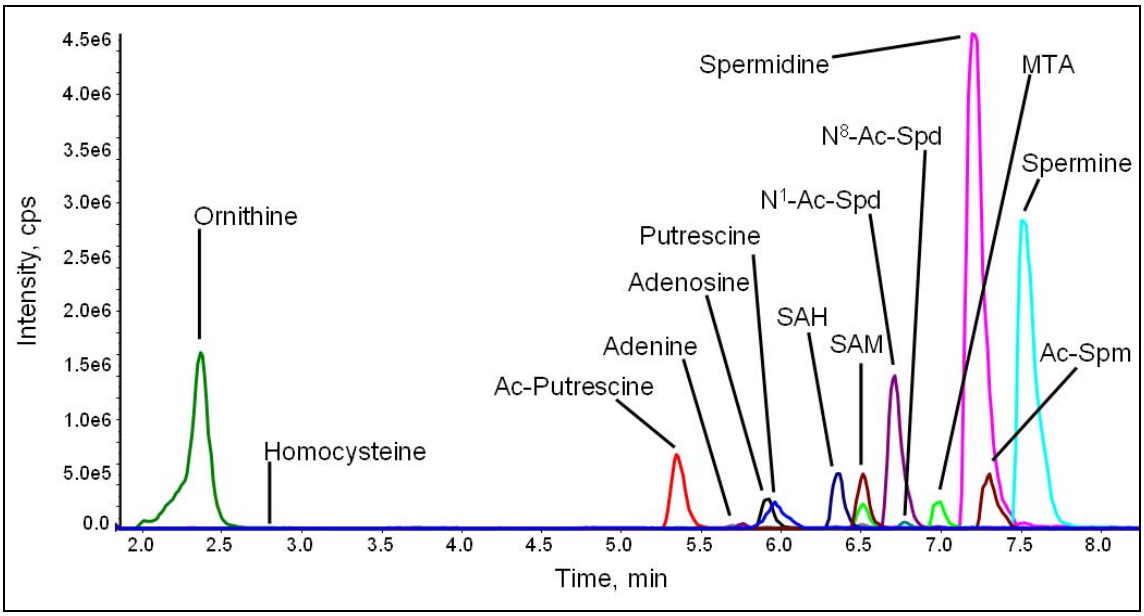

Figure 18: Chromatogram of intermediates of the methionine and polyamine pathways in an acidified methanolic extract of a liver tumor biopsy (Ac - Acetyl, Spd – Spermidine, Spm – Spermine). Chromatography was optimized to the parameters mentioned in chapter 4.2.9.

For absolute quantitative analysis, a calibration was carried out for all analytes in the range of 0.5 nM to 500 µM. Table 4 lists the calibration parameters obtained according to the FDA guidelines for bioanalytical method validation [71]. A general 1/x-weighting factor was used.

Table 4: Calibration parameters. Analytes printed in bold were quantified using the corresponding stable-isotope labeled compound (acetylated polyamines were quantified using the unacetylated analog, SAH using d_3-SAM).

Analyte	LOD[a] [nM]	Linear range [nM] (LLOQ[b] – ULOQ[c])	Slope	Intercept	Coefficient of determination (r^2)
Adenine	2.5	5.0 – 500,000	1.230	0.28600	0.9986
Adenosine	2.5	5.0 – 100,000	0.713	0.04630	0.9975
Homocysteine	2.5	7.5 – 250,000	1.120	0.00636	0.9989
MTA	2.5	5.0 – 100,000	0.670	0.04430	0.9963
Ornithine	25.0	50 – 500,000	1.120	0.07950	0.9959
Putrescine	12.5	50 – 500,000	0.903	0.01090	0.9993
Acetylputrescine	100.0	500 – 50,000	2.170	0.06350	0.9957
SAH	12.5	25 – 10,000	1.460	0.18300	0.9980
SAM	1.0	2.5 – 25,000	0.696	0.00270	0.9929
Spermidine	12.5	50 – 25,000	0.845	0.04090	0.9978
N1-Acetylspermidine	25.0	50 – 2,500	1.530	0.04500	0.9921
N8-Acetylspermidine	1.0	2.5 – 500	2.640	0.00697	0.9979
Spermine	12.5	25 – 100,000	1.610	0.04340	0.9963
Acetylspermine	2.5	5.0 – 100,000	1.730	0.00437	0.9992

[a] LOD, signal-to-noise ratio ≥ 3;
[b] LLOQ, lowest calibration point with five times the response compared to a blank, an accuracy of 80% – 120%, and an imprecision <20%;
[c] ULOQ, highest calibration point with an accuracy of 80% – 120% and imprecision <20%.

Analytes, for which a matching stable-isotope labeled internal standard was available (printed in bold in Table 4), yielded in general lower LODs and LLOQs than the other analytes. The acetylated polyamines were quantified with the corresponding stable isotope labeled unacetylated analog, and SAH with d_3-SAM. The same tendency was observed for the linear range. With the exception of spermidine, all the analytes with a matching stable-isotope labeled internal standard available showed a linear range over three to five orders of magnitude. In contrast, the acetylated polyamines and SAH showed linearity only over two to three orders of magnitude, emphasizing the need for stable-isotope labeled internal standards to account for matrix effects. For all analytes the coefficient of determination (r^2) exceeded 0.99. The average repeatability of triplicate injections was 2.38%.

4.3.2 Extraction optimization for cell pellets

Three different methanol/water combinations (50% MeOH, 80% MeOH and 100% MeOH) were tested to determine the solvent that gave the highest extraction yield of the metabolites under investigation. Figure 19 shows the extracted amounts of analytes and Figure 20 the recovery of the internal standard using the different solvent combinations.

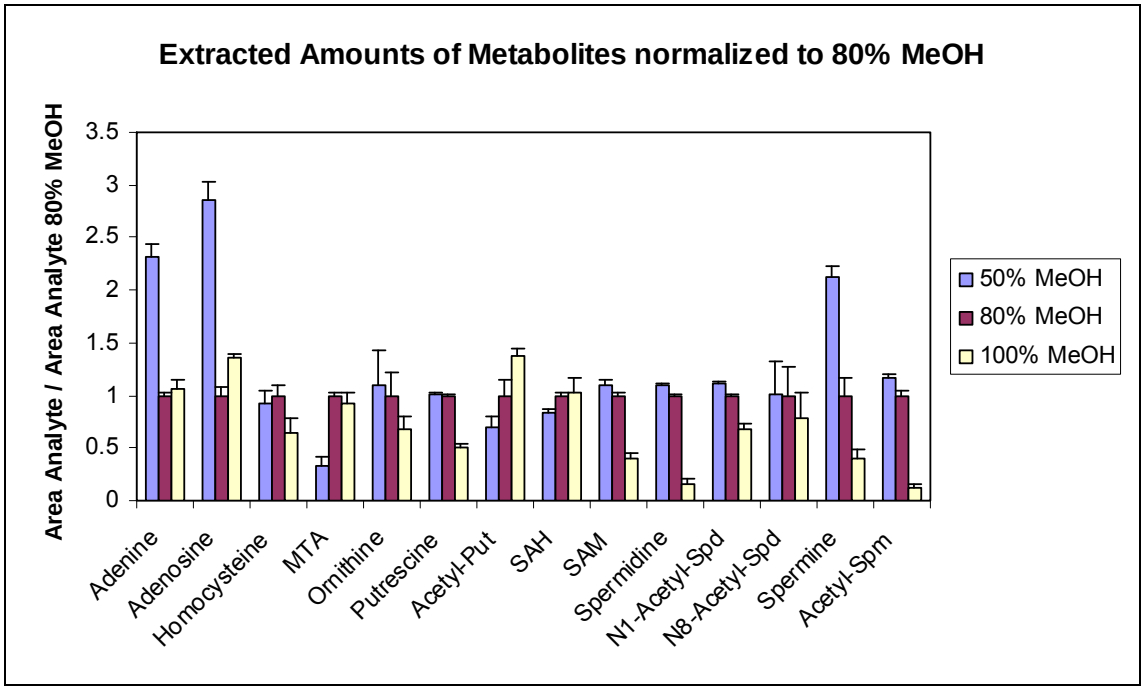

Figure 19: Effect of 50% aqueous methanol and pure methanol on the extraction efficiency of intermediates of the methionine and polyamine pathways in relation to the area integrals measured at 80% methanol (set at 1).

The data presented in Figure 19 were normalized to data obtained using 80% MeOH for better comparability, because the intracellular concentrations of the metabolites differed over three to four orders of magnitude. With this normalization all analytes could be displayed in one diagram. Except for acetylputrescine, SAH and MTA, the extracted amount increased with the water content of the extraction solvent. For adenine, adenosine and spermine the highest yields were obtained with 50% MeOH. The remaining analytes did not show great differences in extraction yield between 50% and 80% methanol.

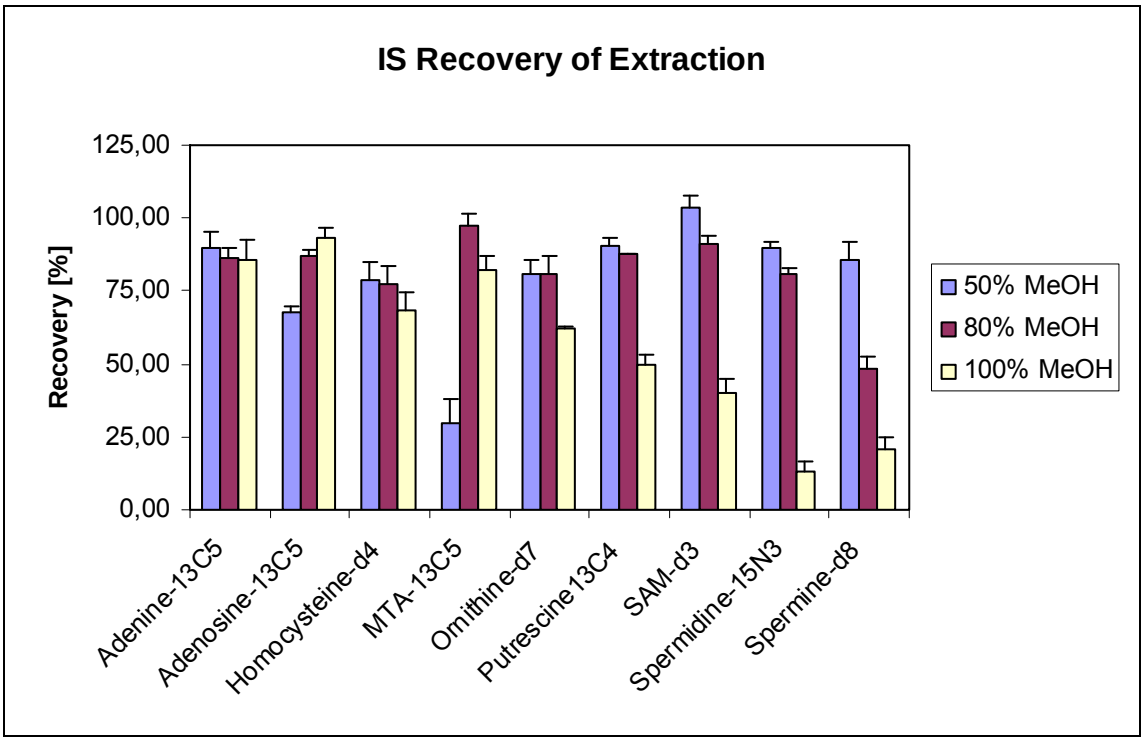

Figure 20: Percent recovery of internal standards at different concentrations of methanol employed for extraction.

For six of nine internal standards, 80% methanol yielded similar or even higher recoveries than 50% methanol (Figure 20). Moreover, 80% methanol resulted in improved protein precipitation, and thus, provided “cleaner” extracts and facilitated the retrieval of supernatant liquid. Consequently, 80% methanol was used for all further extractions. To stabilize SAM, acetic acid was added at a final concentration of 0.1 M. This resulted also in higher extraction yields for spermidine and spermine without affecting the extraction behavior of the other metabolites (data not shown).

4.3.3 Spiking experiment

The recovery of metabolites from Mel Im cell pellets was determined at three different spiking levels (Figure 21).

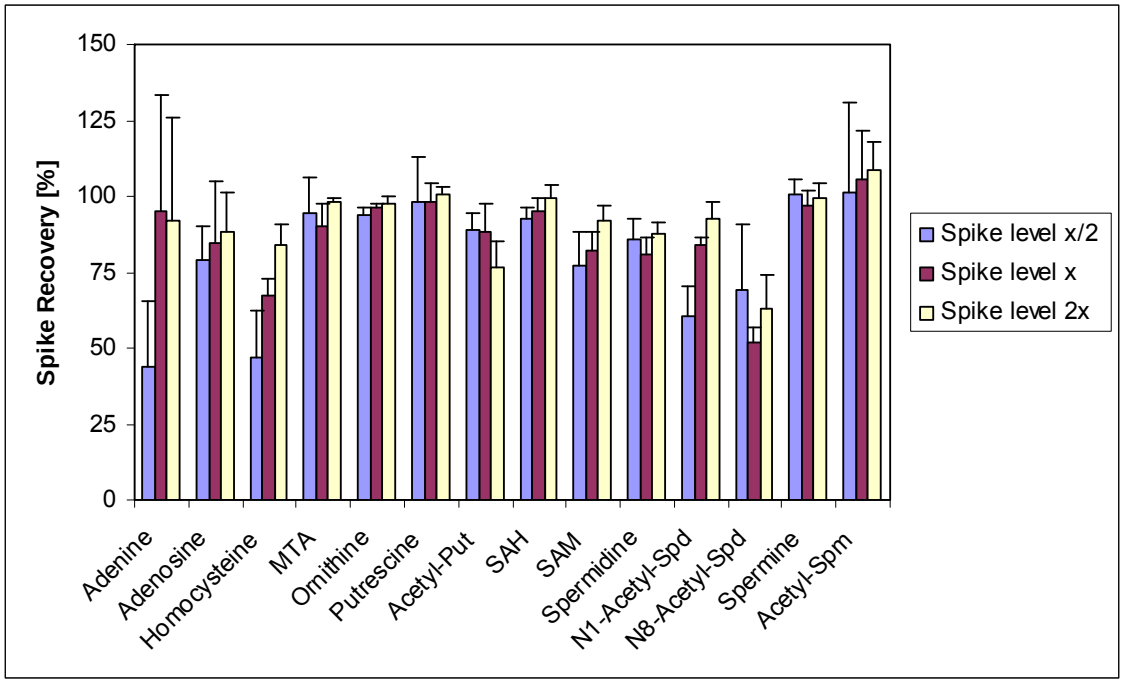

Figure 21: Recovery of analytes in the spike-in experiment.

Most of the analytes yielded spike recoveries exceeding 80%. One of the exceptions was homocysteine, the recoveries of which ranged from 46% to 83% despite the availability of a stable-isotope labeled internal standard generated by the reduction of deuterated homocystine with TCEP prior to its addition to the cell pellet. An explanation for the low recoveries of homocysteine spiked to biological samples might be, that it bound to other thiols in the sample via the formation of covalent disulfide bonds [84], which would result in non-optimal correction for inter-sample differences in extraction and ionization efficiency. Attempts to measure total instead of free homocysteine only by the reduction of the disulfide bond between homocysteine and other thiols or sample proteins before analysis by the addition of TCEP to the cell extracts showed a significant at least tenfold increase in peak area for homocysteine. However, the addition of TCEP also exerted a detrimental effect on

chromatography shifting the retention of most analytes into the void volume (data not shown). Low recoveries were also seen for adenine, likely due to the fact that its intracellular concentrations were close to the LLOQ of the method. For the acetylated polyamines, the corresponding non-acetylated polyamines were used to account for inter-sample differences in extraction and ionization efficiency. This might explain the lower recovery (60-80%) and higher RSD (15-25%) values for these analytes.

4.3.4 Tumor cell lines

The molar amounts of intermediates of the methionine and polyamine metabolism determined in two different melanoma cell lines, namely HTZ-19 and Mel Im, and the HCC cell line PLC are listed in Table 5. All values are given in nmol/million cells.

Table 5: Molar amounts of intermediates of the methionine and polyamine pathways determined in four replicate methanol:water (80:20, v/v) extracts each for the melanoma cell lines HTZ-19 and Mel Im, as well as the hepatoma cell line PLC. Analytes printed in bold were quantified using the internal standard quantification trace of the corresponding stable-isotope labeled compound.

	HTZ-19		Mel Im		PLC	
	Mean nmol/mio cells	S.D.	Mean nmol/mio cells	S.D.	Mean nmol/mio cells	S.D.
Adenine	3.74	0.48	5.24	0.86	296.15	62.15
Adenosine	209.25	26.59	223.00	18.51	87.02	88.80
Homocysteine	5.43	0.88	4.66	0.93	5.93	0.79
MTA	18.35	1.44	16.90	0.71	25.39	2.69
Ornithine	896.75	155.59	507.50	148.81	351.40	40.75
Putrescine	641.75	52.54	875.00	9.97	1761.07	338.23
Acetylputrescine	13.88	1.31	27.68	4.74	67.54	10.62
SAH	108.15	11.45	82.60	2.73	15.19	3.38
SAM	1162.50	86.17	942.50	15.33	939.39	178.57
Spermidine	3487.50	233.43	2727.50	401.86	7354.31	1241.14
N1-Acetylspermidine	734.00	61.81	496.00	9.83	134.03	35.09
N8-Acetylspermidine	5.67	0.60	4.83	1.46	4.07	1.04
Spermine	2487.50	189.98	2487.50	80.98	7162.00	1041.83
Acetylspermine	935.00	216.59	1427.50	172.51	35.36	9.20

The most abundant metabolites in the melanoma cell lines were spermidine, spermine, acetylspermine, and SAM, the molar amounts of which ranged from approximately 0.9 to 3.5 µmol per million cells. Spermidine and spermine were also

the most abundant metabolites in the HCC cell line PLC, with molar amounts as high as 7.35±1.24 and 7.16±1.04 µmol per million cells. The third most abundant metabolite in PLC cells was putrescine (1.76±0.33 µmol/million cells), which was found at concentrations about two- to three-fold higher than in the melanoma cell lines. The concentration of SAM in PLC cells was similar to that observed in the melanoma cell lines. The least abundant metabolites in the three cancer cell lines were homocysteine (4.66±0.93 - 5.93±0.79 nmol/million cells) and N^8-acetylspermidine (4.07±0.93 - 5.67±0.60 nmol/million cells). Interestingly, the molar amount of adenine observed in PLC cells was 56- to 79-fold greater than in the melanoma cell lines. A detailed explanation of the partly significant differences in metabolite concentrations observed among the cell lines will have to await measurements of the abundance and activity of the enzymes involved in the methionine and polyamine pathways.

4.3.5 Liver tissue

Metabolite concentrations observed *in vitro* might differ significantly from those found *in vivo*. To account for such differences we also analyzed 80% methanol extracts of seven human hepatocellular carcinoma (HCC) and three normal liver tissue specimens. As in the HCC cell line PLC, spermidine and spermine were among the most abundant metabolites (Table 6).

Table 6: Metabolite concentrations in human hepatocellular carcinoma (n=7) and normal liver tissue (n=3) biopsy specimens. Analytes printed in bold were quantified using the internal standard quantification trace of the corresponding stable-isotope labeled compound.

	Carcinoma (n=7)		Normal (n=3)	
	Mean [pmol/mg]	S.D. [pmol/mg]	Mean [pmol/mg]	S.D. [pmol/mg]
Adenine	4.42	2.65	3.94	1.57
Adenosine	21.44	11.02	55.87	37.59
Homocysteine	0.34	0.16	0.91	0.77
MTA	2.84	2.52	1.31	0.38
Ornithine	559.72	281.04	497.30	158.60
Putrescine	163.92	108.39	83.85	29.76
Acetylputrescine	44.53	14.35	106.72	66.14
SAH	43.94	23.44	55.51	8.96
SAM	74.51	60.67	38.00	11.77
Spermidine	458.82	246.24	317.36	107.57
N1-Acetyspermidine	15.94	3.44	36.04	44.76
N8-Acetylspermidine	1.09	0.63	1.39	0.92
Spermine	602.29	140.78	647.32	76.96
Acetylspermine	14.91	2.96	23.45	29.35

While the average molar ratios of spermidine and spermine to putrescine in PLC cells (4.2 and 4.1, respectively) and the tumor biopsies (2.8 and 3.7, respectively) were quite similar, the molar amount of ornithine, relative to spermidine and spermine, determined in the tumor biopsies was about 20-fold greater than in the PLC cells. Finally, the molar amount of adenine observed in the tumor biopsies was comparatively much lower than in the PLC cells.

Figure 22 shows the normalized concentrations of the methionine metabolites and polyamines measured in the HCC and normal liver tissue biopsy specimens.

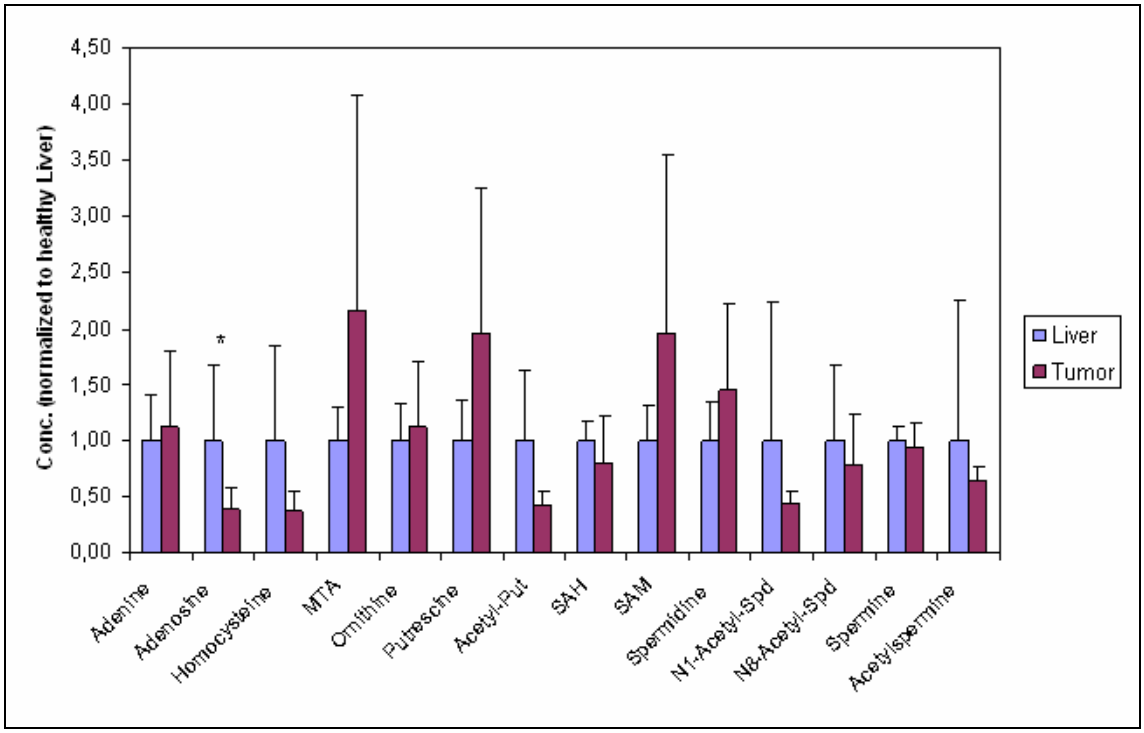

Figure 22: Metabolite concentrations (pmol/mg tissue) in seven hepatocellular carcinoma specimens normalized to tissue specimens from normal liver (n=3). Depicted are arithmetic means and standard deviations. * p<0.05; ** p<0.01

As expected, the average concentration of MTA in tumor exceeded significantly the MTA level in normal tissue presumably due to the reported lack of MTAP in the former [5]. Similar increases in concentration were observed for SAM and putrescine. This indicates that accumulated MTA reduces the metabolism of SAM and putrescine via a feedback loop. The elevated level of spermidine is an indication for a higher cell proliferation in tumors [85-88] and together with the nearly constant spermine level it is suggested that the metabolism of SAM and putrescine in only partly reduced, in case of a total inhibition of this reaction, a decrease in the polyamines is expected.

4.3.6 Non-alcoholic steatohepatitis

Figure 23 shows the normalized concentrations of the methionine metabolites and polyamines measured in the liver of mice with and without non-alcoholic steatohepatitis (NASH). Absolute concentrations are listed in Table A 1 in the appendix.

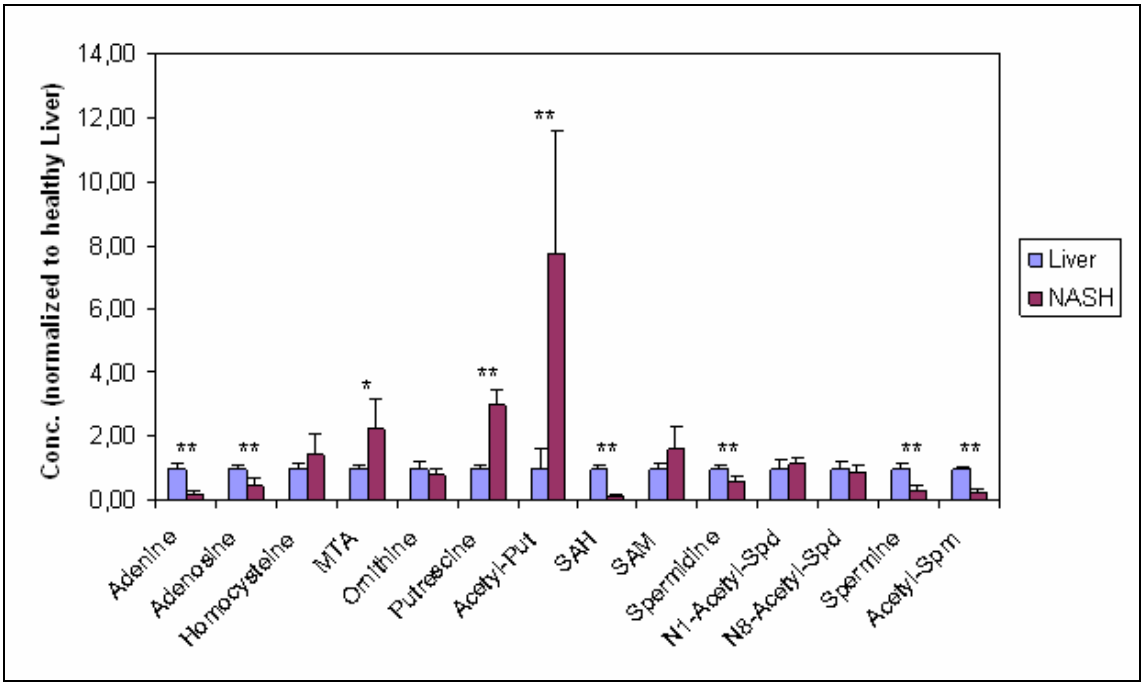

Figure 23: Metabolite concentrations (pmol/mg tissue) in fatty livers normalized to tissue specimens from healthy liver (n=5). Depicted are arithmetic means and standard deviations. * p<0.05; ** p<0.01

Significant changes in the profile of methionine and polyamine metabolites could be observed. As observed in human liver, the most abundant metabolites were ornithine (6223 vs. 5125 nmol/g), spermidine (665 vs. 380 nmol/g) and spermine (526 vs. 146 nmol/g). The highest increases except for N-acetyl-putrescine (0.01 vs. 0.07 nmol/g) were observed for putrescine, MTA and SAM (3.0-, 2.6- and 1.6-fold). The liver of NASH mice has a high percentage of fat and, therefore, the cell count per mg total tissue weight is lower compared to healthy liver. The increase of MTA, putrescine and SAM together with the decrease of spermidine and spermine indicates that the overall MTAP activity in NASH mice is reduced. The reason for the decreased overall

MTAP activity could be a lower expression, a lower MTAP concentration caused by the incubated fat or an inhibition of the enzymatic activity.

4.3.7 Liver cirrhosis

Figure 24 shows the normalized concentrations of the methionine metabolites and polyamines measured in the liver of mice with and without CCl_4 induced liver cirrhosis. Absolute concentrations are listed in Table A 2 in the appendix. The acetylated polyamine levels are missing, because the samples were measured before inclusion of these analytes in the method.

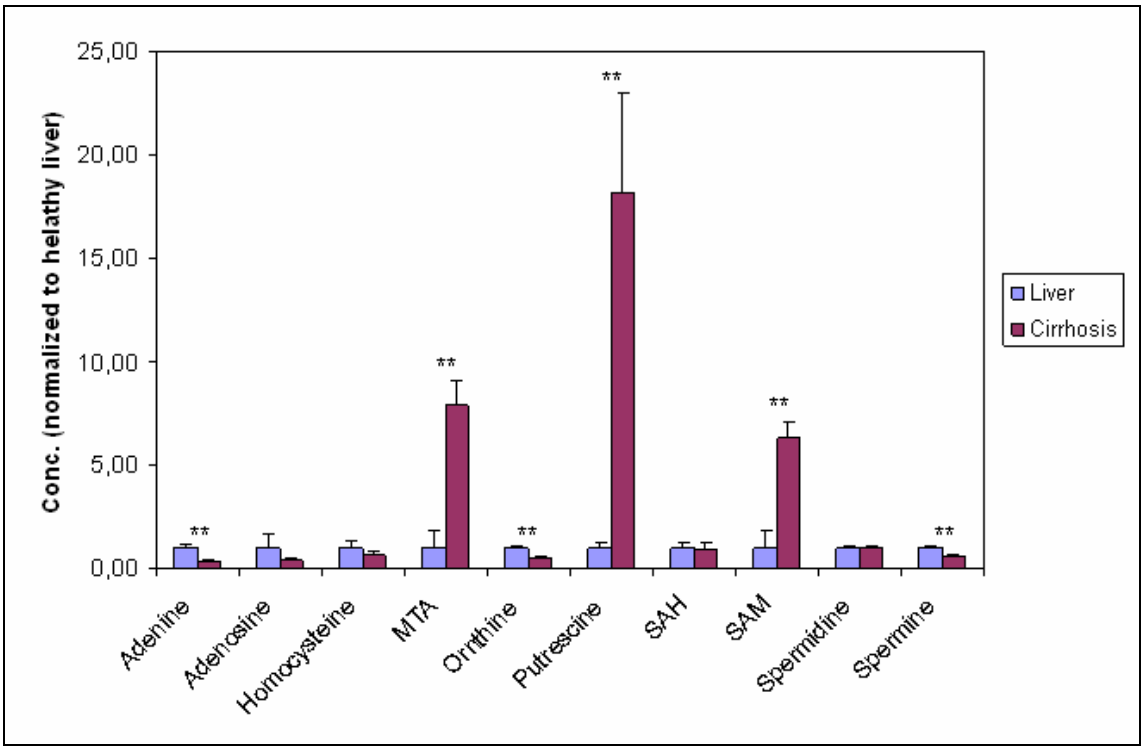

Figure 24: Metabolite concentrations (pmol/mg tissue) in liver cirrhosis normalized to tissue specimens from healthy liver (n=3). Depicted are arithmetic means and standard deviations. * p<0.05; ** p<0.01

Changes during cirrhosis are mainly observed in the concentrations of MTA, putrescine and SAM. The increase is much more intensive than in NASH, probably due to more severe liver tissue damage than in the NASH model. It was also observed by Berasain et al [89] that MTAP expression in cirrhosis is much lower than

in tumors as well as in healthy liver. Hence, the accumulation of MTA was likely caused by a decrease in MTAP expression/activity. The significantly lower level of spermine might be explained with the inhibitory effect of MTA on spermine synthase. As observed by Hibasami et al. [90], MTA has a stronger inhibitory effect on spermine synthase (50% inhibition at 10-15 µM MTA) than spermidine synthase (50% inhibition at 30-45 µM MTA). The lower concentrations of ornithine could be caused by a higher activity of ornithine decarboxylase [91,92], another reason for the elevated putrescine concentration.

4.3.8 Brain tumor samples

Mice glioma tissue samples were analyzed to examine changes in the methionine and polyamine pathways in another tumor. As expected, MTA increases highly significant in the tumor samples due to the lack of MTAP in brain tumors [93]. SAM and putrescine levels also increased significantly, as observed in other tumors. For most analytes no significant difference between the controls (left brain region) and the non-tumorous tissues of the right brain region could be observed. Only analytes with a strong (more then 10-fold) accumulation in the tumor, such as homocysteine, ornithine, putrescine, N1- and N8-acteyl-spermidine and acetyl-spermine, show a slight accumulation in the non-tumorous tissue. In case of putrescine and N1-acetyl-spermidine this accumulation is significant. This could be caused by diffusion of the high concentrated metabolites out of the tumor. For the other analytes no differences between the left (control) and right brain parenchyma were observed, so the changes in the metabolite concentrations are restricted to the tumor (Figure 25). Non-normalized values are given in Table A 3 in the appendix.

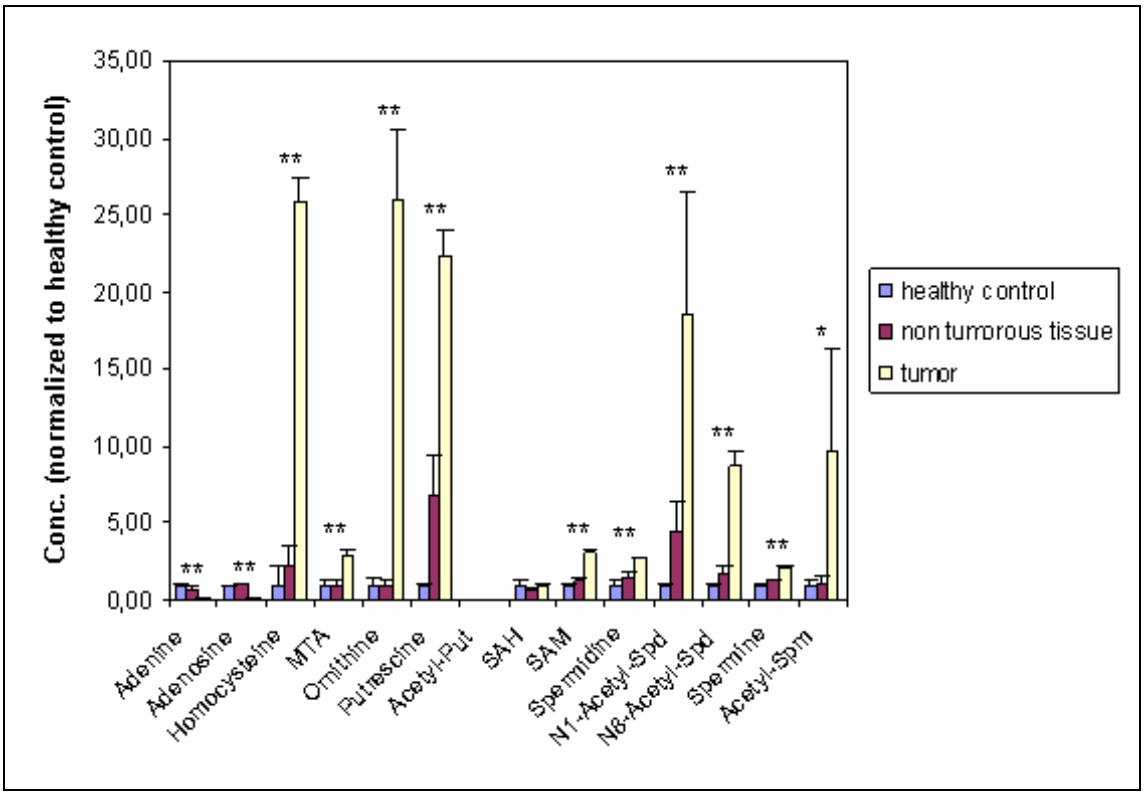

Figure 25: Metabolite concentrations (pmol/mg tissue) in mice glioma normalized to healthy brain parenchyma. Healthy control – left brain parenchyma, non tumorous tissue – right brain parenchyma surrounding the glioma, tumor – glioma sample. (n=4). Significances are shown for tumor vs. healthy control.* p<0.05; ** p<0.01

As can be seen, homocysteine increased dramatically by a factor of 25, a behavior observed for the first time in tumors analyzed in this work. A possible explanation could be found in methylation reactions and a subsequent formation of homocysteine. Due to a defect of the methionine synthase (EC 2.1.1.13), homocysteine could not be recycled back to methionine. This hypothesis is supported by Fiskerstrand et al, who observed the loss of the ability to form methionine from homocysteine in glioma cell lines [94]. The increase of spermidine and spermine (2- and 2.5-fold) is an indication for a higher cell proliferation [85-88], the massive increase of putrescine (22-fold) is an indication for a higher ornithine decarboxylase (ODC) activity, supported by Subhi et al. [29], who postulated that MTA inhibits ODC by downstream metabolites and observed a loss of MTAP and elevated ODC in pancreatic cancer [95]. Since MTA is slower metabolized in the tumor, the inhibitory effect on ODC caused by downstream metabolites of MTA could be lower. The lower

relative standard deviation compared to HCC is the result of the higher homogeneity of the sample group. Instead of different humans here a group of four inbred mice were used.

4.3.9 Renal carcinoma

To examine changes in the methionine and polyamine pathways in a third tumor species, renal carcinomas were analyzed. Figure 26 shows the normalized concentrations of the metabolites in the methionine and polyamine pathway measured in human kidney with and without renal carcinoma. Absolute concentrations are listed in Table A 4 in the appendix.

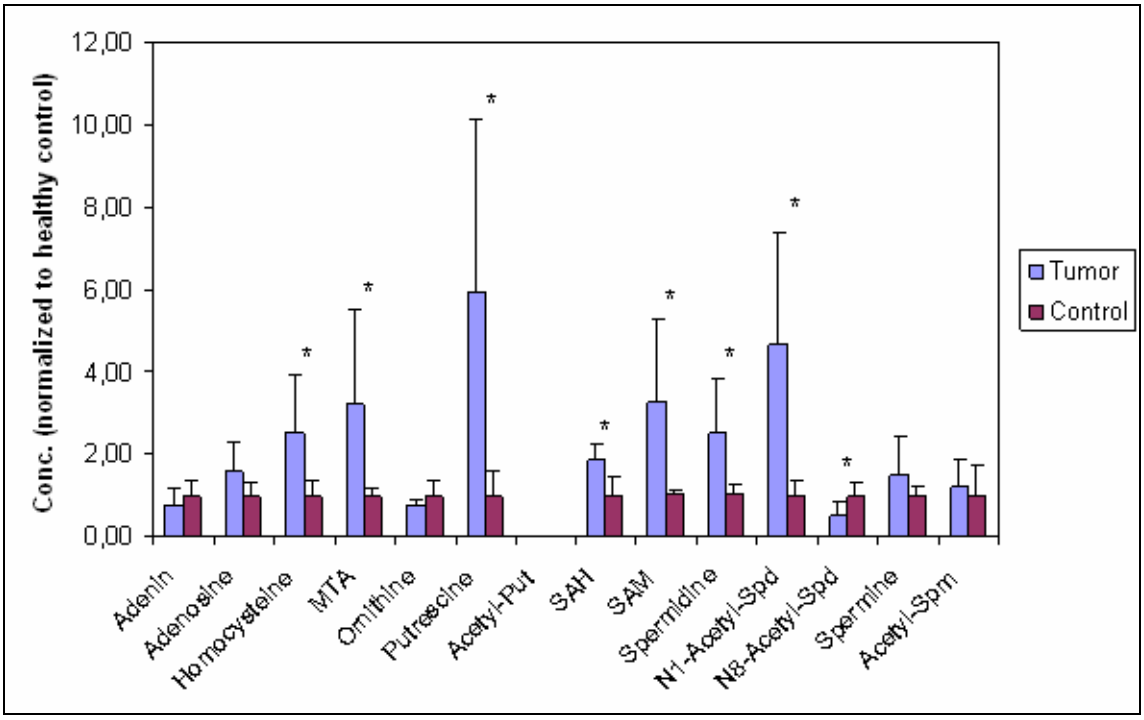

Figure 26: Metabolite concentrations (pmol/mg tissue) in renal carcinomas normalized to tissue specimens from healthy kidneys (n=5). Depicted are arithmetic means and standard deviations.* p<0.05; ** p<0.01

As observed in other tumors and also expected here, MTA (due to the lack of MTAP in tumors), SAM and putrescine are significantly increased. The acetylated putrescine was in all cases below the LOD. Since spermidine and spermine levels are elevated,

an increased polyamine synthesis is assumed, which indicates higher cell proliferation in the tumor [85-88]. For the first time here a nearly 2-fold increase of SAH was observed, in all other analyzed samples SAH stayed nearly constant. An explanation could be a higher methylation rate in renal carcinomas and therefore a higher production of SAH. Della Ragione and Pegg observed an inhibition of S-adenosylhomocysteine hydrolase (EC 3.3.1.1) by increased levels of MTA [96]. This enzyme cleaves SAH to homocysteine and adenosine. Since SAH is an inhibitor of methylation reactions [97], the higher levels of SAH could be another reason for the elevated levels in SAM. Both directions for the metabolism of SAM (methylation and polyamine synthesis with the formation of MTA) are restricted. As observed in the human liver tumor samples, the standard deviation is much higher compared to all experiments with a mouse model. This is again caused by the higher variation of the different human individuals compared to laboratory mice.

4.4 Conclusions

An LC-ESI-MS/MS method was developed for the quantitative determination of intermediates of the methionine and polyamine pathways. With LODs and LLOQs in the lower nanomolar range, the method was sufficiently sensitive for the analysis of the intermediates in aqueous methanol extracts of cell culture samples, human liver biopsies and mural brain tumors. The use of stable-isotope labeled internal standards proved critical in achieving an analytical reproducibility of 1 - 3% and linear dynamic ranges over 3 - 5 orders of magnitude. The method shall prove useful in the field of finding diagnostic and/or prognostic tumor markers. Possible candidates are MTA, putrescine and SAM, which each increase in different tumors.

Caused by a lower overall-activity of MTAP (the reasons of the lower activity could be a lack of MTAP protein or a lower activity of the protein and are not discussed here) MTA accumulates and as a consequence of this the precursors of MTA, namely putrescine and SAM, do also accumulate. The decarboxylated form of SAM (dcSAM) and putrescine are the educts of MTA synthesis. Due to its instability it was not possible to quantify dcSAM. Cataldi et al. published a method, where they have estimated the concentrations of dcSAM using the calibration curve of SAM assuming a similar ionization behavior [30]. A separate calibration curve was not performed due to the instability of this metabolite. The accumulation of MTA, putrescine and SAM could be observed in all studied tumors as well as in different stages of liver damage. However the tumors show also special difference in the metabolite pattern, e.g. the tremendous increase of homocysteine in gliomas due to a deficiency in methionine synthase.

5. Determination of the activity of methylthioadenosine phosphorylase

5.1 Introduction

During the analysis of the metabolite concentrations in the methionine and polyamine pathways it was observed, that the concentration of MTA does not always correlate with MTAP protein abundance. This resulted in the hypothesis that not only protein concentration but also enzyme activity is an important parameter for changes in metabolite concentration. Consequently, an activity assay for MTAP is needed to elucidate, if the accumulation of MTA is caused by changes in MTAP enzyme activity. A few methods have been already described to analyze MTAP activity [2,4,41]. All these assays use a potassium phosphate buffer (concentration 20 – 50 mM, pH 7.4) and DTT as reducing agent. Interestingly, no cofactors were used. The reaction temperature was 37°C in case of human MTAP. Cells were directly lysed in the buffer and the MTAP activity was determined by measuring the formation of [methyl-^{14}C]5-methylthioribose-1-phosphate from [methyl-^{14}C]-MTA. In the present work, the assay was adapted to measure MTAP activity in liver biopsies. Following the literature, the biopsy samples were homogenized in potassium phosphate buffer (50 mM, pH 7.4) and the reaction temperature was set to 37°C. In contrast to the literature, stable isotope labeled MTA was chosen as substrate and the turnover was determined by liquid chromatography-mass spectrometry. This makes the handling of this assay easier and safer. As reducing agent TCEP was used, because it has a non pungent odor and is also not volatile, and a quantitative reduction will be obtained in less than 5 minutes of reaction. Pyridoxal phosphate was added as a cofactor although it should not be necessary for the enzymatic degradation of MTA. However, it is

planned to expand this assay to the measurement of ODC activity in the same reaction mixture, which requires Pyridoxal phosphate [98].

The assay is based on the principle of continuous reaction monitoring. Therefore, aliquots of the reaction mixture were taken at different time points and the reaction was quenched with pure MeOH. The concentration of MTA was determined by liquid chromatography-mass spectrometry based on the method described in chapter 4. The activity was calculated with a response-over-time diagram. The results of this chapter will be part of a manuscript in preparation.

5.2 Experimental

5.2.1 Chemicals

Solvents for sample preparation and LC-MS analysis were HPLC grade and purchased from Fisher-Scientific (Schwerte, Germany) and Merck (Darmstadt, Germany). Heptafluorobutyric acid (HFBA) was from Fluka (Taufenkirchen, Germany), while tris-(2-carboxyethyl) phosphine hydrochloride (TCEP) and pyridoxal phosphate were from Sigma Aldrich (Taufenkirchen, Germany). [1',2',3',4',5'-$^{13}C_5$]-adenosine was from Omicron Biochemicals (South Bend, IN, USA), [1',2',3',4',5'-$^{13}C_5$]-MTA was prepared in house according to Robins et al. [69] (see chapter 3.2.2). KH_2PO_4 and K_2HPo_4 were from Merck (Darmstadt, Germany). The water used was purified by means of a PURELAB Plus system (ELGA LabWater, Celle, Germany).

5.2.2 Internal standard preparation and stock solutions

To obtain a 50 mM potassium phosphate buffer (pH=7.4) 4.01 mL of an 1 M K_2HPO_4 solution were mixed with 0.99 mL of an 1 M KH_2PO_4 solution and filled up to 100 mL.

The pH value was checked and adjusted with phosphoric acid or potassium hydroxide, if necessary.

A stock solution of stable-isotope labeled adenosine was prepared in aqueous 50 mM potassium phosphate buffer (pH=7.4) and diluted to obtain a working solution of 200 nM $^{13}C_5$-adenosine in 50 mM potassium phosphate buffer. A solution of stable-isotope labeled MTA (1 mM) in 0.1 M acetic acid was diluted in 50 mM potassium phosphate buffer (pH=7.4) to obtain a working solution of 1 µM $^{13}C_5$-MTA. Pyridoxal phosphate and TCEP solutions were prepared in 50 mM potassium phosphate buffer (pH=7.4) with a concentration of 1mM and 10 mM, respectively.

5.2.3 Hepatic tissue samples of mice with non alcoholic steatohepatitis

Liver tissue samples from NASH and control mice described in 4.2.6 were also analyzed for MTAP activity.

5.2.4 Preparation of liver samples

Liver samples (10 – 30 mg) were weighted and homogenized in 500 µL of a 50 mM potassium phosphate buffer using “Precelly-Keramik-Kit 1.4 mm vials” (Peqlab Biotechnologie GmbH, Erlangen, Germany). The samples were homogenized twice at 5,500 rpm for 15 s with an intermediate 30-s pause using a Precellys® 24 homogenizer (Peqlab Biotechnologie GmbH). Homogenates were stored on ice until measurement of MTAP activity, for which an aliquot corresponding to 1 mg liver was taken, diluted with buffer to a total volume of 200 µL and spiked with 25 µL each of pyridoxal phosphate and TCEP. The kinetic analysis was started by the addition of 25 µL of 1 µM $^{13}C_5$-MTA solution and 25 µL aliquots were taken at 0, 30, 60, 90, 120, 150, 180, 240, 300 and 600 seconds. To quench the reaction, the aliquots were

transferred into 1.5-mL Eppendorf-cups containing 500 µL MeOH and 10 µL $^{13}C_5$-adenosine as internal standard. The sample was centrifuged at 9,000xg for 5 min at 4°C and the supernatant was transferred to a 1.5-mL glass vial. The solvent was evaporated and the residues were reconstituted in 100 µL of aqueous 0.1 M acetic acid.

5.2.5 Immunoblot of methylthioadenosine phosphorylase and mRNA determination

The determination of total protein and MTAP for liver samples from NASH and control mice was performed as described previously [5]. Briefly, quantitative analysis of MTAP was performed by immunobloting. For protein isolation, samples were lysed in cell lysis-buffer (Cell Signaling, Danvers, MA, USA). Protein concentrations were determined using BCA protein assay reagent (Pierce, Rockford, IL, USA). Equal amounts of protein were denatured at 94°C for 10 min after addition of Roti-load-buffer (Roth, Karlsruhe, Germany) and subsequently separated on NuPage-SDS-gels (Invitrogen, Groningen, The Netherlands). After transferring the proteins onto nitrocellulose-membranes (Invitrogen), the membranes were blocked in 5% milk/TBST for 1 h and incubated with a 1:1,000 dilution of primary monoclonal mouse anti-MTAP antibody (Abcam, Cambridge, UK) overnight at 4°C. A 1:3,000 dilution of mouse anti-Ig-AP (Santa Cruz) was used as secondary antibody. Detection was performed by Amersham ECL detection system (GE healthcare, München, Germany) using Amersham Hyperfilm TM ECL (GE Healthcare).

Isolation of total cellular RNA and reverse transcription were performed as described previously [99]. Quantitative real time-PCR was performed with specific sets of primers by means of LightCycler technology (Roche, Mannheim, Germany) [99].

The experimental work described in chapter 5.2.6 was performed by Barbara Czech in the working group of PD Dr. Claus Hellerbrand, Department of Internal Medicine I.

5.2.6 Instrumentation for methylthioadenosine phosphorylase activity determination

The chromatographic conditions and the instrumentation were the same as used in chapter 4. Briefly, LC-ESI-MS/MS was performed using an Agilent 1200 SL HPLC system (Böblingen, Germany) and a PE Sciex API 4000 QTrap mass spectrometer (Applied Biosystems, Darmstadt, Germany). LC separation was carried out using an Atlantis T3 3µm (2.1 i.d. x 150 mm) reversed phase column (Waters, Eschborn, Germany) and a water-acetonitrile gradient with 0.1% acetic acid and 0.025% HFBA in both solvents.

The API 4000 QTrap mass spectrometer was operated in positive mode with a source temperature of 500°C. Quantitative determination was performed with multiple-reaction monitoring (MRM) using the parameters listed in Table 3 (chapter 4.2.9). Data acquisition and analysis were performed by Analyst version 1.5.1.

5.2.7 Data analysis

Determination of relative rate constants (workflow shown in Figure 27) was carried out using the analyte area response (area $^{13}C_5$-MTA / area $^{13}C_5$-adenosine) over time. A ln transformation results in a linear curve, whose slope is the value of the rate constant of the reaction.

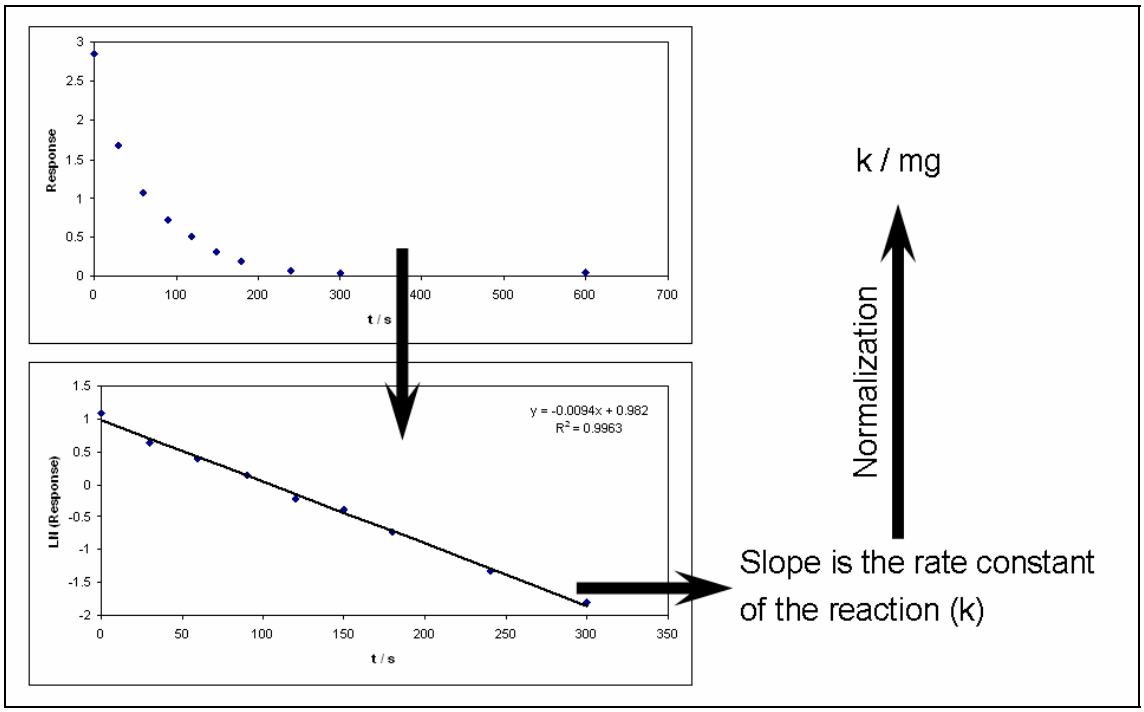

Figure 27: Schematic workflow of the MTAP activity assay.

After normalization, in a first approach to tissue weight, the rate constants of tumor and non-tumor tissue were compared with MTAP protein and MTA concentration. MTA concentrations were determined as described previously [55] (see also chapter 4).

5.3 Results and Discussion

Figure 28 (left) shows that MTA accumulates by a factor of 2.25 in mice with NASH compared to control mice ($p = 0.014$). The activity assay of these samples results in a 50 % decrease in MTAP activity ($p = 5.4E\text{-}5$) in NASH mice compared with healthy mice (Figure 28, middle).

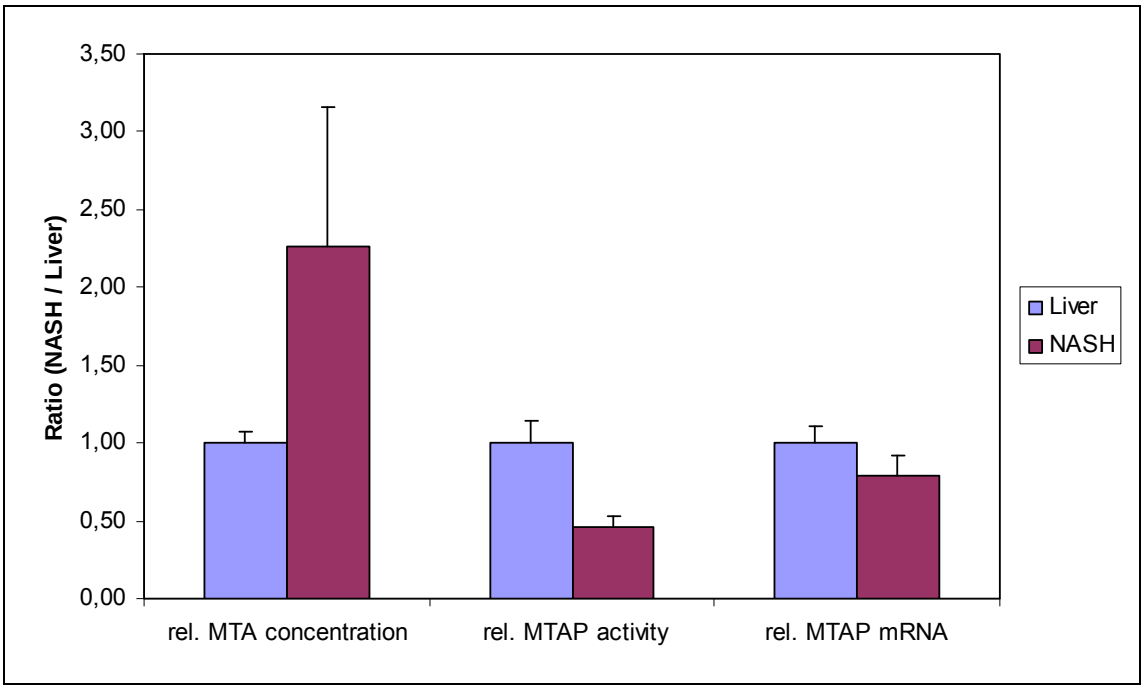

Figure 28: MTA concentration (p=0.014), MTAP activity (p=5.4E-5) and MTAP mRNA levels (p=0.69) in mice (n=5) with and without NASH. Values are normalized to healthy liver.

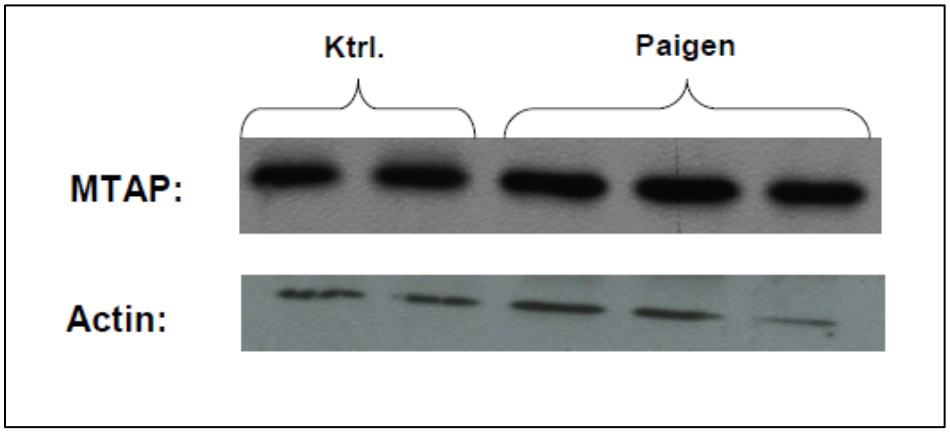

Figure 29: Western blot of MTAP and actin (subset of all samples).

As shown in Figure 28 (right) no significant differences in MTAP mRNA levels were observed (p = 0.69). The same holds true for MTAP protein levels (Figure 29, only a subset of all samples is shown). Therefore, one reason for an accumulation of MTA in NASH mice is a reduced activity of MTAP.

A problem of this data set is that the MTA concentration and MTAP activity is normalized to tissue weight, while MTAP protein is corrected with actin, a marker for cell count. The Paigen/NASH mice show the same MTAP amount in total protein, but the liver of the Paigen/NASH mice contains fat. So the MTAP amount corrected with

total weight should be lower in liver of the Paigen/NASH mice compared to liver of healthy mice. And this normalization will result in no change of MTAP activity (data not shown) but will also increase the MTA concentration in the liver of the Paigen/NASH mice.

This problem clearly indicates that a good parameter for normalization has to be selected and that it is necessary to have a method to determine MTAP quantitatively.

5.4 Conclusions

A stable isotope mass spectrometry based assay for the determination of MTAP activity in different samples was implemented and used in different types of liver biopsies. A decrease in MTAP activity was observed in the liver of NASH mice compared to healthy mice after normalization to tissue weight, which is the easiest normalization parameter.

The quantification of MTAP protein was carried out in a first approach by Western Blot, but this method has the limitation, that it is only semi quantitative because the blots were detected on films.

Nevertheless, the first preliminary results demonstrate the general applicability of the assay to determine MTAP activity in liver samples without using radio-isotopes. However, further steps are needed to optimize the method. This includes the use of protease inhibitors, which were in accordance with the literature not used in the preliminary experiments. Furthermore, buffer selection will be optimized to allow the determination of MTAP protein abundance in the same sample. The optimized assay will be useful to determine MTAP activity in different types of samples.

6. Summary and Outlook

The methionine and polyamine metabolism is an interesting target in the study of tumor metabolism, e.g. polyamine synthesis is a measure of cell proliferation. Since many tumors lack MTAP, they are not capable of metabolizing MTA and metabolic changes in these pathways are expected caused by the assumed accumulation of MTA. An important prerequisite to study these changes is a sensitive and selective method to quantify MTA in samples like cell culture medium, cell pellets and different types of tumor biopsies. In the first part of this thesis a method for the quantification of MTA was developed and validated. The method was successfully used to prove the hypothesized accumulation of MTA in tumors *in vitro* and *in vivo*.

In the next step, this method was expanded to key metabolites of the methionine and polyamine pathways and alterations in these pathways caused by a lack of MTAP were analyzed. Different types of tumors, including malignant melanoma, glioma, hepatocellular and renal carcinoma, and liver tissue samples from different types of liver diseases, including NASH and cirrhosis, showed in all cases an increase of MTA, SAM and putrescine *in vitro* as well as *in vivo*.

To clarify further consequence of a loss of MTAP a mass spectrometry based activity assay was developed and MTAP activity in diseased and healthy tissue samples was measured. In case of NASH mice an inverse correlation between MTA concentration and MTAP activity was found after normalization to tissue weight, while MTAP protein and mRNA remained nearly constant. In further experiments this assay was successfully applied to human liver biopsies (a decrease of $^{13}C_5$-MTA was observed over time), but for these samples the assay has to be further optimized.

At the moment MTAP quantification is carried out by immunobloting and detection with photographic films. This procedure was improved by the usage of a CCD

camera, which results in densitometric analysis with the possibility to get quantitative values. As a standard recombinant MTAP (rMTAP) was used, but the MTAP antibody showed different binding kinetics to the native and recombinant MTAP. To solve this problem a quantification of MTAP via so called AQUA-peptides is planed. In 2003 the group of Steve Gygi presented a new technique for the quantification of proteins [100]. Using the common principle of a stable isotope labeled analog as an internal standard, the group synthesizes an AQUA-peptide. This is a synthetic tryptic peptide corresponding to a protein of interest and contains one stable isotope labeled amino acid resulting in a slight increase in molecular weight. The synthetic and native peptide will show the same properties during chromatography and ionization. However, by mass spectrometry both peptides are distinguished. For quantification a known amount of the AQUA-peptide is added to the protein sample and after tryptic digestion the sample is analyzed by HPLC-MS/MS. Using the AQUA-peptide as internal standard quantification is performed by the peak ratio. For quantification of MTAP it was decided to use two different AQUA-peptides and three MRM-transitions each. It is planed to set up an MRM-method for MTAP quantification at the 4000 QTrap mass spectrometer.

Normalization to tissue weight was not possible for human liver biopsies because the control samples were cirrhotic have more extra cellular matrix. Normalization to β-actin or total protein content was tested, but the results were not satisfying. A possible explanation is that the liver biopsies do not contain any protease inhibitor because they were sampled for histological examination and the samples are now still stored over years. However, inhomogeneities in the samples are still remaining and not correctable with only one sample. To correct for inhomogeneities multiple sampling of biopsies is necessary.

Nevertheless, an activity assay using stable isotope labeled compounds is still not known in literature and will make the handling of the enzymatic activity a bit easier and safer.

7. References

[1] A.E. Pegg, Cancer Res 48 (1988) 759.

[2] F. Della Ragione, M. Carteni-Farina, V. Gragnaniello, M.I. Schettino, V. Zappia, J Biol Chem 261 (1986) 12324.

[3] H.G. Williams-Ashman, J. Seidenfeld, P. Galletti, Biochem Pharmacol 31 (1982) 277.

[4] J. Seidenfeld, J. Wilson, H.G. Williams-Ashman, Biochem Biophys Res Commun 95 (1980) 1861.

[5] C. Hellerbrand, M. Muhlbauer, S. Wallner, M. Schuierer, I. Behrmann, F. Bataille, T. Weiss, J. Scholmerich, A.K. Bosserhoff, Carcinogenesis 27 (2006) 64.

[6] I. Behrmann, S. Wallner, W. Komyod, P.C. Heinrich, M. Schuierer, R. Buettner, A.K. Bosserhoff, Am J Pathol 163 (2003) 683.

[7] S.A. Christopher, P. Diegelman, C.W. Porter, W.D. Kruger, Cancer Res 62 (2002) 6639.

[8] Y. Hori, H. Hori, Y. Yamada, C.J. Carrera, M. Tomonaga, S. Kamihira, D.A. Carson, T. Nobori, Int J Cancer 75 (1998) 51.

[9] N. Kamatani, D.A. Carson, Cancer Res 40 (1980) 4178.

[10] N. Kamatani, W.A. Nelson-Rees, D.A. Carson, Proc Natl Acad Sci U S A 78 (1981) 1219.

[11] T. Nobori, K. Takabayashi, P. Tran, L. Orvis, A. Batova, A.L. Yu, D.A. Carson, Proc Natl Acad Sci U S A 93 (1996) 6203.

[12] A.P. Stevens, B. Spangler, S. Wallner, M. Kreutz, K. Dettmer, P.J. Oefner, A.K. Bosserhoff, J Cell Biochem 106 (2009) 210.

[13] P.J. Wild, S. Meyer, M. Landthaler, F. Hofstaedter, A.K. Bosserhoff, J Dtsch Dermatol Ges 5 (2007) 456.

[14] K.A. Mowen, J. Tang, W. Zhu, B.T. Schurter, K. Shuai, H.R. Herschman, M. David, Cell 104 (2001) 731.

[15] S. Meyer, P.J. Wild, T. Vogt, F. Bataille, C. Ehret, S. Gantner, M. Landthaler, M. Klinkhammer-Schalke, F. Hofstaedter, A.K. Bosserhoff, Exp Dermatol 19 (2010) e251.

[16] B. Kammerer, A. Frickenschmidt, C.E. Muller, S. Laufer, C.H. Gleiter, H. Liebich, Anal Bioanal Chem 382 (2005) 1017.

[17] B. Kammerer, A. Frickenschmidt, C.H. Gleiter, S. Laufer, H. Liebich, J Am Soc Mass Spectrom 16 (2005) 940.

[18] M. Porcelli, G. Cacciapuoti, A. Oliva, V. Zappia, J Chromatogr 440 (1988) 151.

[19] F. Della Ragione, A. Oliva, V. Gragnaniello, M. Fioretti, A. Fioretti, L.F. Menna, V. Papparella, V. Zappia, J Chromatogr 440 (1988) 141.

[20] K. Kaneko, S. Fujimori, N. Kamatani, I. Akaoka, Biochim Biophys Acta 802 (1984) 169.

[21] J. Bremer, Biochimica et Biophysica Acta 48 (1961) 622.

[22] S.S. Oja, M.L. Karvonen, P. Lähdesmäki, Brain Research 55 (1973) 173.

[23] P. Bjornstad, J. Bremer, J Lipid Res 7 (1966) 38.

[24] S.H. Kirsch, J.P. Knapp, J. Geisel, W. Herrmann, R. Obeid, J Chromatogr B Analyt Technol Biomed Life Sci 877 (2009) 3865.

[25] H. Gellekink, D. van Oppenraaij-Emmerzaal, A. van Rooij, E.A. Struys, M. den Heijer, H.J. Blom, Clin Chem 51 (2005) 1487.

[26] R. Djurhuus, Anal Biochem 113 (1981) 352.

[27] D.L. Kramer, P. Diegelman, J. Jell, S. Vujcic, S. Merali, C.W. Porter, J Biol Chem 283 (2008) 4241.

[28] A.P. Stevens, K. Dettmer, S. Wallner, A.K. Bosserhoff, P.J. Oefner, J Chromatogr B Analyt Technol Biomed Life Sci 876 (2008) 123.

[29] A.L. Subhi, P. Diegelman, C.W. Porter, B. Tang, Z.J. Lu, G.D. Markham, W.D. Kruger, J Biol Chem 278 (2003) 49868.

[30] T.R. Cataldi, G. Bianco, S. Abate, D. Mattia, Rapid Commun Mass Spectrom 23 (2009) 3465.

[31] J. Krijt, A. Duta, V. Kozich, J Chromatogr B Analyt Technol Biomed Life Sci 877 (2009) 2061.

[32] J.A. Byun, S.H. Lee, B.H. Jung, M.H. Choi, M.H. Moon, B.C. Chung, Biomed Chromatogr 22 (2008) 73.

[33] P.J. Oefner, S. Wongyai, G. Bonn, Clin Chim Acta 205 (1992) 11.

[34] M.R. Hakkinen, T.A. Keinanen, J. Vepsalainen, A.R. Khomutov, L. Alhonen, J. Janne, S. Auriola, J Pharm Biomed Anal 45 (2007) 625.

[35] H. Kaspar, K. Dettmer, W. Gronwald, P.J. Oefner, J Chromatogr B Analyt Technol Biomed Life Sci 870 (2008) 222.

[36] J. Le Boucher, C. Charret, C. Coudray-Lucas, J. Giboudeau, L. Cynober, Clin Chem 43 (1997) 1421.

[37] T. Soga, Y. Kakazu, M. Robert, M. Tomita, T. Nishioka, Electrophoresis 25 (2004) 1964.

[38] M. Piraud, C. Vianey-Saban, K. Petritis, C. Elfakir, J.P. Steghens, D. Bouchu, Rapid Commun Mass Spectrom 19 (2005) 1587.

[39] G. Cacciapuoti, C. Bertoldo, A. Brio, V. Zappia, M. Porcelli, Extremophiles 7 (2003) 159.

[40] G. Cacciapuoti, S. Gorassini, M.F. Mazzeo, R.A. Siciliano, V. Carbone, V. Zappia, M. Porcelli, Febs J 274 (2007) 2482.

[41] G. Cacciapuoti, M. Porcelli, C. Bertoldo, M. De Rosa, V. Zappia, J Biol Chem 269 (1994) 24762.

[42] K. Dettmer, P.A. Aronov, B.D. Hammock, Mass Spectrom Rev 26 (2007) 51.

[43] O. Fiehn, Plant Mol Biol 48 (2002) 155.

[44] S.G. Villas-Boas, S. Mas, M. Akesson, J. Smedsgaard, J. Nielsen, Mass Spectrom Rev 24 (2005) 613.

[45] M. Guilhaus, J. Mass Spectrom. 30 (1995) 1519.

[46] B.A. Mamyrin, Int. J. Mass Spectrom. 206 (2001) 251.

[47] M. Guilhaus, D. Selby, V. Mlynski, Mass Spectrom Rev 19 (2000) 65.

[48] K. Wille, J. Vanden Bussche, H. Noppe, E. De Wulf, P. Van Caeter, C.R. Janssen, H.F. De Brabander, L. Vanhaecke, J Chromatogr A 1217 (2010) 6616.

[49] K. Wille, J.A. Kiebooms, M. Claessens, K. Rappe, J. Vanden Bussche, H. Noppe, N. Van Praet, E. De Wulf, P. Van Caeter, C.R. Janssen, H.F. De Brabander, L. Vanhaecke, Anal Bioanal Chem (2011) doi 10.1007/s00216.

[50] P.A. Lara-Martin, E. Gonzalez-Mazo, B.J. Brownawell, J Chromatogr A (2011) doi:10.1016/j.chroma.2011.02.031.

[51] B. Timischl, K. Dettmer, H. Kaspar, M. Thieme, P.J. Oefner, Electrophoresis 29 (2008) 2203.

[52] E.M. Thurman, I. Ferrer, A.R. Fernandez-Alba, J Chromatogr A 1067 (2005) 127.

[53] J.D. McCarter, S.G. Withers, J Biol Chem 271 (1996) 6889.

[54] A.L. Stolker, W. Niesing, R. Fuchs, R.J. Vreeken, W.M. Niessen, U.A. Brinkman, Anal Bioanal Chem 378 (2004) 1754.

[55] A.P. Stevens, K. Dettmer, G. Kirovski, K. Samejima, C. Hellerbrand, A.K. Bosserhoff, P.J. Oefner, J Chromatogr A 1217 (2010) 3282.

[56] K. Gevaert, J. Vandekerckhove, Electrophoresis 21 (2000) 1145.

[57] B. Schubert, M. Pavlic, K. Libiseller, H. Oberacher, Anal Bioanal Chem 392 (2008) 1299.

[58] X. Zhao, J. Fritsche, J. Wang, J. Chen, K. Rittig, P. Schmitt-Kopplin, A. Fritsche, H.U. Haring, E.D. Schleicher, G. Xu, R. Lehmann, Metabolomics 6 (2010) 362.

[59] M. Zhou, J.F. McDonald, F.M. Fernandez, J Am Soc Mass Spectrom 21 (2010) 68.

[60] J.W. Hager, Rapid Commun. Mass Spectrom 16 (2002) 512.

[61] J.C. Le Blanc, J.W. Hager, A.M. Ilisiu, C. Hunter, F. Zhong, I. Chu, Proteomics 3 (2003) 859.

[62] J.W. Hager, J.C. Le Blanc, J Chromatogr A 1020 (2003) 3.

[63] Commission of the European Communities. Official Journal of the European Communities. 2002; 221:8. (available online at: http://eur-lex.europa.eu/LexUriServ/LexUriServ.do?uri=OJ:L:2002:221:0008:0036:EN:PDF).

[64] T.N. Decaestecker, S.R. Vande Casteele, P.E. Wallemacq, C.H. Van Peteghem, D.L. Defore, J.F. Van Bocxlaer, Anal Chem 76 (2004) 6365.

[65] A.C. Li, D. Alton, M.S. Bryant, W.Z. Shou, Rapid Commun Mass Spectrom 19 (2005) 1943.

[66] L. Politi, L. Morini, A. Polettini, Clin Chim Acta 386 (2007) 46.

[67] T.M. Annesley, Clin Chem 49 (2003) 1041.

[68] P. De Bievre, Fresenius J Anal Chem 337 (1990) 766.

[69] M.J. Robins, F. Hansske, S.F. Wnuk, T. Kanai, Can. J. Chem. 69 (1991) 1468.

[70] K. Jacob, F. Wach, U. Holzapfel, R. Hein, E. Lengyel, R. Buettner, A.K. Bosserhoff, Melanoma Res 8 (1998) 211.

[71] F.a.D.A. U. S. Department of Health and Human Services, Center for Drug Evaluation and Research (CDER), Center for Veterinary Medicine (CVM), (2001).

[72] M.K. Riscoe, A.J. Ferro, J Biol Chem 259 (1984) 5465.

[73] H. Hibasami, J.L. Hoffman, A.E. Pegg, J Biol Chem 255 (1980) 6675.

[74] K. Singer, Dissertation (Universität Regensburg) 2010 (available online at: http://epub.uni-regensburg.de/17309/1/20100929_Diss_Singer.pdf).

[75] J. Ray, D.A. Peterson, M. Schinstine, F.H. Gage, Proc Natl Acad Sci U S A 90 (1993) 3602.

[76] G. Kirovski, A.P. Stevens, B. Czech, K. Dettmer, T.S. Weiss, P. Wild, A. Hartmann, A.K. Bosserhoff, P.J. Oefner, C. Hellerbrand, Am J Pathol 178 (2011) 1145.

[77] T. Hara, Y.J. Xu, H. Sasaki, M. Niitu, K. Samejima, J. Labelled Cpd. Radiopharm. 43 (2000) 1005.

[78] J. Wagner, N. Claverie, C. Danzin, Anal Biochem 140 (1984) 108.

[79] J.M. Clark, A.M. Diehl, Jama 289 (2003) 3000.

[80] N. Matsuzawa, T. Takamura, S. Kurita, H. Misu, T. Ota, H. Ando, M. Yokoyama, M. Honda, Y. Zen, Y. Nakanuma, K. Miyamoto, S. Kaneko, Hepatology 46 (2007) 1392.

[81] C. Dorn, M.O. Riener, G. Kirovski, M. Saugspier, K. Steib, T.S. Weiss, E. Gabele, G. Kristiansen, A. Hartmann, C. Hellerbrand, Int J Clin Exp Pathol 3 (2010) 505.

[82] C. Hellerbrand, B. Stefanovic, F. Giordano, E.R. Burchardt, D.A. Brenner, J Hepatol 30 (1999) 77.

[83] O.M. Grauer, S. Nierkens, E. Bennink, L.W. Toonen, L. Boon, P. Wesseling, R.P. Sutmuller, G.J. Adema, Int J Cancer 121 (2007) 95.

[84] P.M. Ueland, H. Refsum, S.P. Stabler, M.R. Malinow, A. Andersson, R.H. Allen, Clin Chem 39 (1993) 1764.

[85] C.W. Tabor, H. Tabor, Annu Rev Biochem 45 (1976) 285.

[86] C.E. Seyfried, D.R. Morris, Cancer Res 39 (1979) 4861.

[87] J. Janne, H. Poso, A. Raina, Biochim Biophys Acta 473 (1978) 241.

[88] R.H. Fillingame, C.M. Jorstad, D.R. Morris, Proc Natl Acad Sci U S A 72 (1975) 4042.

[89] C. Berasain, H. Hevia, J. Fernandez-Irigoyen, E. Larrea, J. Caballeria, J.M. Mato, J. Prieto, F.J. Corrales, E.R. Garcia-Trevijano, M.A. Avila, Biochim Biophys Acta 1690 (2004) 276.

[90] H. Hibasami, R.T. Borchardt, S.Y. Chen, J.K. Coward, A.E. Pegg, Biochem J 187 (1980) 419.

[91] K. Nishioka, V.B. Grossie, T.H. Chang, J.A. Ajani, D.M. Ota, J Surg Oncol 47 (1991) 117.

[92] T. Narisawa, M. Takahashi, M. Niwa, H. Koyama, H. Kotanagi, N. Kusaka, Y. Yamazaki, O. Nagasawa, K. Koyama, A. Wakizaka, et al., Cancer 63 (1989) 1572.

[93] T. Suzuki, M. Maruno, K. Wada, N. Kagawa, Y. Fujimoto, N. Hashimoto, S. Izumoto, T. Yoshimine, Brain Tumor Pathol 21 (2004) 27.

[94] T. Fiskerstrand, B. Christensen, O.B. Tysnes, P.M. Ueland, H. Refsum, Cancer Res 54 (1994) 4899.

[95] A.L. Subhi, B. Tang, B.R. Balsara, D.A. Altomare, J.R. Testa, H.S. Cooper, J.P. Hoffman, N.J. Meropol, W.D. Kruger, Clin Cancer Res 10 (2004) 7290.

[96] F. Della Ragione, A.E. Pegg, Biochem J 210 (1983) 429.

[97] R.T. Borchardt, J Med Chem 23 (1980) 347.

[98] D. Russell, S.H. Snyder, Proc Natl Acad Sci U S A 60 (1968) 1420.

[99] C. Hellerbrand, T. Amann, J. Schlegel, P. Wild, F. Bataille, T. Spruss, A. Hartmann, A.K. Bosserhoff, Gut 57 (2008) 243.

[100] S.A. Gerber, J. Rush, O. Stemman, M.W. Kirschner, S.P. Gygi, Proc Natl Acad Sci U S A 100 (2003) 6940.

8. Appendix

Table A 1: Metabolite concentrations in liver samples of mice with non-alcoholic steatohepatitis (NASH).

	Sample	Adenine	Adenosine	Homocysteine	MTA	Ornithine	Putrescine	Acetyl-Put	SAH	SAM	Spermidine	N1-Acetyl-Spd	N8-Acetyl-Spd	Spermine	Acetyl-Spm
Healthy control [nmol / g]	BPE01_001	8,35	33,57	0,82	0,68	7481,69	9,90	0,00	99,18	27,14	699,57	6,39	1,41	522,95	2,84
	BPE02_008	11,05	34,82	0,92	0,79	6084,33	11,57	0,01	109,89	23,43	654,33	5,46	1,58	588,17	2,95
	BPE03_015	11,15	30,38	0,88	0,68	7634,80	10,35	0,02	97,14	19,85	615,38	3,88	1,02	463,62	2,68
	BPE04_022	8,53	35,65	0,68	0,68	4521,61	11,11	0,01	87,50	22,25	625,38	3,67	1,03	464,12	2,83
	BPE05_029	10,87	36,64	0,67	0,66	5393,15	9,91	0,01	115,81	26,33	732,37	6,08	1,22	591,41	3,15
	Mean:	**9,99**	**34,21**	**0,79**	**0,70**	**6223,12**	**10,57**	**0,01**	**101,91**	**23,80**	**665,41**	**5,10**	**1,26**	**526,05**	**2,89**
	Stdev.:	**1,42**	**2,42**	**0,12**	**0,05**	**1339,78**	**0,74**	**0,01**	**11,12**	**2,99**	**49,70**	**1,25**	**0,24**	**62,99**	**0,17**
	rel. Stdev.:	**0,14**	**0,07**	**0,15**	**0,08**	**0,22**	**0,07**	**0,63**	**0,11**	**0,13**	**0,07**	**0,25**	**0,19**	**0,12**	**0,06**
NASH [nmol / g]	BPE06_002	0,72	19,85	0,57	0,73	4271,24	27,66	0,04	14,05	26,42	326,83	5,10	1,05	137,48	0,60
	BPE07_009	3,16	26,66	1,56	2,43	6939,10	38,27	0,03	22,09	66,30	568,05	7,32	1,45	293,18	1,18
	BPE08_016	0,96	13,98	0,56	1,64	4901,53	28,52	0,08	10,52	34,25	358,27	6,35	1,12	134,69	0,68
	BPE09_023	1,90	11,27	1,54	1,30	4378,67	34,33	0,11	7,02	28,80	245,85	4,79	0,76	52,46	0,23
	BPE10_030	2,07	11,02	1,38	1,80	5273,19	29,86	0,09	6,61	34,22	403,18	5,46	1,10	115,02	0,44
	Mean:	**1,76**	**16,56**	**1,12**	**1,58**	**5152,75**	**31,73**	**0,07**	**12,06**	**38,00**	**380,43**	**5,81**	**1,09**	**146,57**	**0,63**
	Stdev.:	**0,97**	**6,67**	**0,51**	**0,63**	**1077,60**	**4,47**	**0,03**	**6,37**	**16,18**	**119,58**	**1,03**	**0,25**	**88,84**	**0,35**
	rel. Stdev.:	**0,55**	**0,40**	**0,46**	**0,40**	**0,21**	**0,14**	**0,50**	**0,53**	**0,43**	**0,31**	**0,18**	**0,22**	**0,61**	**0,56**

Table A 2: Metabolite concentrations in liver samples of mice with liver cirrhosis.

	Sample	Adenine	Adenosine	Homocysteine	MTA	Ornithine	Putrescine	SAH	SAM	Spermidine	Spermine
Contol [mol / g]	1	3,86	13,70	0,38	0,22	1512,33	5,01	16,03	6,22	2271,23	635,62
	2	4,98	7,66	0,63	0,22	1736,24	3,81	21,19	6,56	2454,13	623,85
	3	4,33	31,19	0,74	0,81	1532,18	5,89	27,72	24,03	2329,21	675,74
	Mean	**4,39**	**17,52**	**0,58**	**0,42**	**1593,58**	**4,90**	**21,65**	**12,27**	**2351,52**	**645,07**
	Stdev.:	**0,56**	**12,22**	**0,18**	**0,34**	**123,94**	**1,05**	**5,86**	**10,19**	**93,47**	**27,21**
	rel. Stdev.:	**0,13**	**0,70**	**0,31**	**0,82**	**0,08**	**0,21**	**0,27**	**0,83**	**0,04**	**0,04**
Cirrhosis [nmol / g]	13	1,05	8,94	0,43	3,68	927,17	94,09	13,92	77,95	2047,24	405,51
	14	2,07	6,35	0,31	3,46	894,44	110,19	17,76	86,48	2388,89	405,56
	15	0,92	7,23	0,48	2,73	672,35	63,26	28,03	69,32	2348,48	363,64
	Mean	**1,35**	**7,51**	**0,41**	**3,29**	**831,32**	**89,18**	**19,90**	**77,92**	**2261,54**	**391,57**
	Stdev.:	**0,63**	**1,31**	**0,09**	**0,50**	**138,64**	**23,85**	**7,30**	**8,58**	**186,68**	**24,19**
	rel. Stdev.:	**0,47**	**0,18**	**0,22**	**0,15**	**0,17**	**0,27**	**0,37**	**0,11**	**0,08**	**0,06**

Table A 3: Metabolite concentrations in mice glioma samples.

	Sample	Adenine	Adenosine	Homocysteine	MTA	Ornithine	Putrescine	Acetyl-Put	SAH	SAM	Spermidine	N1-Acetyl-Spd	N8-Acetyl-Spd	Spermine	Acetyl-Spm
Healthy control [nmol / g]	HC1_001	19,38	492,27	0,07	0,85	9,85	7,16	< 0	13,20	24,43	329,90	1,01	0,20	144,33	0,34
	HC2_005	13,41	468,99	0,01	0,63	5,93	5,43	< 0	12,25	20,08	204,26	1,30	0,17	138,76	0,46
	HC3_009	13,14	439,22	< 0	0,47	4,35	4,59	< 0	7,33	19,49	185,88	1,24	0,19	132,55	0,44
	HC4_013	16,00	478,26	< 0	0,81	5,51	5,57	< 0	8,17	23,04	219,13	1,57	0,25	155,65	0,66
	Mean:	**15,48**	**469,68**	**0,04**	**0,69**	**6,41**	**5,69**	< 0	**10,24**	**21,76**	**234,79**	**1,28**	**0,20**	**142,82**	**0,47**
	Stdev.:	**2,90**	**22,45**	**0,05**	**0,17**	**2,39**	**1,08**	**n.d.**	**2,91**	**2,36**	**64,84**	**0,23**	**0,03**	**9,81**	**0,13**
	rel. Stdev.:	**18,74**	**4,78**	**121,12**	**25,07**	**37,23**	**18,93**	**n.d.**	**28,47**	**10,87**	**27,62**	**18,13**	**16,37**	**6,87**	**28,23**
Non tumorous tissue [nmol / g]	NT1_002	11,38	545,87	0,08	0,95	7,66	60,09	0,04	8,90	33,12	423,39	5,37	0,37	168,35	0,36
	NT2_006	9,85	515,00	0,07	0,69	6,90	24,10	< 0	6,65	27,40	220,50	3,24	0,25	185,50	0,69
	NT3_010	10,42	455,76	0,16	0,63	7,58	35,45	< 0	5,84	24,61	353,94	4,94	0,27	179,39	0,67
	NT4_014	16,04	503,57	0,03	0,55	4,50	35,25	< 0	6,29	23,18	385,71	9,21	0,50	153,21	0,50
	Mean:	**11,92**	**505,05**	**0,09**	**0,70**	**6,66**	**38,72**	**0,04**	**6,92**	**27,08**	**345,89**	**5,69**	**0,35**	**171,61**	**0,56**
	Stdev.:	**2,81**	**37,40**	**0,05**	**0,17**	**1,48**	**15,20**	**n.d.**	**1,36**	**4,39**	**88,28**	**2,52**	**0,12**	**14,17**	**0,15**
	rel. Stdev.:	**23,60**	**7,41**	**59,75**	**24,77**	**22,21**	**39,25**	**n.d.**	**19,69**	**16,23**	**25,52**	**44,37**	**33,25**	**8,26**	**27,61**
Tumor [nmol / g]	T1_003	1,19	24,79	1,07	2,07	195,86	127,81	0,57	10,12	68,64	656,80	17,46	1,75	297,63	2,21
	T2_007	1,84	36,62	1,02	1,95	172,62	120,91	0,64	9,96	66,92	646,39	19,85	1,98	322,05	3,11
	T3_011	1,03	53,18	1,00	2,25	172,24	120,07	0,14	9,40	68,23	608,70	39,13	1,83	289,63	9,13
	T4_015	1,86	53,08	0,93	1,92	127,47	140,66	0,74	11,65	62,64	675,82	18,24	1,48	301,10	3,79
	Mean:	**1,48**	**41,92**	**1,00**	**2,05**	**167,05**	**127,36**	**0,52**	**10,28**	**66,61**	**646,93**	**23,67**	**1,76**	**302,60**	**4,56**
	Stdev.:	**0,43**	**13,82**	**0,06**	**0,15**	**28,60**	**9,52**	**0,27**	**0,96**	**2,75**	**28,25**	**10,36**	**0,21**	**13,83**	**3,11**
	rel. Stdev.:	**29,21**	**32,96**	**5,83**	**7,47**	**17,12**	**7,47**	**51,18**	**9,36**	**4,12**	**4,37**	**43,75**	**11,83**	**4,57**	**68,27**

Table A 4: Metabolite concentrations in human renal carcinoma samples.

	Sample	Adenin	Adenosine	Homocysteine	MTA	Ornithine	Putrescine	Acetyl-Put	SAH	SAM	Spermidine	N1-Acetyl-Spd	N8-Acetyl-Spd	Spermine	Acetyl-Spm
Tumor [nmol / g]	Tumor 1	0,62	1,68	1,28	6,99	0,71	12,53	< LOD	2,19	6,26	4,15	5,73	0,38	3,11	1,26
	Tumor 2	0,91	0,43	2,35	3,12	0,69	4,75	< LOD	1,41	3,85	2,13	2,85	1,08	1,26	0,50
	Tumor 3	1,42	1,50	1,05	2,74	0,97	1,80	< LOD	1,95	3,31	3,61	6,51	0,38	1,42	2,11
	Tumor 4	0,28	2,32	4,10	2,54	0,68	7,28	< LOD	2,24	2,05	1,27	7,40	0,40	0,96	1,54
	Tumor 5	0,47	1,92	3,77	0,66	0,63	3,46	< LOD	1,41	0,81	1,41	0,87	0,25	0,74	0,53
	Mean:	**0,74**	**1,57**	**2,51**	**3,21**	**0,74**	**5,97**	**n.d.**	**1,84**	**3,25**	**2,51**	**4,67**	**0,50**	**1,50**	**1,19**
	Stdev.:	**0,44**	**0,71**	**1,39**	**2,31**	**0,13**	**4,18**	**n.d.**	**0,40**	**2,05**	**1,31**	**2,73**	**0,33**	**0,94**	**0,69**
	rel. Stdev:	**0,60**	**0,45**	**0,56**	**0,72**	**0,18**	**0,70**	**n.d.**	**0,22**	**0,63**	**0,52**	**0,58**	**0,67**	**0,63**	**0,58**
Healthy [nmol / g]	Healthy 1	0,51	0,69	1,34	1,11	1,42	1,62	< LOD	1,37	1,05	1,32	1,08	1,11	1,27	1,60
	Healthy 2	1,40	0,78	0,86	0,96	0,58	1,25	< LOD	0,62	0,98	0,94	0,89	0,85	0,89	0,63
	Healthy 3	1,16	1,50	1,10	0,77	0,66	0,55	< LOD	0,44	0,91	0,68	0,52	0,55	0,73	0,47
	Healthy 4	1,18	0,90	1,20	0,92	1,20	0,26	< LOD	1,33	0,88	0,88	0,98	1,36	1,07	0,37
	Healthy 5	0,76	1,12	0,50	1,24	1,14	1,32	< LOD	1,25	1,18	1,18	1,53	1,13	1,05	1,94
	Mean:	**1,00**	**1,00**	**1,00**	**1,00**	**1,00**	**1,00**	**n.d.**	**1,00**	**1,00**	**1,00**	**1,00**	**1,00**	**1,00**	**1,00**
	Stdev.:	**0,36**	**0,32**	**0,33**	**0,18**	**0,36**	**0,57**	**n.d.**	**0,44**	**0,12**	**0,25**	**0,36**	**0,31**	**0,20**	**0,72**
	rel. Stdev:	**0,36**	**0,32**	**0,33**	**0,18**	**0,36**	**0,57**	**n.d.**	**0,44**	**0,12**	**0,25**	**0,36**	**0,31**	**0,20**	**0,72**

9. Curriculum Vitae

Personal Data:

Name: Axel Peter Stevens

Nationality: German

Date of Birth: 30.11.1981

Education:

10/2006 – present:	Natural Sciences Graduate Student at the Institute of Functional Genomics, University of Regensburg, Germany: Analysis of intermediates of the methionine and polyamine metabolism by liquid chromatography-tandem mass spectrometry (Advisor: Prof. Dr. Peter J. Oefner)
09/2005 – 07/2006:	Diploma Thesis at the Institute of Analytical Chemistry, University of Leipzig, Germany: Adaption of the capillary batch injection to the capillary electrophoresis with electrochemical detection (Advisor: Prof. Dr. F.-M. Matysik)
10/2001 – 07/2006	Chemistry studies at the University of Leipzig, Germany
08/1992 – 07/2001	High school in Bad Homburg
08/1988 – 07/1992	Primary school in Friedrichsdorf

Awards:

- 3rd Place in the 2nd round of "Jugend forscht" (German youth research competition) in the chemistry section (2001)
- Travel grant of the AK Separation Science (Society of German Chemists) for the ISC 2010 held in Valencia / Spain
- Travel grant of the AK Separation Science (Society of German Chemists) for the HPLC 2009 held in Dresden / Germany.
- Travel grant of the Division of Analytical Chemistry (Society of German Chemists) for the ANAKON 2009 held in Berlin / Germany.
- Travel grant of the AK Separation Science (Society of German Chemists) for the ISC 2008 held in Münster / Germany.

10. Publications & Presentations

10.1 Publications

[1] G. Kirovski, **A. P. Stevens**, B. Czech, K. Dettmer, T. S. Weiss, P. Wild, A. Hartmann, A. K. Bosserhoff, P. J. Oefner, C. Hellerbrand; Downregulation of methylthioadenosine phosphorylase (MTAP) induces progression of hepatocellular carcinoma via accumulation of 5'-deoxy-5'-methylthioadenosine (MTA); Am. J. Pathol. 2011; 178(3): 1145 – 1152.

[2] K. Dettmer, **A. P. Stevens**, S. R. Fagerer, H. Kaspar, P. J. Oefner; Amino acid analysis in physiological samples by GC-MS with propylchloroformate derivatization and iTRAQ-LC-MS/MS; Amino Acid Analysis Handbook, Humana/Springer, in press.

[3] **A. P. Stevens**, K. Dettmer, G. Kirovski, K. Samejima, C. Hellerbrand, A. K. Bosserhoff, P. J. Oefner; Quantification of intermediates of the methionine and polyamine metabolism by liquid chromatography-tandem mass spectrometry in cultured tumor cells and liver biopsies; J. Chromatogr. A 2010;1217(19): 3282 – 3288.

[4] **A. P. Stevens**, K. Dettmer, A. K. Bosserhoff, P. J. Oefner; Bestimmung von 5'-Deoxy-5'-methylthioadenosin in Melanomzellen – Ein potentieller Marker für das Ansprechen auf eine Interferon-Therapie?; GIT Special – Separation 2009 (1): 7 – 9.

[5] **A. P. Stevens**, B. Spangler, S. Wallner, M. Kreutz, K. Dettmer, P. J. Oefner, A. K. Bosserhoff; Direct and tumor microenvironment mediated influences of 5'-deoxy-5'- (methylthio)adenosine on tumor progression of malignant melanoma; J. Cell Biochem. 2009; 106(2): 210 – 219.

[6] **A. P. Stevens**, K. Dettmer, S. Wallner, A. K. Bosserhoff, P. J. Oefner; Quantitative analysis of 5'-deoxy-5'-methylthioadenosine in melanoma cells by liquid chromatography-stable isotope ratio tandem mass spectrometry; J. Chromatogr. B 2008; 876(1): 123 – 128.

[7] **A. Stevens**, F.-M. Matysik; Kapillar-Batch-Injektion: Ein neues Injektionskonzept für die Kapillarelektrophorese mit kurzen Kapillaren - eine Alternative zur Chipelektrophorese?; in U. Guth und W. Vonau (Hgs.): „Elektrochemische Grundlagenforschung und deren Anwendung in der Elektrochemie", Die Deutsche Bibliothek, 2006, ISBN 978-3-00-019932-5, Seite 119 – 124

10.2 Oral & Poster Presentations

[1] ISC 2010: **Activity assay of methylthioadenosine phosphorylase in tissue specimens by means of stable isotope labeled methylthioadenosine and LC-MS/MS** (oral)

[2] HPLC 2009: **Quantification of Intermediates of the Methionine and Polyamine Pathways in Different Tumor Cell Lines** (poster)

[3] Anakon 2009: **Quantification of intermediates of the methionine and polyamine cycles in different tumor cell lines** (oral)

[4] 19. Doktorandenseminar des AK „Separation Sciences" der GDCh 2009: **Quantification of metabolites of the methionine and polyamine pathways in different tumor cell lines** (oral)

[5] ISC 2008: **Determination of 5'-deoxy-5'-(methylthio)adenosine in melanoma cell line samples** (poster)

[6] 1st European Chemistry Congress 2006: **Capillary batch injection: A novel injection concept for capillary electrophoresis - an alternative to chip electrophoresis?** (poster)

[7] MSB 2006: **Capillary batch injection: A new injection concept for microfluidic systems** (poster)

11. Summary

5'-Deoxy-5'-methylthioadenosine (MTA) is formed in the course of the synthesis of polyamines from S-adenosylmethionine (SAM). Tumors lack the enzyme methylthioadenosine phosphorylase (MTAP), which metabolizes MTA, and should accumulate MTA. In a first step, a method for quantification of MTA by liquid chromatography-mass spectrometry was developed and the postulated accumulation of MTA in tumors and tumor cell lines lacking MTAP could be demonstrated. To elucidate further consequences of a lack of MTAP in tumor cells, the method was expanded to most of the metabolites in the methionine and polyamine pathways. With this method it could be shown, that MTA, putrescine and SAM correlate in concentration. So, the accumulation of MTA has a direct influence on the synthesis of the polyamines. This correlation could be observed in different tumor species, e.g. malignant melanoma, HCC, renal carcinoma and brain tumors, as well as in different liver diseases (fibrosis, cirrhosis and hepatocellular carcinoma). To clarify a relation between MTA concentration and MTAP abundance a mass spectrometry based activity-assay for MTAP has been set up, using stable isotope labeled MTA as substrate. The decrease in stable isotope labeled MTA was measured over time by liquid chromatography-mass spectrometry and rate constants were determined. For mice with fatty liver disease an inverse correlation of MTA concentration and MTAP activity (both normalized to tissue weight) was observed. The assay works also in human tumor biopsies, but the analysis of the results is much more difficult because the control tissue is cirrhotic. Normalization to tissue weight is not possible due to the different nature of both tissue specimens.

In a next step MTAP protein should be quantified by AQUA peptides and liquid chromatography mass spectrometry for a better understanding of the still measured activity.

12. Zusammenfassung

5'-Deoxy-5'-methylthioadenosin (MTA) entsteht im Zuge der Polyaminsynthese aus S-Adenosylmethionin (SAM). Das für den Abbau von MTA nötige Enzym Methylthioadenosinphosphorylase (MTAP) ist in vielen Tumoren nicht vorhanden oder zumindest in seiner Aktivität stark vermindert und somit wird postuliert, dass in Tumoren MTA akkumuliert. Zuerst wurde eine Methode zur quantitativen Bestimmung von MTA mit Flüssigkeitschromatographie-Tandem-Massenspektrometrie entwickelt, mit der dann die vermutete Akkumulation von MTA in Tumoren und Tumor-Zell-Linien mit reduziertem MTAP-Level nachgewiesen werden konnte. Um weitere Folgen eines reduzierten MTAP-Levels in Tumoren zu klären, wurde die Methode auf die meisten Metabolite des Methionin- und Polyaminstoffwechselweges erweitert und es konnte gezeigt werden, dass eine positive Korrelation zwischen MTA, SAM und Putrescin besteht, die sowohl in verschiedenen Tumoren (z. B. Melanom, Gliom, Nierenkarzinom und Lebertumor) als auch unterschiedlichen Lebererkrankungen (Fettleber, Zirrhose und Lebertumor) beobachtet werden konnte. Zur Klärung des Zusammenhangs zwischen MTA-Konzentration und Menge an MTAP wurde ein Aktivitäts-Assay für MTAP entwickelt, bei dem stabil isotopen markiertes MTA verwendet wurde. Die zeitliche Abnahme des Substrates wurde mit Flüssigkeitschromatographie-Tandem-Massenspektrometrie verfolgt und Geschwindigkeitskonstanten ermittelt. Bei Mäusen mit Fettleber konnte eine inverse Korrelation von MTA-Konzentration und MTAP-Aktivität (normalisiert auf Lebergewicht) beobachtet werden. Somit akkumuliert MTA in den Lebern der kranken Mäuse auf Grund eines langsameren MTA-Abbaus. In humanem Lebergewebe, welches mit diesem Assay ebenfalls analysiert wurde, sind die Ergebnisse schwerer zu interpretieren, da das Kontrollgewebe in diesem Fall

bereits zirrhotisch ist. Eine Normalisierung auf Gewicht ist auf Grund des großen Unterschiedes zwischen gesundem und zirrhotischem Lebergewebe nicht sinnvoll.

In einem nächsten Schritt soll die MTAP-Proteinmenge mit AQUA-Peptiden und Flüssigkeitschromatographie-Tandem-Massenspektrometrie bestimmt werden, um die gewonnenen Aktivitätswerte besser verstehen zu können.

Erklärung

Hiermit versichere ich, dass ich die vorliegende Arbeit selbst verfasst und keine anderen als die angegebenen Hilfsmittel und Quellen verwendet habe.

Regensburg,

Axel P. Stevens